University of Kent

School of Engineering and Digital Arts

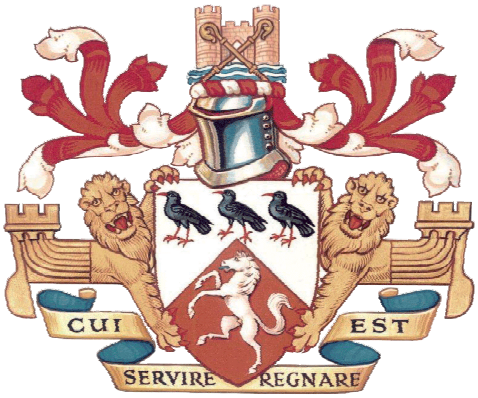

Seamless Mobility under a Dedicated Distributed Antenna System for High-Speed Rail Networks

A Thesis Submitted to The University of Kent

For The Degree of Doctor of Philosophy

In Electronic Engineering

By

Wael W. Ali

December-2018

External Examiner: Associate Professor Justin Coon

University of Oxford

Internal Examiner: Associate Professor Christos Efstratiou

University of Kent

SUPERVISOR

Prof. Jiangzhou Wang

DEDICATION

To my father Waqar Ali, mother Eman Muhsen, wife Noor Al-Janabi, brothers Yasser and Asser, sisters Walaa and Hala, and to my beloved kids Yazan and Ian.

I am so grateful for your continuous inspiration, love, and support.

ACKNOWLEDGEMENTS

First and foremost, I would like to thank my supervisor, Professor Jiangzhou Wang, for his continuous help, support, and guidance during my Ph.D. journey at the University of Kent. Without his constructive comments and invaluable feedback, this thesis would not be possible.

Secondly, I would like to express my sincere appreciation to my co-supervisor, Dr. Huiling Zhu, for her continuous advice, fruitful and constructive meetings and discussions. Her feedback was instrumental in developing my ideas and work to become high value research.

Thirdly, I would like to indicate my deepest gratitude to Dr. Junyuan Wang from the university of Edge Hill for her perpetual help, advice, fruitful meetings and constructive discussions throughout my Ph.D. journey. Without her knowledge, insightful notes and comments, this thesis would not have been possible to complete.

Fourthly, I was very fortunate to become acquainted with my fellow colleagues at the school of engineering and digital arts especially the wireless communication research group: Ramiz Raoof, A. Daghal, Ali J. Mahbas, Kenan Alhares, Hind Albasry, Osama Alluhaibi, Manish Nair, Yan Kai, R. Husbands, A. Khadka and Estela, for the wonderful

time shared at the wireless communication research group.

Further, I would like to thank my sponsor, The Higher Committee For Education Development in Iraq for their financial support. Without this support, it would have been impossible to undertake my Ph.D. program at the University of Kent.

Last but not least, I would like to thank my father and mother for their continuous motivation and for always believing in me, and also for their endless love and support. Also, I am profoundly indebted to my beloved wife for her continuous love, support, and understanding of my Ph.D. pressure and lack of time. In addition to all the time she has given to taking care of our small family during those four years. Without her this thesis would not have been possible.

ABBREVIATIONS

1G ..... First Generation

2G ..... Second Generation

3G ..... Third Generation

4G ..... Fourth-Generation

5G ..... Fifth Generation

3GPP ..... Third Generation Partnership Project

ACK ..... Acknowledgement

ADC ..... Analogue to digital conversion

AI ..... Artificial intelligence

AP ..... Access point

BBU ..... Baseband Unit

BER ..... Bit error rate

bps ..... Bit per second

BS ..... Base Station

BW ..... Bandwidth

CAPEX ..... Capital expenditure

CB ..... Coordinates beamforming

CBP ..... Call blocking probability

CDF ..... Cumulative Distribution Function

CDMA ..... Code division multiplexing

CDP ..... Call dropping probability

COMP ..... Coordinated multi point transmission/reception

CPRI ..... Common Public Radio interface

C-RAN ..... Cloud radio access network

C-RNTI ..... Cell radio network temporary identifier

CS ..... Coordinated scheduling

CSI ..... Channel state information

CU ..... Central unit

DAC ..... Digital to analogue conversion

DAS ..... Distributed antenna system

dB ..... Decibel

dBm ..... Decibel referenced to milliwatts

DCS ..... Dynamic cell selection

DL ..... Downlink

EB ..... Exabytes

EC ..... Extended cell

ECGI ..... E-UTRAN cell global identifier

eICIC ..... Enhanced inter-cell interference

eNB ..... Evolved Node B

E-RAB ..... Evolved Universal Terrestrial Radio Access radio access bearer

E-UTRAN .. Evolved universal terrestrial radio access

e.t.c ..... etcetera

FDMA ..... Frequency division multiple access

FSW ..... Frequency switch

Gbps ..... Gigabits per second

GSM ..... Global system for mobile

HARQ ..... Hybrid automatic repeat request

HetNet ..... Heterogeneous network

HHO ..... Hard handover

HO ..... Handover

HOF ..... Handover failure

HSR ..... High-speed railway

Hz ..... Hertz

ICI ..... Inter carrier interference

ICIC ..... Inter-cell interference coordination

IP ..... Internet protocol

JT ..... Joint transmission

km ..... Kilometre

LOS ..... Line-of-sight

LTE-A ..... Long Term Evolution-Advanced

LTE ..... Long Term Evolution

m ..... Meter

MAC ..... Media access control

MAHO ..... Mobile assisted handover

Mbps ..... Megabits per second

MC ..... Measurement control

MFC ..... Moving frequency concept

MIB ..... Master information block

MIMO ..... Multiple input multiple output

MMIMO .... Massive multiple input multiple output

MME ..... Mobility management entity

MR ..... Mobile relay

MRT ..... Measurement report

mmWave .... Millimetre wave

NCHO ..... Network controlled handover

NLOS ..... Non line-of-sight

OA ..... Onboard antenna

OADM ..... Optical add drop multiplexer

OCU ..... Onboard CU

OFDMA .... Orthogonal Frequency Division Multiple Access

OFDM ..... Orthogonal Frequency Division Access

OPEX ..... Operating expenditure

OFSW ..... Onboard FSW

PCI ..... Physical cell identification

PDCP ..... Packet data convergence protocol

PHY ..... Physical

P-GW ..... Packet gateway

PS ..... Port server

QoS ..... Quality of service

RA ..... Random access

RACH ..... Random access channel

RAR ..... Random access response

RAU ..... Remote antenna unit

RCR ..... Radio resource control connection reconfiguration

RF ..... Radio frequency

RLF ..... Radio link failure

RRC ..... Radio resource control

RRH ..... Remote radio head

RSRQ ..... Reference signal received quality

RSRP ..... Reference signal received power

RSQ ..... Received signal quality

RSS ..... Received signal strength

S-GW ..... Serving gateway

SHO ..... Soft handover

SIB ..... System information block

SIR ..... Signal to Interference Ratio

SINR ..... Signal to Interference plus Noise Ratio

SN ..... Sequence number

TDMA ..... Time division multiple access

TFSW ..... Trackside FSW

TTT ..... Time to trigger

TCU ..... Trackside CU

UE ..... User equipment

UL ..... Uplink

UMTS ..... Universal mobile telecommunications system

VCN ..... Virtual cellular networks

WLAN ..... Wireless local area networking

LIST OF SYMBOLS

A ..... Constant

f ..... Carrier frequency

c ..... Speed of light in vacuum

k ..... RAU $k \in \{S, T\}$ [serving, target]

j ..... OA $j \in \{f, m\}$ [front, middle]

T_s ..... Symbol duration

σ_i^k ..... Shadow fading deviation

$\sigma_{i_j}^K$ ..... Shadow fading deviation between OA j and RAU k

β_1, β_2, β ..... Triggering thresholds

N ..... Total number of RAUs in each cell

M ..... Total number of subcarriers

r ..... RAU radius

L ..... Train's length

d_i^k ..... Distance between RAU k and the MR

$d_{i_j}^k$ ..... Distance between RAU k and OA j

d_v ..... Distance between RAU and the track

U ..... Minimum signal threshold required to recover the commands successfully

$J_0(\cdot)$ ..... Zeroth-order Bessel function of the first kind

Δ ..... Normalized ICI power of OFDM system

v ..... MR/train speed

d_i^T ..... Distance between the MR and the target RAU

d_i^S ..... Distance between the MR and the serving RAU

D ..... Inter-RAU distance between two successive RAUs

y_i/x_i ..... MR's current location

h_R ..... RAU's height

h_T ..... Train's height

d_{BR} ..... Breaking point distance

g_i^k ..... Shadow fading between RAU k and the MR

$g_{i_j}^k$ ..... Shadow fading between RAU k and OA j

$Q(x)$ ..... The Q-function

σ_o^2 ..... The noise power

σ_i^T ..... Shadow fading deviation between the MR and the target RAU

σ_i^S ..... Shadow fading deviation between the MR and the serving RAU

ρ_{RCR} ..... Overlapping area percentage dedicated to perform HO algorithm decision and to recover RCR command

$\chi^{\boldsymbol{tradH}}$ ..... Overlapping area associated with the traditional HO scheme

γ ..... The maximum number of retransmission trials associated with the target access procedures of the traditional HO scheme

δ ..... The maximum number of retransmissions for the RCR command of the traditional HO scheme

δ^{prop} ..... The maximum number of retransmissions for the RCR command of the proposed HO scheme

α/α_{mrt} ..... Maximum possible transmission trials for recovering the measurement report of the FSW scheme

ϑ ..... the maximum number of retransmission trials associated with RCR of the enhanced fast HO scheme

ξ ..... Maximum retransmission trials associated with the target access procedures of the enhanced fast HO scheme

$\overline{\delta_s}$ ..... Average value of δ

$\overline{\gamma_s}$ ..... Average value of γ

$\overline{\alpha_s}$ ..... the expected value of the random variable α

$\overline{\xi_s}$ ..... Average value of ξ

$\chi^{\boldsymbol{efH}}$ ..... Overlapping area of the Enhanced fast HO scheme

$\chi^{\boldsymbol{tradH}}/\chi$ ..... Overlapping area of traditional HO case

$\chi^{\boldsymbol{Tfsw}}/\chi^{\boldsymbol{fsw}}$ ... Overlapping area of the trackside FSW scheme

$log_{10}(\cdot)$ ..... Natural logarithmic function

$E(\cdot)$ ..... Expected value

$\in$ ..... Belong sign

$\lfloor \cdot \rfloor$ ..... The floor function

I_i^k ..... The normalized noise and ICI power

I_{ij}^k ..... The normalized noise and ICI power between OA j and RAU k

$I_{i,z}^S$ ..... The normalized noise and ICI power for the retransmission trial z between the serving RAU and the MR

$I_{i,z}^T$ ..... The normalized noise and ICI power for the retransmission trial z between the target RAU and the MR

P_i^k ..... The received power of the MR from RAU k

P_{ij}^k ..... The received power of OA j from RAU k

P_t ..... The transmitted power per RAU

P_T ..... The total transmitted power of CU

Ω_i^S ..... RSQ of the MR from the serving RAU

Ω_i^T ..... RSQ of the MR from the target RAU

Ω_{ij}^k ..... RSQ of OA j from RAU k

$P_{L_i}^k$ ..... Large scale fading between RAU k and the MR

$P_{L_{ij}}^k$ ..... Large scale fading between RAU k and OA j

$\mathbf{P}_{trigg}^{\boldsymbol{tradH}}/\mathbf{P}_{trigg}$. Triggering probability of the traditional HO scheme

$\mathbf{P}_{trigg}^{\boldsymbol{fsw}}$ ..... FSW triggering probability

$\mathbf{P}_{trigg}^{\boldsymbol{efH}}$ ..... Triggering probability of the fast enhanced HO scheme

$\mathbf{P}_{f_{RCR}}^{\boldsymbol{tradH}}$ ..... RCR failure probability for multiple retransmissions of the traditional HO scheme

$\mathbf{P}_f^{\boldsymbol{fsw}}$ ..... Failure probability of the FSW scheme per RAU

$\mathbf{P}_{f_f}^{\boldsymbol{Tfsw}}$ ..... Failure probability of the TFSW scheme per RAU of the front OA

$\mathbf{P}_{f_{mc}}^{\boldsymbol{Tfsw}}$ ..... Failure probability of the MC of the TFSW scheme per RAU of the front OA

$\mathbf{P}_{int}^{\boldsymbol{Tfsw}}$ ..... the interruption probability of the TFSW scheme

$\mathbf{P}_{int}^{\boldsymbol{Ofsw}}$ ..... the interruption probability of the OFSW scheme

$\mathbf{P}_{out_m}^{\boldsymbol{Ofsw}}$ ..... the outage probability of the OFSW scheme of the middle OA

$\mathbf{P}_{f_{mc}}^{\boldsymbol{Ofsw}}$ ..... Failure probability of the MC of the OFSW scheme per RAU of the front OA

$\mathbf{P}_{unint}^{\boldsymbol{Ofsw}}$ ..... The uninterrupted probability of the OFSW scheme per RAU of the OFSW scheme

$\mathbf{P}_{f_f}^{\boldsymbol{Ofsw}}$ ..... Failure probability of the OFSW scheme per RAU of the front OA

$\mathbf{P}_{f_{RCR}}^{\boldsymbol{efH}}$ ..... the RCR failure probability of the enhanced fast HO scheme

$\mathbf{P}_{f}^{\boldsymbol{efH}}$ ..... HOF probability of the enhanced fast HO scheme

$\mathbf{P}_{f_{tar}}^{\boldsymbol{efH}}$ ..... Proposed target access failure probability

$\mathbf{P}_{f}^{h}$ ..... HOF probability of the traditional HO scheme without retransmission

$\mathbf{P}_{f}^{\boldsymbol{tradH}}$/ $\mathbf{P}_{f_T}^{h}$ .. HOF probability of the traditional HO scheme with retransmission

$\mathbf{P}_{f_c}$ ..... Single command failure probability of the target access of the traditional HO scheme

$\mathbf{P}_{f_{tar}}^{\boldsymbol{tradH}}$ ..... Target access failure of the traditional HO scheme for single transmission

$\mathbf{P}_{f_{tar_z}}$ ..... Target access failure of the traditional HO scheme for multiple transmissions

$\mathbf{P}_{f_{tar_z}}$ ..... Target access failure of the traditional HO scheme for single transmission

$T_{mr}^{\boldsymbol{fsw}}$ ..... One-time transmission delay to recover the measurement report of FSW scheme

$T_{succ}^{\boldsymbol{efH}}$ ..... HO success latency

$T_{dec}^{\boldsymbol{fsw}}$ ..... Delay required to perform the FSW scheme decision algorithm

$T_{succ}^{\boldsymbol{tradH}}$ ..... the success HO latency for the traditional HO scheme

$T_{int}^{\boldsymbol{tradH}}$ ..... Interruption time of the traditional HO scheme

$T_{int}^{\boldsymbol{efH}}$ ..... Interruption time of the enhanced fast HO scheme

$T_{succ}^{\boldsymbol{fsw}}$ ..... Success latency of the FSW scheme

$T_{int}^{\boldsymbol{fsw}}$ ..... The interruption time for this scheme

$T_{rec}^{w[RCR]}$ ..... Total recovery time of the enhanced fast HO scheme

$T_{311}^{w[RCR]}$ ..... Cell re-selection time of the enhanced fast HO scheme

$T_{avg}^{\boldsymbol{tradH}}$ ..... The average time of the traditional HO scheme

$T_{succ}^{\boldsymbol{tradH}}$ ..... The success latency of the traditional HO scheme

$T_{avg}^{\boldsymbol{efH}}$ ..... The average time of the enhanced fast HO scheme

$T_{succ}^{\boldsymbol{efH}}$ ..... The success time of the enhanced fast HO scheme

$\overline{T_{int}^{\boldsymbol{tradH}}}$ ..... The average interruption time of the traditional HO scheme

$\overline{T_{int}^{\boldsymbol{efH}}}$ ..... The average interruption time of the enhanced fast HO scheme

$T_{rec}^{\boldsymbol{fsw}}$ ..... Recovery latency of the FSW scheme

$T_{avg}^{\boldsymbol{fsw}}$ ..... The average latency of the FSW scheme

$T_{succ}^{\boldsymbol{fsw}}$ ..... Success latency of FSW scheme

$\overline{T_{int}^{\boldsymbol{fsw}}}$ ..... The average interruption time of FSW scheme

T_{RCR} ..... RCR command transmission time

T_{RCRcom} ..... RCR complete command transmission time

$T_{mr}^{\boldsymbol{fsw}}$ ..... Transmission time of the measurement report

T_{304} ..... Maximum time allowed to finalize the target access procedures

T_{dec} ..... Time required to perform the HO decision algorithm

T_{dec}^{prop} ..... The HO preparation time of the proposed HO scheme

$T_{dec}^{\boldsymbol{fsw}}$ ..... Time required to perform the FSW scheme decision algorithm

T_{adm} ..... Latency of the admission control decision algorithm

T_{psw} ..... Path switch process latency

T_{req} ..... Latency of HO request

$T_{req/ACK}$ ..... Latency of HO request ACK

T_{search} ..... Time required to search for the frequency

$N_{freq}^{w/o[RCR]}$ .... Number of frequencies needed to be scanned without receiving RCR command

$N_{freq}^{w[RCR]}$ ..... Number of frequencies needed to be scanned when receiving RCR command

$T_{SI}^{w/o[RCR]}$ ..... Time required for receiving all the relevant SIBs without recovering RCR command

$T_{SI}^{w[RCR]}$ ..... Time required for receiving all the relevant SIBs when recovering RCR command

LIST OF PUBLICATIONS AND SUBMISSIONS

The presented work in this dissertation is part of the following publications:

1. Wael Ali, Junyuan Wang, Huiling Zhu, Jiangzhou Wang, "An Optimized Fast Handover Scheme Based on Distributed Antenna System for High-Speed Railway," VTC-Fall 2017, pp. 1-5.
2. Wael Ali, Junyuan Wang, Huiling Zhu, Jiangzhou Wang, "Seamless Switching Using Distributed Antenna Systems for High-Speed Railway," VTC Spring 2017, pp. 1-5.
3. Wael Ali, Junyuan Wang, Huiling Zhu, Jiangzhou Wang, "Distributed antenna system based frequency switch scheme evaluation for high-speed railways," ICC 2017, pp. 1-6.
4. Wael Ali, Junyuan Wang, Huiling Zhu, Jiangzhou Wang, "An Expedited Predictive Distributed Antenna System Based Handover Scheme for High-Speed Railway," GLOBECOM 2017, pp. 1-6.
5. Wael Ali, Junyuan Wang, Huiling Zhu, Jiangzhou Wang, "Seamless Mobility under a Dedicated Distributed Antenna System for High-Speed Rail Networks," submitted to IEEE Transaction on Wireless Communications.

ABSTRACT

High-speed railway (HSR) has demonstrated a tremendous growth worldwide, and currently is attaining a maximum velocity of 575 km/h. Such a high speed makes the mobile wireless communications a challenging task for HSR to sustain since the handover (HO) rate increases with speed which might result in a high loss of link connectivity. By employing a dedicated distributed antenna system (DAS) along with the two-hop network architecture for HSR wireless communications, this thesis aims to attain a high system capacity, a more transmission reliability, and consequently a superior mobile wireless communication quality-of-service (QoS) for commuters on HSR.

First, this thesis proposes a frequency switch (FSW) scheme to mitigate the persistent HO issue in conventional HSR wireless communication systems. The proposed scheme significantly alleviates the interruption time and the dense signalling overhead associated with the traditional HO process, providing a much more convenient scheme, i.e. fast and soft which suits the remote antenna unit (RAU) small coverage area and the train's high moving speed. Therefore, FSW scheme provides mobility robustness signalling process that guarantees a more successful frequency switch instead of HO, thereby, reduces the probability of a radio link failure (RLF) compared with HO process in traditional HSR systems.

Second, an enhanced fast predictive HO mechanism is proposed by starting the HO process earlier, when moving from one RAU coverage area to the next where these two RAUs are controlled by different central units (CUs). It shows that the proposed fast

HO scheme achieves a lower HO command failure probability than the traditional HO. This leads to a lower HO failure probability which consequently can considerably enhance the end-users' quality-of-service (QoS) experience. Analytical results verify that the proposed schemes can improve the system performance substantially by delivering ultra-reliable low-latency communications.

Finally, with the aim of providing an ultra-reliable low-latency wireless communications, this thesis also proposes an onboard frequency switch scheme to further simplify our previously proposed FSW scheme.

CONTENTS

LIST OF FIGURES

LIST OF TABLES

CHAPTER 1

INTRODUCTION

Recently, cellular wireless communication systems have seen substantial technological improvements. The need for ubiquitous, high mobility speed, and all time-on data connectivity has driven the quick development of wireless technologies. Specifically, the third generation partnership project (3GPP) standard has witnessed the transformation of universal mobile telecommunications systems (UMTS) into high-speed packet access (HSPA) and lately into the long-term evolution (LTE) and the more recent version long-term evolution advanced (LTE-A) [11]. LTE and its successor versions are anticipated to be a potential standard for the future mobile broadband. LTE-A is currently able to deliver very high data rates in both the downlink (DL) (3 Gbps) and uplink (UL) (1.5 Gbps). This is attained due to using a combination of carrier aggregation and multiple input multiple output (MIMO) techniques along with other technologies [12].

Moreover, packet delay in the radio access network is considerably decreased by using a fast scheduling and fast hybrid automatic repeat request (HARQ) scheme. The scheduling interval is decreased to 1 ms, while in HSPA, it is 2 ms, which consequently means a tight coordination between physical (PHY) and medium access control (MAC) layers is imperative. A second crucial aspect is the evolution of an end-to-end Internet protocol (IP)-based network architecture which relatively has lower levels of hierarchy than second/third generation [(2/3)G] networks. This results in decreasing the end-to-end latency [11]. In addition, LTE enables interconnecting with the Legacy 3GPP technologies

i.e., global system for mobile communications (GSM), HSPA, and also with non-3GPP technologies i.e., wireless local area network (WLAN) and code division multiple access (CDMA) [13].

Heterogeneous Network (HetNet) deployment is also enabled in LTE, in which a macro cell is deployed for a global coverage, whereas pico/femto/relay cells are deployed for data rates/coverage improvements and an increased spectral efficiency. However, HetNets have challenges in terms of interference management and mobility [14, 15]. In this thesis, we focus on mobility management, more specifically on the frequent handover (HO) issue.

1.1 Motivation

Today, humanity is plunged into the age of mobile services. Various motivations underpin global wireless connectivity not only for business purposes, but most importantly for a personal use, or even for security objectives. In this context, a massive range of services currently coexist in a very intricate and heterogeneous network architecture, which can be managed by multiple operators [16]. 5G networks are expected to encounter 10^4 times more traffic especially in ultra-dense scenarios (stadium) compared with the current technology. 10-100 times more devices, battery life of 10 years, and ultra low cost devices are all associated with the introduction of the machine-to-machine communications [17]. Peak data rates of 10 Gbps for some applications, such as augmented reality, and at least 100 Mbps data rates whenever needed (cell edge). Together with a latency level of 1 ms needed for vehicle-to-everything technology [18]. Additionally, most of these services and applications are yearned for ultra-reliability performance [19, 20].

High-speed trains, as a 5G scenario, will be required to provide most of the aforementioned QoS even though the high mobility speed. However, a number of challenges should be addressed in order to achieve the required QoS. First, due to the massive number of users allocated along the train's carriages, the serving cell footprint should be in the range of tens of metres in order to satisfy the user's needs in terms of capacity, otherwise a capacity shortage occurs. Consequently, small cell deployment in conjunction with high

mobility speed means necessarily increasing the HO rate. Increasing the HO rate will deteriorate the end-user's QoS, as this can increase the failure probability, which will lead to increasing the HO latency. A crucial part of this latency is the interruption time during which neither the transmitter nor the receiver can send or receive any packets. This would result in high packet loss, and high call dropping probability, and consequently low throughput would take place due to the frequent HO issue.

This thesis aims to alleviate the problem of recurrent HO of HSR, by proposing schemes which can considerably reduce the signalling overhead. Subsequently, leads to a higher success probability, or by proposing a scheme which guarantees a higher success probability by optimising the original scheme (the original scheme is optimised for the traditional hexagonal cell layout and for the user's random mobility pattern) for the high-speed railway (HSR) scenario. In which the train can move linearly from cell to cell in a one dimensional cell layout along a predetermined itinerary as will be shown in the upcoming chapters.

1.2 Challenges

This subsection discusses the challenges imposed by the HSR scenario as follows.

- HSR broadband wireless communication is encountering many challenges due to the train's special environment and its high moving speed. For example, a mobile relay (MR) has been proposed in [2, 21] to form a two-hop architecture to avoid the carriage's large penetration loss as well as to solve the group handover (HO) for tens to hundreds of users equipments (UEs) located within each carriage which leads them to send a request to HO concurrently. The utilized MR represents all the UEs attached to it and therefore forwards one request to hand over all its associated UEs, which then can reduce the network burden considerably. When employing the MR, in the downlink, the first hop is the base station (BS) to the MR while the second hop is the MR to the access point (AP) or the MR to the UE if no AP is employed. In the uplink, on-board users are connected to the APs located inside

each carriage, and thereafter the APs direct the users' data streams to the BS via the on-board MRs.

- The densely deployed UEs inside each carriage is the other inherent issue in HSR, which requires high data rates and larger network capacity to fulfil UEs' needs. Network intensification can be applied to partially satisfy the users' needs. However, the ultimate solution is to marry network intensification with a millimetre wave (mmWave) frequency spectrum (30-300 GHz).

- Additionally, HSR itinerary might include a variety of environments mainly deemed as suburban or rural areas [22]. Yet, HSR might also travel through viaducts [23, 24], tunnels [25], hilly terrains [26], stations [27], and cuttings [28], which are quite different from the usual suburban or rural environments. This kind of diversity imposes another challenge represented in channel measurement and modelling.

- Further, the train's high moving speed results in a Doppler shift that increases as the speed and/or the used frequency increases. For instance, a Doppler shift of 666.66 Hz is incurred as a consequence of a speed of 360 km/h and a frequency of 2 GHz. This leads to a carrier frequency offset resulting in an inter carrier interference (ICI) which poses a serious impact on the overall system performance.

- Another impact of the high moving speed is the Doppler spread which results in a fast time varying channel which consequently leads to an obsolete channel state information. However, the Doppler shift has a higher impact on HSR scenario compared with the Doppler spread, as the available energy in the line-of-sight (LOS) path is higher than the multipath energy, and the multipath delay is relatively small [29].

- More importantly, a high moving speed requires a frequent HO. For example, a HO would be imperative every 10s supposing a footprint of 1km conjointly with a velocity of 100 m/s. The recurrent HO would lead to a long delay, a high packet loss, and a high drop off rate, and therefore could seriously deteriorate the system

throughput. The reason for this is the long HO interruption time which might be exacerbated manifold due to the HO failure (HOF) case.

These challenges; however, motivate us to propose a few robust solutions to deal with some of the above issues, specifically on the frequent HO issue, by proposing schemes which have a better HO success probability compared to the traditional HO scheme. Although, most of the current research focuses on enhancing the HO success probability by using either dual antennas/systems or by splitting the user and control planes onto different frequencies (as discussed later in the upcoming chapters), here with, and in contrast to other research work we focus on modifying and optimising the traditional HO scheme by utilizing the HSR's one dimensional layout in conjunction with DAS system architecture. Thus, the proposed schemes should have a higher success probability and therefore we can achieve a better performance (as discussed later in the upcoming chapters).

1.3 Contribution of the Thesis

The objective of this thesis is to improve the performance metrics associated with moving a certain user from cell to cell in terms of the scheme's failure probability, which depends mainly on the received signal quality being higher than, or equal to, the minimum threshold required to recover the negotiated messages associated either with the serving cell or with the target cell. The presented work of this thesis is based on a novel system model neither of the available works are similar to it as we take into consideration the following points. 1) The analysis of the HO failure scheme takes into account each step of the HO process unlike the current work which divided the HO failure probability into HO failure probability associated with only one step with the target and an outage probability of one command with the serving cell. The available HO failure probability analysis thus does not reflect the real HO failure probability, as it does not consider the serving commands into the failure probability. 2) We also take into account the required retransmission trials both the upper bound and the average and no available work consider them. 3) We also analyze the effect of the overlapping area and its effect on the overall performance, and there is no work which analyzes the effect of the overlapping area analytically only a

simulation based result is available. 4) The average latency and the average interruption time is calculated, also a very few works calculated these metrics. 5) In this thesis we focus on optimizing the original HO scheme for the HSR scenario and thus delivering a better performance unlike most the available works which focuses more on the system architecture not the scheme itself. The detailed contributions of this thesis include:

1. A predictive HO scheme is proposed whereby part of the preparation phase is triggered in advance, so that the overall system performance is enhanced. This scheme is realized by utilizing the HSR linear one-dimensional cell layout, where there is only one possible candidate cell to camp on when moving between RAUs belonging to different CUs. The HO command failure probabilities of the proposed and traditional HO scheme are derived and compared by means of simulation as are the access failure probabilities of both cases. The schemes' failure probabilities are derived as well as the average latency and the required overlapping areas of both schemes. Moreover, the effect of retransmission trials on the overall system performance is investigated.

2. BY employing the DAS architecture along with the two-hop architecture, we are able to propose the following:

   (a) A new mechanism, known as the frequency switch (FSW) scheme to supplant the conventional HO between RAUs under the control of the same CU by applying the MFC into CU. In this mechanism, a frequency switch is triggered based on satisfying a predefined threshold. Therefore, the MR triggers a measurement report back to CU via the current associated RAU. This scheme aims to deliver a fast and robust mobility signalling which ensures a lower failure probability than the traditional HO scheme. Unlike other schemes, which use location based triggering scheme by utilizing the GPS signalling which is unsuitable in case of tunnel scenarios which exists frequently in HSR scenario. Instead we propose a more practical approach to activate the FSW scheme. This approach is based on the current channel measurement i.e., the received signal quality (RSQ). Since HSR's routes have a large number of tunnels which

are considered as outage zones for the GPS signalling, we prefer a more robust approach represented by employing RSQ to trigger the scheme. The proposed approach is backward compatible with LTE standard, also the existing work is based only on laboratory experiment using Ethernet cable instead of fibers [21].

(b) Furthermore, a simplified yet a more robust HO scheme is offered when moving between RAUs which belong to different CUs, through utilizing a dedicated one-dimensional DAS network architecture which provides more degree of freedom to optimize the HO scheme for high mobility users. Since a HO process generally occurs when the MR moves from one RAU's coverage area linked to the serving CU to another RAU's coverage area linked to the target CU under a dedicated DAS architecture deployment, the target CU could be known in advance as it will be the only possible candidate that the MR will eventually be handed over to, so that the measurement report and HO command/RCR can be triggered in advance to assure an improved system performance.

(c) Moreover, we have considered the ICI effect on the overall system performance by employing the RSQ to trigger HO/FSW process. We further consider the retransmission trial times and their effect on the overall system performance. Finally, closed-form expressions for triggering probability, HO command failure probability, the total failure probability, average latency, average interruption time, overlapping area distance are derived through theoretical analyses for the proposed schemes as well as for the traditional HO scheme. Please note that there is no available work analyses the ICI effect except [30], which analyze it incorrectly.

3. In addition, an onboard FSW scheme is proposed to replace the traditional FSW scheme, by adopting the original concept of FSW scheme but this time to be performed within the train network instead of the track side network (DAS). The proposed scheme reduces the overlapping area and the average latency by delivering less negotiated signalling. Thereby achieving a lower failure probability and better QoS with less capital expenditure (CAPEX) and operating expenditure (OPEX) compared with the traditional scheme. Moreover, the issue of partial interruption

associated with the traditional FSW scheme is avoided using multiple antennas linked to the same frequency. The additional antennas not only avoids the interruption scenario but also improves the switching performance by enhancing the reliability and therefore reducing the latency. Enhancing reliability can be achieved using multiple antennas, using multiple antennas can reduce the required number of retransmission. Thus, obtaining the needed reliability with ultra less latency.

The work provided in this thesis does not provide comparison with other work in the literature due to our work's unique proposed schemes and the singular analytical models and assumptions which is mentioned above. However, we give a comparison with other schemes in terms of the schemes' negotiated signalling overhead count and size as these will not get affected by neither the used analytical model approach nor the assumptions, as we will see in chapter 4.

1.4 Thesis Outline

This thesis contains six chapters and an appendix. The main contributions of this thesis are summarized, and then structured as follows:

- In Chapter 1, the motivation and the main challenges associated with HSR communication are discussed.
- In Chapter 2, the available literature proposed to solve the recurrent HO issue is presented, in which the state-of-the-art, advantages and disadvantages of each scheme is investigated. In addition, the research works related to the FSW scheme are explained.
- In Chapter 3, an expedited predictive HO scheme is proposed and compared analytically and by means of simulation with the traditional HO scheme with and without using retransmission trials.
- In Chapter 4, the proposed enhanced fast HO scheme as well as the FSW scheme are proposed, discussed, and analytically investigated along with the traditional

HO scheme. A comparison is made in terms of some crucial performance metrics used to verify the proposed schemes' superiority over the traditional HO scheme by means of simulations, such as the measurement report/HO command failure probability, access failure probability, total scheme's failure probability, the required overlapping area, the average and maximum allowed retransmission trials, and the average latency of each scheme.

- In Chapter 5, an onboard FSW scheme is proposed, investigated, and compared analytically and by means of simulation with the traditional FSW scheme in terms of the schemes' failure probabilities, the interruption probabilities and the average latency.

- In chapter 6, the conclusions of this thesis are drawn, and possible future work is discussed.

- In Appendix A, Theorem 1 is analytically derived.

CHAPTER 2

LITERATURE REVIEW

2.1 Introduction

In the first part of this chapter, an overview of HO, distributed antenna system (DAS) and relay network is presented. These topics pertain to the work carried out and discussed in this dissertation. More specifically, the HO types, prerequisites, relationship with resource management, triggering criteria, and evaluation metrics are examined. Then, DAS architecture and its advantages are discussed. Finally, the relay network concept is discussed. A considerable amount of research has been done on high-speed railway wireless communication systems, and especially on the frequent HO issue. Hence, the focus of the second part of this chapter, is the state-of-the-art of the proposed HO solutions. We provide a brief description of each scheme and its associated architecture which have been proposed to alleviate this issue.

2.2 Introduction to Handover Concept

Currently, wireless communication plays a crucial role in the contemporary world due to its mobility and flexibility with more than 5 billion users worldwide and with expected traffic to reach 49 Exabytes (EB) per month by the end of 2021 [31]. This huge data traffic is due to the greedy nature of trendy applications and services, i.e. the wide variety

of multimedia services, such as wireless HDTV, wireless home entertainment and the virtual wireless office. As a result of developments in modern technology, there are more and more applications, locations (home, office, and anywhere in between), and handsets (mobile phone, tablet, etc.) with various purposes, all of which need to be connected tetherlessly and served conveniently and effectively [32]. To support these applications, wireless system technologies should offer user equipment (UE) with a huge capacity by incorporating a variety of different techniques, such as antenna diversity, an advanced and complex coding scheme, beam-forming, small cells, etc [1]. The millimetre wave spectrum is a possible candidate to meet tomorrow's unprecedented user demand [33].

The handover is a crucial aspect in the wireless communication paradigm due to the user's movement. HO is a scheme by which a user moves between cells while keeping a continuing call or data session uninterrupted. This can be carried out by changing the UE's channel in the serving cell to a new channel offered by the target cell. In general, HO is imperceptible to the user, yet it can affect the quality of service (QoS). HO can be categorized into two types: horizontal HO and vertical HO. Horizontal HO takes place when a UE moves out of the coverage of the serving cell and into the coverage of the target cell where both cells belong to the same system. Vertical HO, on the other hand, can be defined as a HO which happens between the serving cell and the target cell where both cells use different wireless communication technologies, e.g. a WLAN to a wireless cellular network and vice versa [33].

Normally, the HO process is performed around the middle point between two cells, namely the serving cell and the target cell in a region known as the HO region or the overlapping area. Fig. 2.1 depicts a typical HO scenario in which the UE moves from cell to cell and the received signal strength (RSS) or RSQ of the serving cell gradually decreases while the RSS of the target cell gradually increases [32]. Note that the RSS is continuously measured by the UE for both the serving cell and surrounding cells. At a certain point in the overlapping area the RSS of the serving cell becomes worse than the RSS of the target cell. Therefore, triggering the handover process becomes an urgent necessity to preserve the user's QoS. The triggering process can be initiated by sending a measurement report from the UE back to the serving cell. A successful handover triggering

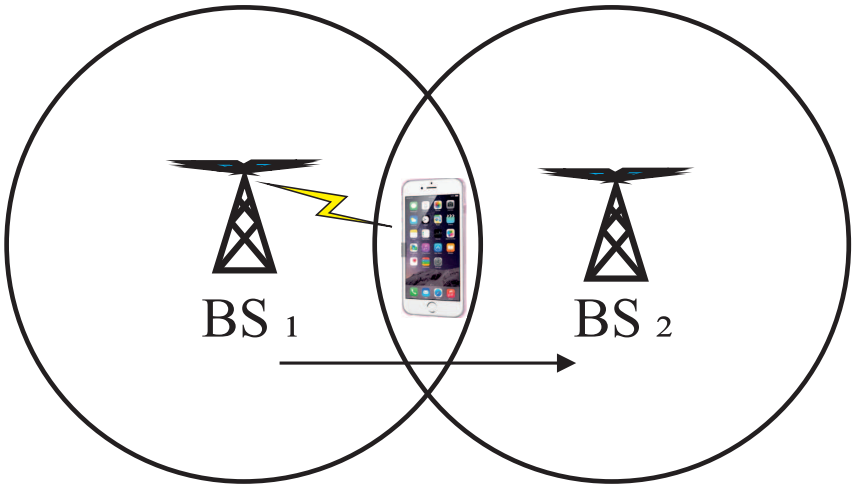

Figure 2.1: HO scenario in a wireless network takes place within the overlapping area.

process is finalized if the target cells are able to provide the UE with the required resources by issuing the HO command from the serving cell to the UE. If the target cell is unable to provide the user with the required resources, the target cell will reject the serving cell HO request. This results in a session dropping. The call dropping probability (CDP) can be consequently defined as the probability that an ongoing session is compelled to end due to a shortage in the target cell's resources. A blocked connection is the process by which the target cell rejects a new connection access request to the network. Therefore, the call blocking probability (CBP) is the probability that a new communication session is refused access into the system. Both CDP and CBP are important QoS parameters for the wireless communication system as they provide a good indication of the network's ability to support mobility [33].

Generally, a HO is formed from a couple of procedures that can be classified into three main phases. The first phase is the measurement phase, which is concluded by issuing the measurement report after satisfying a predefined triggering condition. The second phase is the preparation phase during which the HO decision and admission control decision are performed by the serving cell and the target cell, respectively. These decisions are carried out by algorithms which consider certain parameters and criteria as an input to obtain the optimal decision according to the current inputs. The third phase is the execution phase during which the link established with the serving cell is terminated and the link with the target cell is established by assigning a new channel to the UE being handed

over [33]. From a control point of view, a HO can be classified into three basic types: a network controlled HO (NCHO), a mobile assisted HO (MAHO) and a mobile controlled HO (MCHO). During the decision phase, if the network makes the handover decision by utilizing the measurements of the UE at a number of cells, then it is a NCHO. A HO is said to be a MAHO if the UE provides the measurements and the network carries out the HO decision. When the UE completely controls the handover scheme, it is a MCHO. A NCHO has been used in the first generation (1G) analogue system with latency in the range 5-10 s, while a MCHO has been used by the second generation (2G) system with a delay of 1 s in the global system for GSM [34]. Long-term evolution as a fourth generation (4G) digital system and its successors are network controlled mobile assisted HOs. In the MCHO, the handover process has a short latency in the range of 0.1 s which makes it suitable for microcellular systems. MCHO is considered to have the highest degree of decentralization and the most important feature of this type is the fast HO decision compared with other types. Also, MCHO reduces the burden on the network side by performing the HO process independently from the network especially when the number of users is extremely large. This type is used in the European Standard for cordless telephones [34].

A HO can also be divided into two main types from the point of view of a connection: a hard HO (HHO) and a soft HO (SHO). A HHO is also known as a break-before-make connection, as the link between the UE and the serving cell is broken before establishing a new one. A SHO, on the other hand, is a make-before-break connection, that is, the connection of the serving cell is broken only after the connection of the new cell has already been made [33]. A special case of the SHO is the softer HO which occurs when the UE moves between two sectors belonging to the same serving cell. In the softer HO the channel is preconfigured to send the signalling messages to multiple sectors and use diversity combining techniques to process the signals collected from them [35]. Furthermore, a HHO which happens within the same cell is called an intra-cell HO, while the HHO which happens when a UE crosses into another cell is called an inter-cell HO. Frequency division multiple access (FDMA) and time division multiple access (TDMA) use the HHO as the UE can only be linked to one base station (BS) at a time. Basically, SHO can be utilized

by any wireless technology, however it might be very costly and it is worth mentioning that the support for SHO may not be good for specific wireless technologies. SHO is used only in CDMA [33].

2.2.1 Handover Prerequisites

Both the QoS and the network capacity can be affected by the HO. As a result, there are a couple of points which should be taken into account to alleviate any adverse effects of the HO scheme. These features can be summarized as follows:

- The delay incurred during the HO should be very short. The HO should be transient in order to keep the HO process transparent to the UE so that it cannot perceive any service deterioration or connection disruption during the HO operation [33].
- For a specific itinerary of a UE, the number of HO attempts should be kept to a minimum and the percentage of successful HOs to the number of HO trials should be maximized [33].
- CDP and CBP should be minimized, so that the effect on the QoS is minimal [33].
- The negotiated signalling messages associated with the HO process should also be minimized [33].

To realize these prerequisites, designers should consider factors which affect the HO scheme and these are as follows:

- Wireless technology: The wireless technology utilized will determine the cell footprint, cell architecture, and the traffic model. Multiple wireless technologies might be utilized simultaneously, which results in new prerequisites for HO procedures that occur between different wireless technologies, that is, vertical HO [33].
- Cell footprint: The cellular footprint decides the HO rate due to the cell coverage area. Cell size can be described in a descending order as follows: umbrella-cell, macro-cell, micro-cell, pico-cell and femto-cell. The smaller the cell, the more frequent the HO and the stricter the time constraint will be for a given itinerary [33].

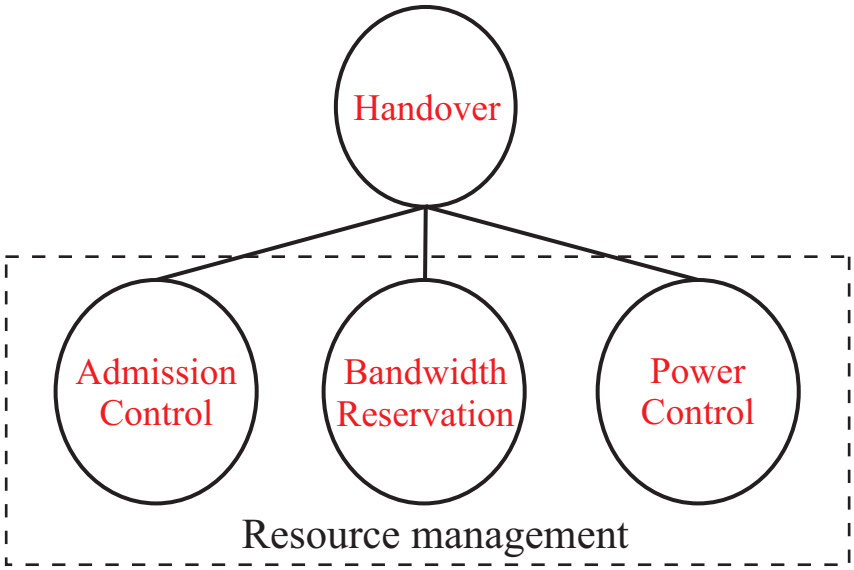

Figure 2.2: Handover and Resources Management

- System topology: Topology, with antenna positions being one example, is a crucial factor in the design of a wireless system, and this in conjunction with the UE's itinerary controls HO performance [33].

- User's mobility speed: The speed and direction of the UE plays an important role in the HO process. Namely, as the UE moves faster, the time for a HO becomes shorter given a fixed overlapping area length. Thus, the HO scheme should consider this effect [33].

- QoS: QoS evaluating parameters can be used to indicate the need to trigger a HO when it reaches a specific preconfigured threshold, such as the bit error rate (BER), packet loss, throughput, etc. A HO is requested to preserve the QoS by camping on a new BS which can guarantee the QoS [33].

2.2.2 Handover and Resources Management

Wireless resources, such as channel frequency, time slots, transmission power, and battery energy can assist in reducing the probability of a HO failure (HOF) and maintaining the required QoS during and after the HO. If the target BS has a radio resource shortage, then it is impractical to preserve the QoS parameters and, as a result, the call might be dropped

after the HO. Therefore, to avoid this situation, some resource management should be considered, such as admission control, bandwidth (BW) reservation, and power control, as illustrated in Fig. 2.2. In admission control, new calls can be managed differently from an ongoing call, and this can prevent the network from being overloaded. For example, new calls might be queued and HO requests might be prioritized. Requirements from UE and applications, channel state information, MAC protocol and scheduling policy are the information required for admission control. Furthermore, admission control can be either centralized or distributed. If there is a BW reservation or a free channel, a HO request can be admitted. Hence, an easy solution is to preserve part of the cell BW in order for it to be used for HO purposes only. Yet, a careful balance which maintains the maximum BW utilization and suppresses the maximum failure rate of the incoming HOs under an acceptable level should be considered. This is due to the fact that the BW is a scarce and precious resource to wireless communication systems. In this context, complete sharing and complete partitioning are schemes proposed to dynamically control the BW resource allocation. In the former scheme, all data traffic tiers share the whole BW, while in the latter scheme, the BW is partitioned into a specific portion, with each corresponding to a particular traffic type [36].

Power control is a fundamental scheme in mobile wireless communication systems due to its vital role in spectrum allocation, resource allocation, battery life, and safety. Power control schemes can be either centralized or distributed. Power can also be used as a parameter of the input measurement, which is used to assist in performing the HO decision especially in vertical HO between a UMTS and other systems [37].

2.2.3 Handover Schemes

HO schemes can be divided into two types according to the HO criteria employed.

1. Traditional HO schemes are schemes that depend on the RSS/RSQ, distance, speed, and power budget.

2. Intelligent HO schemes are schemes that depend on artificial intelligence technologies, e.g. fuzzy logic, prediction, and neural networks [33].

2.2.3.1 Traditional Handover Schemes

In this approach, the RSSs of the neighbouring evolved Node Base stations (eNBs) are measured continuously and a HO is executed with the eNB that has the highest RSS. Whenever the UE reaches a point at which the RSS of the serving eNB starts to recede compared with the RSS of the target eNB, the UE then should be handed over to the target eNB. In case the RSS of the serving eNB increases to be stronger than the RSS of the target eNB, the UE will be handed over to the original serving eNB. This happens either due to the multipath effect or the user is being moved along the edge of another cell or multiple adjacent cells, which might cause a fluctuated RSS. As a result, the HO process might be repeated with either eNB a couple of times. Consequently, this results in what is known as the ping-pong phenomena, where all the HOs performed are unnecessary. These redundant HOs increase the call failure probability during the HO. The ping-pong problem also increases the network load, so to avoid this issue several HO techniques have been proposed, such as the RSS with a threshold, the RSS with hysteresis and the RSS with a threshold and hysteresis. Traditional HO schemes can be divided into the following:

1. RSS with a Threshold Schemes

   The HO is triggered if and only if the target eNB becomes better than a specific threshold, or the RSS of the serving eNB is worse than a threshold and the target eNB is better than that of the serving eNB. The problem with this approach is to find a suitable threshold value. For example, when the threshold is too low in the second case, the link might be disrupted, while, if the threshold is too high, this might result in a ping-pong scenario [38].

2. RSS with Hysteresis Schemes

   The HO is requested if the target eNB is better than the RSS of the serving eNB by a hysteresis h value. This technique might eliminate the ping-pong effect however again the same problem might arise, i.e. to find a suitable/optimal hysteresis value. In case h is too high, the RSS of the serving eNB might drop to a very low level and

the link might consequently be dropped. If h is too low, HO might happen early whilst the RSS of the serving eNB is still of a good quality [33].

3. RSS with a Threshold and Hysteresis

   In this approach, both a threshold and hysteresis are used to reduce the number of HOs. Therefore, a HO is requested only if the RSS of the serving eNB is lower than a threshold value and the RSS of the target eNB is better than the RSS of the serving eNB by a hysteresis value [39]. This approach is utilized in GSM technology [33].

4. Signal to Interference (SIR) Schemes

   SIR is considered as a metric which reflects the quality of the communication. In this scheme, a HO is triggered if the SIR of the serving eNB is worse than a threshold and the SIR of the target is better. However, this approach results in cell dragging which takes place when a UE is moving at low-speed away from the serving eNB. As a result, the serving eNB does not realize it due to the strong average signal. This method might also prevent HOs near geographical cell boundaries [5].

5. Velocity Schemes

   Call dropping probability increases as the UE speed increases due to excessive HO delay. As a result, this approach was proposed to deal independently with each UE according to its speed. Since each UE might have a different speed, an adaptive threshold was proposed to deal with this issue. For instance, the UE that has a higher speed will be assigned a lower threshold compared with the UE that has a lower speed, as the UE with the lower speed needs more time to traverse the same overlapping area [33].

6. Direction-Biased Schemes

   This approach is significant for high-speed UE specifically in a non-line-of-sight (NLOS) scenario [33]. This method can enhance the handover performance not only by minimizing the number of HOs, but also by lowering HO latency [3]. In such schemes, the direction information can be exploited to expedite the HO process towards a certain target and also can be used to prevent the ping-pong effect by handing over to the same serving cell, thereby reducing the number of handovers.

2.2.3.2 Artificial Intelligence Schemes

In terms of the artificial intelligence HO schemes, we discuss two main types:

1. Pattern recognition schemes: in this type of scheme, the RSS measurements are taken from the surrounding eNBs. If the current measurements match the pattern in terms of the RSS values and their location to those of the pattern, then a HO is performed in a speedy fashion. This method decreases the ping-pong effect and HO latency especially for the HO decision phase. Nonetheless, choosing an appropriate threshold and hysteresis is still an issue [33].

2. Prediction schemes: these methods use the prediction of a certain HO criteria to trigger a HO process, i.e. the RSS. For example, grey prediction methods can be used to predict the next RSS so that the HO can be triggered earlier. As a result, this method can reduce the HO rate and HO latency [5].

2.2.4 Handover Scheme Evaluation Metrics

Each HO scheme can be evaluated using conventional HO metrics and some of these are discussed below.

- HO triggering input factors are RSS, SIR, BER, speed, and motion direction. Usually the traditional HO scheme uses one or two factors only. More might be used in the case of intelligent HO schemes [33].

- The HO rate can be defined as the number of HOs in a given period of time. The HO rate can be decreased by utilizing hysteresis [33]. Speed and direction can also be used to reduce the HO rate and HO latency [3].

- The ping-pong effect: although this effect can be alleviated using the threshold and hysteresis value, using a small hysteresis value will result in a rise in the ping-pong effect again. However, if the hysteresis value is high, this leads to an increased HO delay [33].

- HO latency is a crucial metric used to analyse the HO scheme [40]. Traditionally, the delay is high if a higher value is allocated to hysteresis in order to reduce the ping-pong effect [33].
- A redundant HO is a metric highly correlated with the ping-pong effect, and similarly to the ping-pong effect, this effect can be avoided using the hysteresis value [33].
- Other metrics, such as interruption time, call dropping probability/HO failure probability, HO blocking probability, and HO signalling size will not be discussed further in this section [33].

2.3 Distributed Antenna System Architecture

Broadband mobile transmission traffic demands are increasing rapidly. Based on [41], their growth is expected to be 13-fold from 2012 to 2017, with mobile phones and tablets being the main reason for this increase. Thus, to meet these ever-increasing demands, operators will have to enlarge the system capacity. This can be achieved via either increasing cell density or by adopting certain techniques, such as MIMO [42] or the more recent massive MIMO (MMIMO) [43], where a massive number of antennas can be employed to serve a number of users using the same time-frequency resource. Nonetheless, this technique also results in an increase in the inter-cell interference level and the deployment cost. Also, increasing the BSs density is not a viable solution, since CAPEX and OPEX increases substantially as the BS density increases. Thence, the idea of a distributed antenna system (DAS) where a large number of remote antenna units (RAUs) are linked to a central unit (CU)/baseband processing pool becomes a necessity. In this architecture, the expensive baseband processing unit (BBU) is shared by a large number of RAUs, thereby reducing the cost and energy consumption compared with traditional architecture.

This type of network can be easily upgraded and maintained due to its distinct advantage of being centralized. Another advantage for BBU centralization is the low interaction latency between these elements. This low latency makes recent technologies, such as the enhanced inter-cell interference (eICIC) [44, 45] and the coordinated multi-point

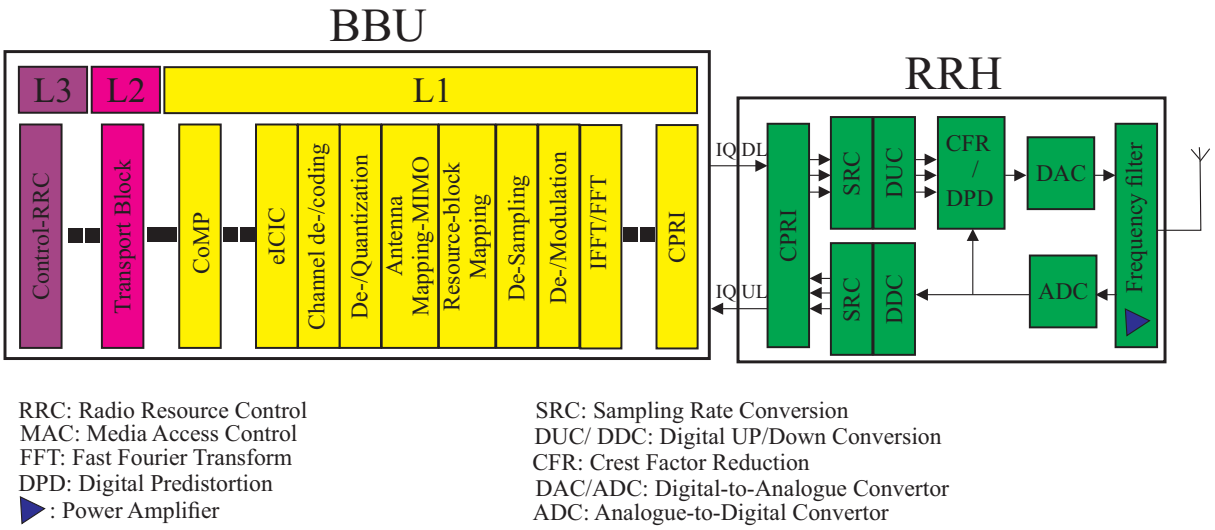

Figure 2.3: DAS architecture entities and their functionalities (adapted from [1]).

(COMP) [46] easier and more efficient to implement. Load balancing techniques will also become more efficient in this particular architecture. Furthermore, the intra-BBU pool HO is greatly simplified and therefore reduces HO latency. This architecture is one of the most important milestones in achieving the 5th generation (5G) mobile network by 2020. Other approaches include small cells [47] and MMIMO. More specifically, small cells are one of the most promising solutions for both outdoor hot-spot and indoor scenarios. Deploying small cells result in network and wireless resources being underutilized especially during off-peak periods. In addition, the feature of collaboration and cooperation will be lost compared with DAS. Moreover, small cells can be more difficult to upgrade and maintain than DAS [1].

2.3.1 Centralized Radio Access Network

In this type of architecture, the BS is detached into a radio module and a signal processing module as shown in Fig. 2.3. The radio module is known as the remote radio head (RRH), the remote radio unit (RRU) or the remote antenna unit (RAU). RAU offers the interface to the fibre, conducts digital processing, digital to analogue conversion (DAC), analogue to digital conversion (ADC), amplification, and filtering [48]. The signal processing module is called the baseband unit (BBU) and it is where all signal processing is performed [49]. The RAU and BBU separation distance can reach 40 km, and the main reason behind

this limitation is the processing and propagation latencies [1]. Both optical fibre and microwave links can be used to link RAU to BBU. BBU contains all the processing units in the same place which makes it easier to maintain compared with traditional architecture in which the BBU needs to be in the proximity of the antenna. In this architecture, RAU can be constructed on poles or rooftops. Analogous to the traditional architecture, RAUs are allocated to a BBU, so that each BBU can serve a large number of RAUs [1].

2.3.2 Centralized Unit

To improve the resource utilization of BBUs, some of which can be highly loaded and some lightly loaded, they are centrally located in the same entity, which is known as the BBU pool, the centralized unit, the central unit, or the control unit. The pooled resources are divided among the cell sites. Furthermore, the BBU is a universal purposes processes utilized to carry out baseband PHY/MAC processing. Therefore, each pool is a virtual cluster linked to the neighbouring cluster through an X2 interface. In general, a central unit (CU) can also be known as a cloud, co-operative radio, collaborative or clean radio network. Moreover, all the components which lie between the RAU unit and the BBU pool are known as the fronthaul while the backhaul links the BBU pool with the core network. RAUs are linked to the CU via a low latency high BW optical link. Digital baseband (IQ samples) are transmitted between the RAU and the CU [1].

2.3.3 Merits of DAS

Both macro cell and small cell distribution can benefit from CU/C-RAN architecture. For macro cell distribution, a CU permits effective utilization of the BBUs and decreases the BS's installation and operation expenditure. Furthermore, the CU can decrease power consumption and can use COMP and interference cancellation techniques more effectively. CU can also provide the high computational processing power required by many users. Furthermore, coverage expansion can be easily achieved by deploying an RAU linked to the already deployed BBU pool/CU [1]. In order to improve network capacity, deployed cells can be sectored or more RAUs can be deployed. In case the overall capacity needs to be increased, this can be fulfilled by upgrading the CU/BBU pool, either by installing

more BBUs or replacing the current BBUs with more powerful units. Another advantage is load balancing on both the CU and RAU. On the CU side, BBUs existing in the same entity can easily achieve load balancing by a suitable resource allocation among the BBUs. On the RAU side, load balancing can be attained by switching users among cells with no constraints if there is an enough capacity to serve them in the pool, as the CU is responsible for allocating capacity dynamically [50]. Some of the advantages of DAS architecture compared with other system architecture are discussed below.

- More Throughput, Less Latency

  One of the most prominent technology options to be widely employed with DAS is LTE technology and its successor LTE-A [51]. Integrating LTE technology with DAS architecture has several advantages. First, since all the BBUs exist in the same entity, LTE features such as the enhanced inter-cell interference (eICIC) and COMP can be greatly facilitated. This simplifies the implementation and decreases processing and transmission latencies. LTE uses a scheduler in the BS (eNB) which is responsible for resource assignment. LTE uses OFDMA as the access scheme [52]. In this scheme, a large number of densely spaced orthogonal carriers can be dynamically assigned in frequency and time domain, which provides a very flexible exploitation of the resources available. In LTE, generally, a frequency reuse factor of 1 is employed, which means that all cells use the same frequency. Therefore, inter-cell interference is relatively high in LTE. Thus, the peak throughput to edge throughput ratio is very high. Addressing the interference issue can be achieved either by minimizing inter-cell interference or by utilizing the interference path constructively and these approaches are discussed below.

1. Minimizing Inter-cell Interference

   Two main approaches are used to preclude inter-cell interference either statically or dynamically in time, frequency, and power domain. The statistical approach is to use different frequency channels in neighbouring cells. This is known as hard frequency reuse, which can eliminate X2 signalling almost entirely. In addition, fractional frequency reuse can be used [53]. However, since spectrum resources are very scarce and precious it is better to utilize other approaches which do not implicate frequency

reuse. In LTE, the inter-cell interference coordination (ICIC) [54] technique was introduced. It can be used in case the UE undergoes a high interference level on specific subcarriers and if this occurs, the UEs can report back to the eNB. Then the eNB can cooperate with the neighbouring cell via the X2 interface to avoid using those subcarriers for this particular UE. It should be noted that this approach can be utilized for cell edge users only, whereas for users at the cell centre where there is no interference, the full resources can be exploited. Therefore, this approach is easy to implement and needs no synchronization of BSs, as only load and scheduling information is required to be negotiated. Considering neighbour cell interference by the scheduler can result in less optimal scheduling decisions being made. However, since the control channels work on fixed resources, these channels can interfere again. This approach is slow enough to work seamlessly on systems with distributed BS deployment. Enhanced inter-cell interference coordination (eICIC) was recently introduced; the main idea of this scheme is to mute a certain subframe so that the subframe will be an interference-free time interval which can be utilized to transmit crucial information, e.g. signalling or reference signals. Furthermore, the power domain can be utilized to avoid interference issues too. These approaches are mainly used in the UL direction in HetNet scenarios. The idea is to dynamically manage the transmission power of the users and therefore control interference between the pico and the micro cells [1].

2. Exploiting the Interference Path Constructively

   Currently, COMP is considered as the most advanced approach to deal with inter-cell interference. COMP is based on the key idea of converting interference into a beneficial signal. As a result, the signal-to-interference plus noise (SINR) ratio increases on the user's side which can result in better bit rates [55–57]. In this scheme, a group of cells, which is called the COMP-set, collaborate on serving one or more of the users by employing feedback from the user(s). In the DL part, this demands a strict synchronization and coordination among the COMP-set entities. In this scheme, a particular user receives transmission from the serving eNB, whereas the rest of the COMP-set assists in minimising interference. This can be achieved by

abandoning the use of specific subcarriers, i.e. coordinated scheduling (CS) and/or employing special, e.g., beamforming, antennas, i.e. coordinated beamforming (CB) [58]. Hence, in this scheme, all the cells in the COMP-set together determine how to carry out scheduling and beamforming to try to reduce interference for all the users. Both CS and CB techniques need BS synchronization similar to LTE, since only one BS is able to transmit to one user at a time. The dynamic cell selection (DCS) scheme [59], which is an expansion of CS/CB, can be also used. In this method, the data needed to be sent to a specific user is made available for the COMP-set entities. Only one eNB is permitted to transmit at any given time, yet the entities coordinate on which should carry out the transmission. This is beneficial since the transmission can be performed from the eNB that has the best channel to the user. This scheme also requires synchronization [1].

Joint transmission (JT) [60, 61] is another type of COMP but it is a more advanced version. In this version, several eNBs jointly and simultaneously transmit to the same user, and again the data will be made available for all the COMP-set entities. JT depends on very timely and accurate feedback from the mobile on the property of the combined channel from several BSs. To achieve this, a new set of channel state information (CSI) reference signals was developed and integrated into the standard [1]. For one user of JT, a couple of cells transmit the same information to the same mobile. Thus, in contrast to ICIC where we mute resources, the JT transmits the same signal from several BSs at the same time to permit the signals to be estimated simultaneously at the receiver and hence obtain a better SINR. The drawback of this method is the resource consumption of several eNBs that effectively produces a reuse factor of 1/3 [1]. Therefore, this approach suits lightly loaded systems. In the case of a highly loaded system, JT can be used for multi-user JT, where a couple of users share the same time-frequency resources. This is actually a combination of multi-user MIMO and JT [1]. This scheme also requires a tight BS synchronization. From the techniques discussed above we note that all of them need tight timing which can be easily achieved using centralized architecture [1]. For example, if the COMP-set belongs to the same BBU pool, then this could enable

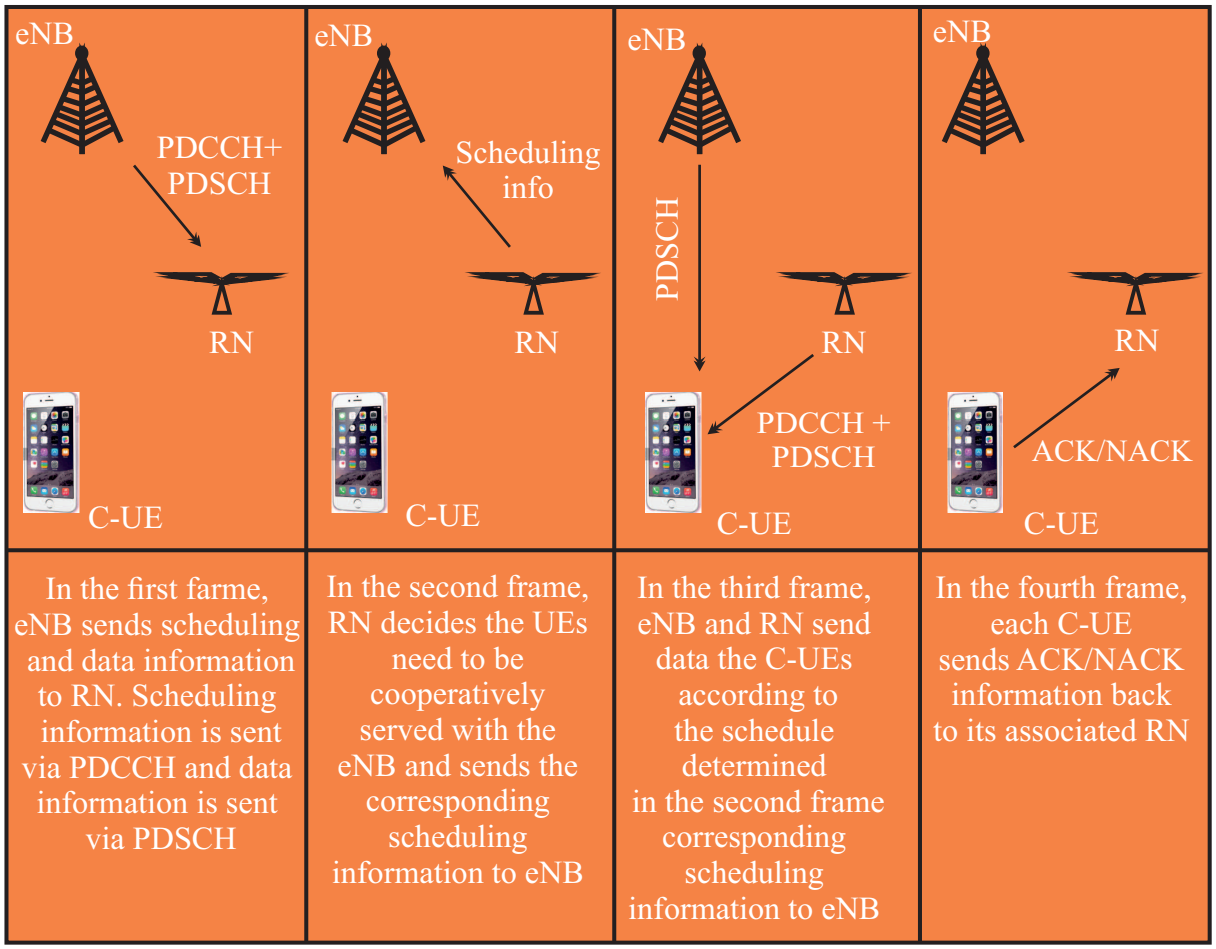

Figure 2.4: COMP scheme for intra-cell scenario (adapted from [2]).

a tighter interaction between the set. Thus, the interference level can be reduced so that the throughput can be enhanced. Moreover, multi-cell MIMO [62] can be improved using centralized architecture due to the tighter cooperation among BSs within the CU [1].

3. Lower Latency

   Since a large number of RAUs can belong to the same CU, then the time needed to carry out HO is considerably reduced as it is performed inside the same BBU pool/CU instead of between eNBs [1].

2.4 Relay Node

Cooperative communication permits the UEs in a network to listen and assist in data transmission to each other. Potential approaches of achieving cooperation include using a relay node to help the communication nodes in a network to assist each other to communicate with their associated destinations. LTE release 10 has adopted cooperative communication as a vital technology for the forthcoming generations of wireless communication systems. A relay network (RN) assists in overcoming obstacles and enhances capacity by reducing the distance, reducing the cost compared with BS, improving power and spectrum efficiency, and enhancing communication reliability, but at a cost of increasing the delay. In this system, initially the source sends its data to the corresponding RN. The RN will transmit the data recovered to the destination after processing it, following a certain cooperation protocol. Then, the destination decodes the data received, which had been transmitted from the corresponding transmitter via the RN [2, 63–65].

Basically, there are three types of cooperation protocol: amplify and forward (AF) [66], decode and forward (DF) [67] and compress and forward (CF) [68]. In the AF protocol, once the RN recovers the signal it scales it to the RN's power constraint and then forwards the scaled message to the destination in the following transmission slot. In the DF case however, the RN firstly decodes the message received, secondly re-encodes it into a new code word, and thirdly sends it in the following transmission slot. In the CF case, the RN maps its recovered message into another message in a decreased signal space, and then encodes and forwards the compressed signal as a new code word by considering the message recovered at the destination as side information. Protocol performance in terms of capacity or diversity may vary depending on the network architecture/topology and the quality of the backhaul connection between the RN and the source. However, generally for a system with a good backhaul link, DF outperforms the others, while for a system with a poor backhaul link, AF or CF are more advantageous [2]. There are three types of relay: fixed, nomadic (special events indoors), and mobile relays (in trains, as we will see in the forthcoming chapters) [69]. An example of relaying scenario is shown in Fig. 2.4.

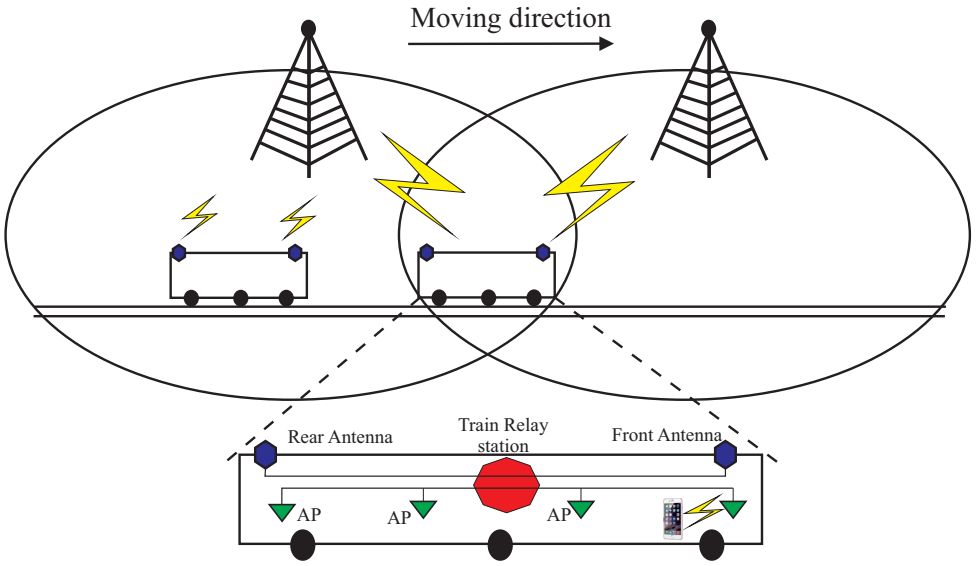

Figure 2.5: The dual link System architecture solution used to enhance the system performance during HO (adapted from [3]).

2.5 An Overview of Handover Schemes for High-Speed Railway

The authors of [3] proposed a seamless HO scheme utilizing two-hop dual-link architecture for HSR. In this scheme, two antennas were used, one was located at the front of the train and the other at the rear. The front antenna performs the HO scheme with the target cell, while the rear antenna keeps the link with the serving cell. If the front antenna performs HO successfully, the rear antenna then switches its frequency according to that employed by the target cell. As a result, the communication link is not disrupted during the HO process. However, if the front antenna fails to HO successfully, the rear antenna has to perform HO again and disruption is inevitable. Moreover, the scheme employs the concept of bi-casting to reduce the latency and the signalling overhead associated with data forwarding from the serving cell to the target cell. However, this requires modifications to the standard HO process mainly in two aspects. Firstly, mobility management entity (MME) requires the maintenance of two different sets of links that connect information about both the mobile relay's (MR) antenna concurrently since the MR may link with both the serving cell and target cell during the HO process. Secondly, the serving gateway (S-GW) should also maintain two forwarding paths within its routing table in order to

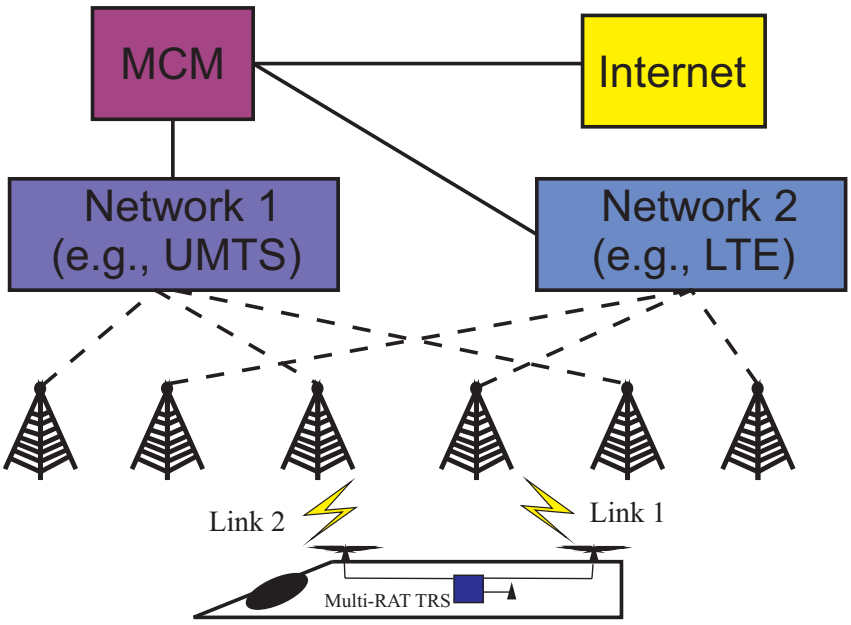

Figure 2.6: System architecture associated with multiple access technology solution to alleviate the recurrent HO problem in HSR (adapted from [4]).

support bi-casting.

The authors of [39] presented an enhanced scheme of the above paper by proposing a new algorithm to achieve an optimal chance for performing HO and therefore avoid early and/or late HO triggering and the unneeded bi-casting when the train reaches a new BS. This could be achieved not only by considering the RSS of the front antenna but also by considering the RSS of the rear antenna. Therefore, the optimized scheme is different from the original concept as the former employs predefined triggering conditions/metrics. Moreover, the optimized scheme provides a better probability of success for the front antenna by assuming almost unlimited retransmission trials. Furthermore, the shortcomings of the original concept still apply to the optimized scheme. Fig. 2.5 shows the system architecture of the dual-link architecture. In [4], a dual link HO is proposed to solve the frequent interruption issue in HSR due to the frequent occurrence of HO. In this scheme, multiple radio access technologies are considered to alleviate the HO issue. A train's MR is assumed to be linked simultaneously to more than one heterogeneous network, e.g. LTE and UMTS. Maintaining more than one link to the HSR at the same time will support a seamless handover as the MR can be connected to another technology while it is performing the HO process using the current technology. Utilizing more than

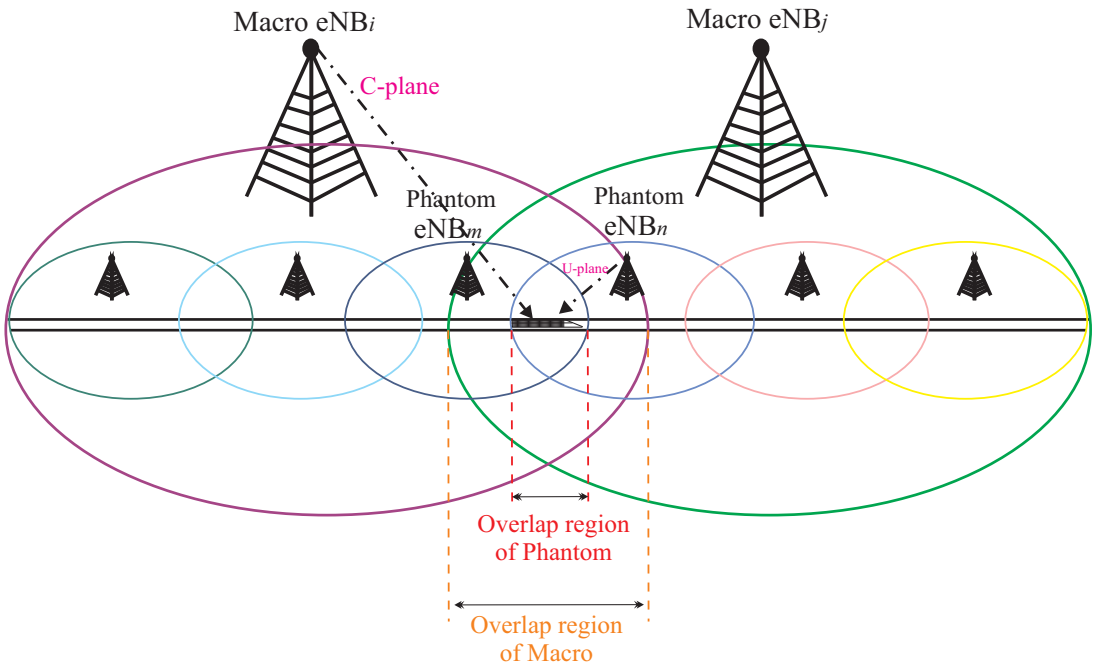

Figure 2.7: System architecture of control/user plane splitting solution under HetNet for HSR (adapted from [5]).

one technology simultaneously also enhances performance by reducing the probability of failure. The system architecture is shown in Fig. 2.6.

With the aim of providing higher system capacity, better transmission reliability, and less co-channel interference for passengers on board a high-speed train, [5] has proposed a decoupled control/user (c/u) plane split architecture for HSR as shown in Fig. 2.7. In this scheme, the c-plane is controlled by the macro eNB utilizing a lower frequency band which provides superior reliability for the control information, while the required capacity for the users on board is supported using a higher frequency band provided by a phantom eNB. Both the control zone signalling and L1/L2/L3 signalling, which belongs to the data zone of the LTE downlink subframe, are part of the c-plane information. Due to its important role in establishing and maintaining communication, the data zones signalling will be supported by the macro eNB to guarantee better reliability. However, this approach's main disadvantages are associated with modifying LTE standard specifications and protocol, such as frame structure, protocol split, and the measurement procedure. This approach further incurs a large signalling overhead due to HO processes associated with intra-macro-cell HO (phantom-to-phantom HO) and inter-macro-cell HO (macro-to-

macro HO). This approach also increases the burden on the macro-cell as the number of controlled cells increases due to the increment of the associated control signalling. Furthermore, it increases the HO latency, connection density, and traffic volume. In addition, inter-macro-cell HO includes both macro-to-macro and phantom-to-phantom handovers resulting in a heavy signalling overhead which might lead to failure at any point during the HO process [70, 71].

In this context, [6] proposed a c/u-plane split architecture in which the small cells are deployed so that the overlapping area between two successive macro-cells contains a small cell as shown in Fig. 2.8. Thereby, the cell edge of the macro-cell is no longer the cell edge of the small cell. As a result, inter-macro-cell HO will not include any small-cell HO. Therefore, there will not be any u-plane interruption during the c-plane HO. On the other hand, and by exploiting this architecture, the u-plane HO will not include any c-plane HO as the small-cell edge will be within the macro-cell coverage area. Consequently, the u-plane HO is simplified to the conventional intra-eNB HO. Therefore, c-plane and u-plane handovers are separated. Furthermore, to achieve a fast and seamless u-plane HO, COMP and bi-casting techniques were used to avoid interruption. However, using these techniques might avoid interruption but at the cost of increasing the in-network signalling overhead which again means a standard modification, less throughput, and more wasted network resources.

Furthermore, [7] proposed a scheme for an enhanced measurement procedure and a group of in-network HO procedures. The scheme utilizes a control mobile relay (CMR) at the front of the train to represent other general MRs during the HO. The general MRs are allocated along the train carriages and are used to serve UEs on board. Thereby, the CMR is used to carry out the proposed scheme. The enhanced measurement procedure is performed by inferring the train's current location and whether it is approaching the neighbouring eNB. This can be fulfilled through employing either a quality-based scheme or a Doppler-based scheme. In the former, the CMR measures and records the signal quality values obtained from the target eNB in a vector. If the vector values have an ascending order, then the CMR decides that the train is approaching some neighbouring eNB. Once detected, the CMR issues a measurement report to start the HO procedure. In

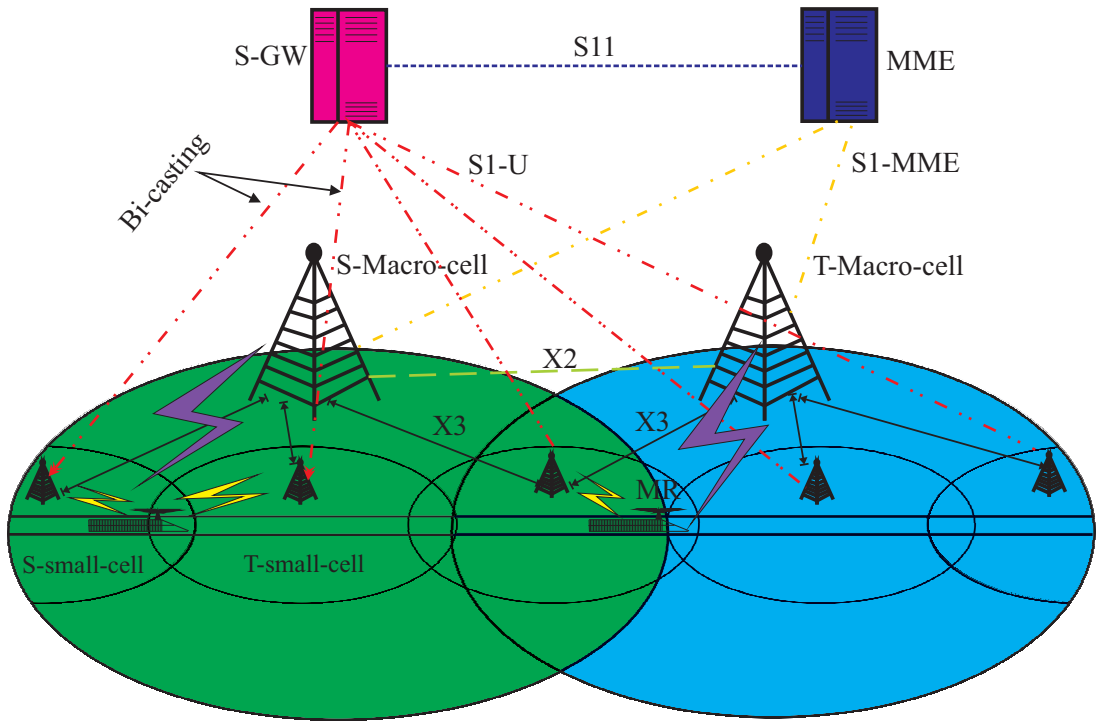

Figure 2.8: A novel system architecture associated with the control/user plane splitting architecture under HetNet for HSR, in which the overlapping area of the Macro and the Micro cell do not have the same overlapping area, thus reducing the HO burden on the network (adapted from [6]).

the latter, the CMR observes the frequency variation of the signal received from the target eNB by following the Doppler shift characteristics. The train is said to be approaching the target eNB if the frequency received is higher than the radiated frequency, and the frequency received remains the same or slightly decreases; the frequency received might increase when the train is accelerating. If this condition holds then the CMR sends a measurement report back to the serving eNB. The enhanced in-network procedures are performed by triggering the in-network signalling right after triggering the HO command. This scheme, therefore, focuses on reducing the handover procedure time. The system architecture of this approach is depicted in Fig. 2.9.

A system architecture based on a network mobility protocol has been proposed in [8] as shown in Fig. 2.10 for the high-speed trains. In this architecture, an enhance femto-cell (HeNB) has two antennas distributed on the front and rear of a train. The enhanced HeNB egress interface has dual links to support a better signal quality which ensures a seamless HO. Different MME and S-GW entities are identified to handle the onboard

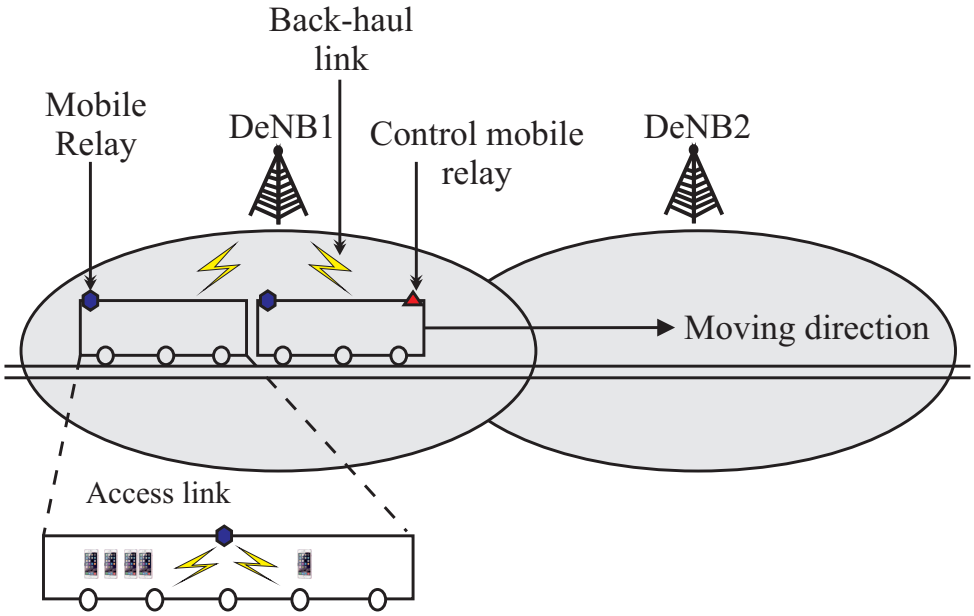

Figure 2.9: System architecture associated with a proposed control MR in front of the train used to represent other MR during the HO process (adapted from [7]).

UEs and the HeNB mobility events separately. One IP address is assigned to the egress interface which is utilized by the enhanced HeNB to link to the corresponding MME and S-GW, while the other MME and S-GW set identifies the enhanced HeNB by its ID, e.g. the international mobile subscriber identity (IMSI) or the temporary mobile subscriber identity (TMSI), and forwards its information data to the serving eNB using its ID. Furthermore, the proposed scheme adds another criterion when determining the need for HO by sending the candidate eNBs via the measurement report. Then, the serving eNB checks if one of the targets has a high RSSI in the same IP domain, and if so it is selected as the target eNB, therefore prioritizing the eNB which is in the same eNB IP domain. This avoids the high interruption time associated with handoff to a target eNB which is not in the same IP address domain. Moreover, in [9], a beamforming technique is employed to adjust the power strength and corresponding signal-to-noise ratio of the onboard transceiver according to the train's current location so that the SNR can be enhanced when the train is about to handover; more specifically in the overlapping area, beamforming can enhance cell coverage. As a result, HO performance can be improved by enhancing the probability of success. The system model is shown in Fig. 2.11.

Communication-based train control (CBTC) is a crucial part of the HSR wireless

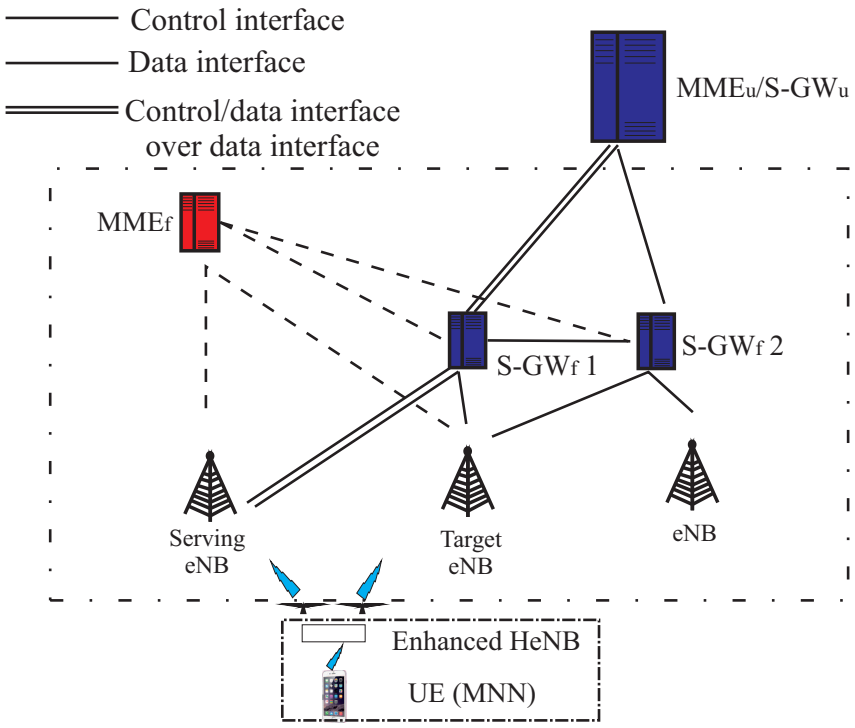

Figure 2.10: System architecture associated with femtocell-based multiple egress network interfaces solution for HO in HSR scenario (adapted from [8]).

communication system to ensure the safety of railways using data communication. It has strict communication latency and reliability requirements. Based on this, [72] has proposed a HO scheme based on MIMO technology. The scheme utilized a wireless local area network (WLAN) approach because of its wide availability. Furthermore, the author has considered the channel estimation error effect along with the MIMO working mode to enhance HO latency performance. Furthermore, [73] has also proposed a MIMO-assisted HO with the aim of reducing HO latency for a CBTC system. In this scheme, during the HO process, one antenna is linked to the serving AP exchanging data packets, while the other antenna is exchanging the HO signalling so that the onboard transmission will not be interrupted during the HO procedure. Zero forcing and the space-time block code are employed to cancel interference from UL and DL, respectively. The result shows that the proposed scheme can optimize HO latency. Location-based triggering is utilized to replace the traditional signal strength-based triggering criteria so that the ping-pong effect can be eliminated.

A COMP soft HO scheme for LTE was proposed in [74] to enhance the conventional

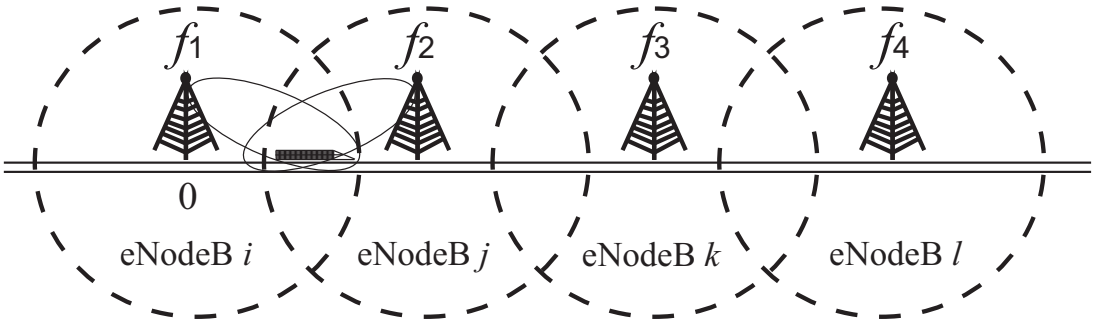

Figure 2.11: System model associated with the beamforming solution which enhances the received signal quality and as a result enhances the overall system performance (adapted from [9]).

HHO performance. Also, a dual-link for the onboard MR was considered, located on both the front and rear carriages of the train. Once the front antenna enters the overlapping area, the source eNB commences the cooperative transmission set (CTS) consisting of the serving eNB and the target eNB. Both eNBs communicate concurrently with the MR forming the CTS. Commencing the CTS depends on the measurement report and the position information provided by the CTBC system. Employing the COMP technique results in both eNBs sending data information to the train's MR. Once the HO predefined condition is satisfied, the c-plane is switched from the serving to the target while the u-plane is still linked to the eNBs which avoids an interruption delay due to the current HHO. Once the HO procedure is finished, the target eNB kicks the source eNB from the formed sets. The results show a better performance in terms of the probability of outage and a successful HO.

2.6 Frequency Switch Scheme Related Literature

HO schemes can be optimized via designing a suitable network architecture. In this context, a virtual cellular network (VCN) was proposed in [75, 76] to avoid the traditional HO. In this architecture, a single frequency network is utilized by deploying a distributed access point (AP), which replaces the traditional BS, to construct an adaptive wireless infrastructure in which a simple antenna, referred to as a port, is deployed within the VCN; this is defined as the coverage area in which the UE transmission can be captured successfully by a port. These ports are linked to and controlled by a port server (PS). More

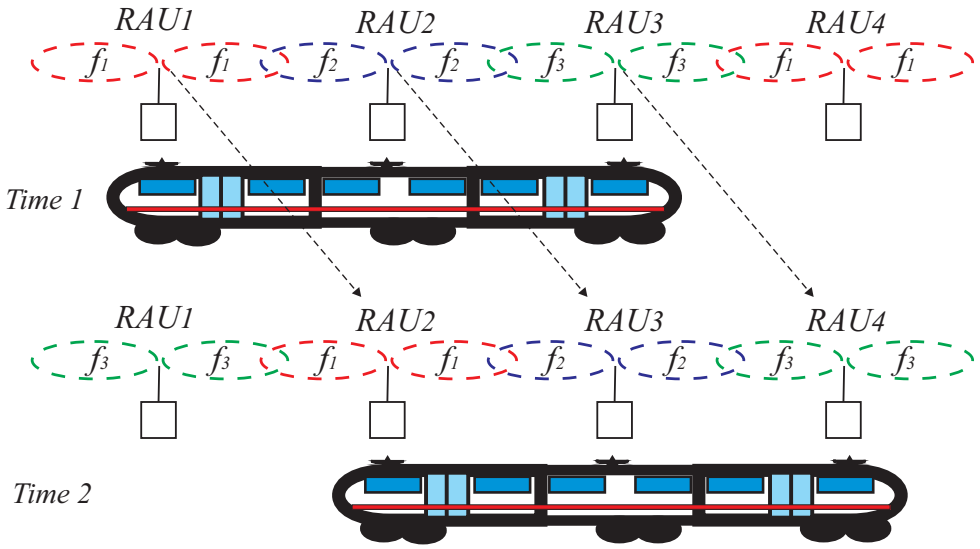

Figure 2.12: Moving frequency concept proposed to alleviate the frequent HO issue for CU (adapted from [10]).

specifically, a VCN is dynamically constructed according to the UE's current location. Therefore, the data stream intended for a UE is dynamically conveyed via the PS to all ports within the VCN. Consequently, the routing table should be updated continuously to keep track of each UE within the network. In this way, the traditional HO can be eliminated thanks to the single frequency channel utilized and the dynamic formed VCN. However, this approach has two main drawbacks. First, one frequency band is shared by a large number of users and, second, a large traffic overhead is needed to handle the ports dynamically.

Moreover, the concept of an extended cell (EC) was proposed in [77]. A group of adjacent cells are dynamically aggregated to form an EC. Thus, the aggregated cells transmit the same data over the same frequency channel. OFDM can also be utilized to alleviate the multipath and shadowing effect on the network. In this network, the HO region is the overlapping area separating two neighbouring ECs. The simulation results depict that this approach can decrease the HO rate and the probability of call dropping by 70% compared with the no EC case. However, challenges such as connectivity, mobility, self-configuration, and cognitive radio still need to be addressed. Furthermore, [21] proposed the concept of the moving cell (MC) to avoid HO in a high-speed railway scenario where the train's speed can reach 100 m/s and a cell footprint is approximately 100 m, which makes the HO rate very high. The MC is based on the physical moving

cell concept presented in [78]. The MC is a group of moving cells which follow/pursue the train's movement. Each cell changes its frequency dynamically according to its own train location so that the trackside cells can be communicating using the same frequency channel during the whole train journey as shown in Fig. 2.12. Therefore, this scheme reduces the HO rate and latency compared with the traditional HO scheme. This scheme takes the merits of RoF technology and marries them to special characteristics of the HSR where the onboard UE moves together at the same speed and in the same direction as we will see more in the following chapters.

A moving extended cell concept was proposed in [79] which is a mix of EC and MC and virtual zone concepts. This scheme can be easily implemented by taking advantage of using RoF technology. More specifically, each UE is covered by a number of cells radiating the same frequency, and these cells move together with the UE and are grouped using the EC concept. The simulation results show that the proposed scheme can realize zero CDP and packet loss for a speed of 40m/s.

2.7 Summary

To this end, the mobility management, more specifically, the HO is one crucial aspect that should be thoroughly studied. In this chapter, we have presented a general overview about the design and the prerequisites needed to propose a suitable HO scheme when moving among cells. Moreover, the evolution of multi-technologies has left us with multiple candidate system architecture either of them can be the best to employ depending on each communication system scenario requirements and characteristics. For example, by employing the C-RAN system architecture, a large number of small RAU cells can be controlled by the same CU. Each CU can include BBU pool. Thereby, the required capacity of the HSR's large number of users can be easily satisfied, so that C-RAN can support the required throughput upgrade in comparison to the usual capacity supported by the traditional BS. This boosting in throughput is also due to the interference management approaches which can be offered using this particular architecture, as explored beforehand, compared with the traditional architecture capability. Further, less HO time

is needed since the HO happens within the same BBU pool (in case each BBU is statically allocated to a group of RAUs) compared with the case of performing HO between two separate eNBs. To support seamless mobility over any network architecture, it is necessary to offer low-latency HO scheme as we will see in the next chapters. Finally, the relay types, benefits, and protocol were investigated as well.

Furthermore, more and more new techniques are expected to play a crucial role in solving the recurrent HO issue when moving among cells at a high mobility speed and this chapter has explored through most of the current techniques. The necessity for the best possible QoS (offering seamless/lossless scheme) has led to the proliferation of many approaches, which aims at reducing the failure probability. These approaches mainly proposed to find some kind of a backup link when moving at the cell edge of two neighbouring cells i.e. HO, by adding an extra antenna/antennas (MIMO) or simultaneously linked to different system technologies, or by splitting the control and user planes onto different frequency bands. Thereby, increasing the scheme's reliability by reducing the possibility of failing, thus reducing the failure probability. However, no one has proposed to optimise the traditional HO procedures for the HSR scenario. Therefore, this thesis aims to enhance the scheme's reliability by either optimising/simplifying the traditional HO scheme either by reducing the negotiated signalling overhead or by triggering part of the process in advance when the RSQ is at the strongest level and/or giving the system the chance to retransmit more trials as we will see in the upcoming chapters.

CHAPTER 3

AN EXPEDITED PREDICTIVE DISTRIBUTED ANTENNA SYSTEM BASED HANDOVER SCHEME FOR HIGH-SPEED RAILWAY

3.1 Introduction

Currently, more and more attempts have been performed to satisfy the ever-growing desire for Internet access due to the trending application which connects people all over the globe. This kind of popularity results in wide diverse requirements, which range from a simple web browsing to a mobile video communication, e.g. video conferencing. Lately, HSR mobile communication system has focused on providing Internet access with high QoS [80] to entice more travellers. Yet, the current available mobile broadband wireless communication technology is only suitable for low-to-medium-mobility scenarios.

HSR broadband wireless communication is encountering many challenges one of the most crucial issue is the frequent handover (HO). For example, a HO would be imperative every 10s supposing a footprint of 1km conjointly with a velocity of 100 m/s. The recurrent HO leads to a long delay, a high packet loss, and a high drop off rate, and therefore could seriously deteriorate the system throughput. The reason for that is the long HO interruption time which might be even exacerbated manifold due to the HO failure (HOF) case.

The current HO solutions can be divided into three main categories. The first category is the location based triggering using the global positioning system (GPS) signalling [9, 81]. This approach results in a standardization overhead, and it is unreliable in the cases of poor GPS signal reception, e.g., in a tunnel scenario. The second approach is the dual link where there are two antennas [3, 39]. One is located on the train's front, and the other is on the train's rear. The front antenna performs the HO scheme with the target cell, while the rear antenna keeps the current link with the serving cell. The third approach is distributed antenna system (DAS) based approach [82]. DAS based system architecture provides a twofold target of enhancing the spectrum efficiency and the HO algorithm performance.

DAS network architecture specially designed for HSR broadband wireless communication system consists of hundreds of remote antenna units (RAUs) deployed linearly along the rail track in a one dimensional fashion, as the new HSR network tends to have less inclination angle nowadays [83]. Each RAU is a simplified radio unit used for transmission/reception. The other part is the central processing unit (CU) where signal processing is performed [84]. RAUs are connected to the CU via either a fibre link or a wireless link. Furthermore, the CU can control RAUs up to 20 km, and no HO is needed between RAUs controlled by the same CU, by employing the frequency switch (FSW) scheme [83].

Newly published results of long-term evolution (LTE) field tests in a dense urban area exhibits a HO failure (HOF) rate of more than 21% [85]. Transmission failure of the HO command, also known as failure of the radio resource control (RRC) connection reconfiguration (RCR) command, is the major reason behind those failure events. Based on this observation, this chapter proposes a faster HO algorithm which aims to reduce the failure probability of RCR command, and thus provide a seamless service for the train's passengers by reducing the HO latency with the target of providing reliable broadband services, and considerably alleviate the effect of frequent HO. This algorithm is inspired by the property of a dedicated linear DAS network architecture, where the target cell is always the next adjacent one. In contrast to the hexagonal cell distribution, where the cells are distributed randomly along the rail track, this algorithm infers the train location to trigger some HO procedures in advance. The performance of the proposed

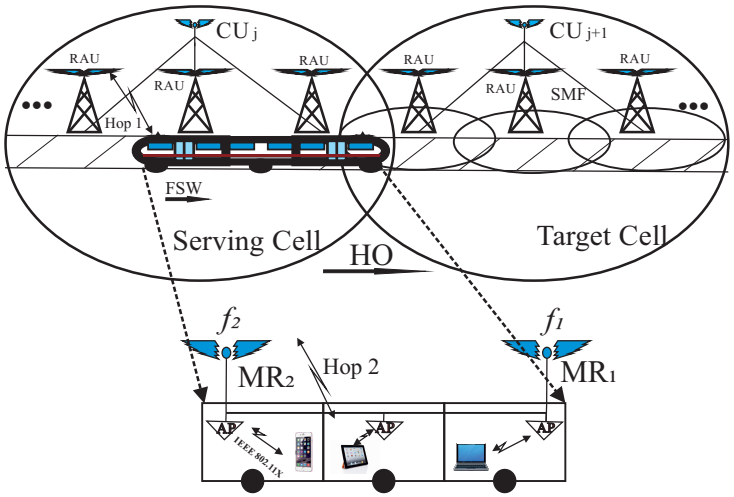

Figure 3.1: DAS based System architecture for high-speed railway.

HO scheme is evaluated when the train moves from coverage area of one RAU linking to serving CU to the coverage area of another RAU linking to the target CU. The proposed HO scheme is backward compatible with long-term evolution advanced (LTE-A) since the international union of railways has decided that the next generation standard for railway wireless communication will be based on LTE. The results show that our proposed scheme outperforms the traditional HO scheme.

The remainder of this chapter is organised as follows. Section 3.2 introduces the system architecture. The proposed scheme is presented in Section 3.3. Finally, Section 3.4 presents the HO performance analysis.

3.2 System Architecture

The DAS network architecture specially designed for HSR broadband wireless communication consists of hundreds of RAUs deployed linearly along the rail track in a one-dimensional fashion as the new HSR network tends to have less inclination angle nowadays. Linear deployment can increase the possibility of continuous line-of-sight (LOS) connections between RAUs and MRs. Each RAU is a simplified radio unit used for transmission/reception, while network optimization and signal processing are performed at the CU. RAUs are connected to the CU via fibre link. By using DAS along with the two-hop architecture, RAUs and MRs can be linked via any mobile wireless communication

system, e.g., LTE/LTE-A. Users inside the train are considered as indoor users and can be served using LTE/LTE-A or 802.11x. This chapter mainly focuses on the stability of the back-haul link (RAU-MR), since the train is moving very fast and the MR needs to perform FSW/HO frequently. Note that the notation used for this system architecture is shown in Fig. 3.1.

3.3 The Proposed Scheme

In contrast to the conventional two-dimensional cell layout where there are multiple candidate target cells located at random distance to the rail track, the linear one-dimensional DAS based layout shown in Fig. 3.1 should lead to a more straightforward HO strategy. Therefore, taking advantage of the specialized DAS network architecture and the HSR linear track deployment are the main motivations behind the proposed HO scheme. Subsequently, this specialized dedicated architecture will result in only one candidate target CU, which is the solely possible cell that the MR requests to handoff to and the details of the proposed scheme are presented in the following subsection.

3.3.1 Proposed Central Unit-Central Unit Handover

In this section, an optimized fast HO scheme is proposed consisting of four phases: handover pre-preparation, handover preparation, handover execution, and handover completion. Fig. 3.2 shows the signalling flow of the traditional HO scheme, while Fig. 3.3 shows the signalling flow of the proposed HO scheme. In the following, and without loss of generality, the HO process of the first MR is described. The details are as follows.

Phase I Handover Pre-preparation

1) Once the MR issues a measurement report for switching the MR from the current RAU to the next under the same serving cell (CU_j) control, CU_j detects if the target RAU is the last controlled RAU. CU_j could detect that easily by using either the RAU ID, which is included in the measurement report sent by the MR or by the unique dedicated wavelength used to modulate the signal with.

2) Once confirmed, CU_j can follow one of the following approaches to trigger phase II

or may use all of them cooperatively to have an accurate predicted result.

A) CU_j monitors the received frequency f_r from the MR (received by the last RAU) until f_r is smaller than the source frequency f_s used by the MR ($f_r < f_s$) and f_r is continuously decreasing for a number of consecutive times such that $f_{r_{m+1}} > f_{r_{m+2}} ... > f_{r_{m+n}}$. Note that n is directly related to the RAU coverage area and the maximum system speed. According to the Doppler frequency shift properties, $f_r > f_s$ when the source (i.e. MR/train) moves towards the fixed observer (i.e. one RAU linking to CU_j); $f_r = f_s$ when the MR passes the observer; $f_r < f_s$ when the MR moves away from the observer according to the formula $f_r = f_s(1 + 2v \cdot cos\theta/c)$. When the MR is approaching, θ increases in the range of $(0, \pi/2)$ and $cos\theta$ decreases resulting in $f_r > f_s$ until $cos\theta = 0$. After the train is passing by the observer, θ increases in the range of $(\pi/2, \pi)$ and $cos\theta$ decreases from zero to negative value.

B) CU_j waits for the MR to trigger the preparation phase by issuing a measurement report after detecting that the received signal quality (RSQ) from target is less than the triggering threshold by some value (two triggering events).

C) CU_j can predict the MR location, for example, if we assume that the MR communicates with CU_j every 10 ms and CU_j can prognosticate the MR speed through the received signal power degradation caused by the ICI effect. The Doppler shift degradation power can be obtained according to $\Delta = 1 - \int_{-1}^{1}(1 - |x|)J_0(2\pi f_D T_s x)dx$ and consequently the MR speed can be obtained. Even if the MR is changing its speed, CU_j can easily calculate that change since the train does not change its speed in a random fashion. For example, it takes 15 minutes for HSR in Taiwan to speed-up from 0 to 83.3 m/s [7]. Also, CU_j should consider the MR's next location by taking into account the round trip time (RTT) of the system. For example, LTE system has a RTT of 70-140 ms [86]. Therefore, CU_j can predict that the MR is very close to the cell edge/normal HO triggering event using one or all the above approaches.

Phase II Handover Preparation

3) If the condition(s) is (are) satisfied, consequently CU_j requests the targeted neighbouring CU (CU_{j+1}) to HO the active UEs in advance by sending the HO request to CU_{j+1}.

4) Afterwards, CU_{j+1} performs the admission control algorithm for the requested UEs to evaluate its ability to accept the request. If CU_{j+1} decides to accept the request, it sends a handover request acknowledgment (ACK) back to CU_j, which represents the RCR command.

5) Employing the event-triggering reporting type would guarantee a fast triggering condition. Therefore, once the RSQ triggering threshold (β) is met for a time-to-trigger (TTT) value. The MR issues the measurement report back to CU_j to trigger the process.

6) As soon as CU_j receives the measurement report, it performs the HO algorithm to determine whether to HO. If CU_j decides to HO the MR, CU_j will command the MR to HO by sending RCR command to the MR immediately. RCR command includes the channel access parameters required to synchronize the MR with CU_{j+1} as well as the crucial integrity protection and ciphering information. The rest of procedures are the same as the standard.

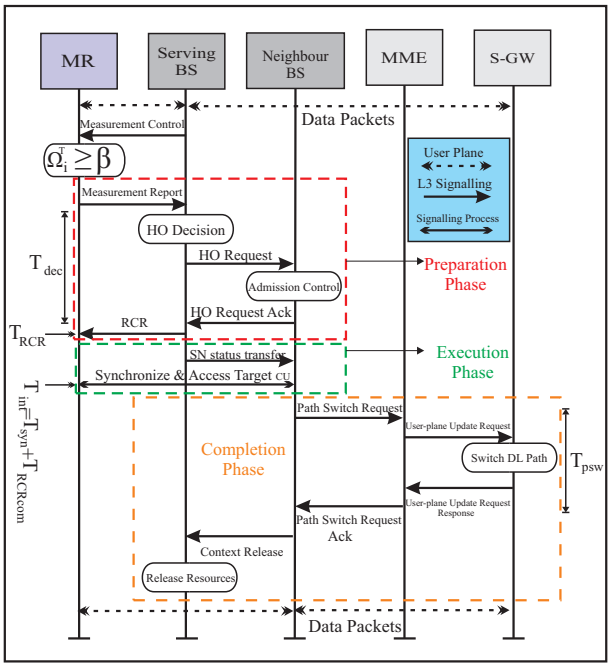

Figure 3.2: Traditional BS-BS handover.

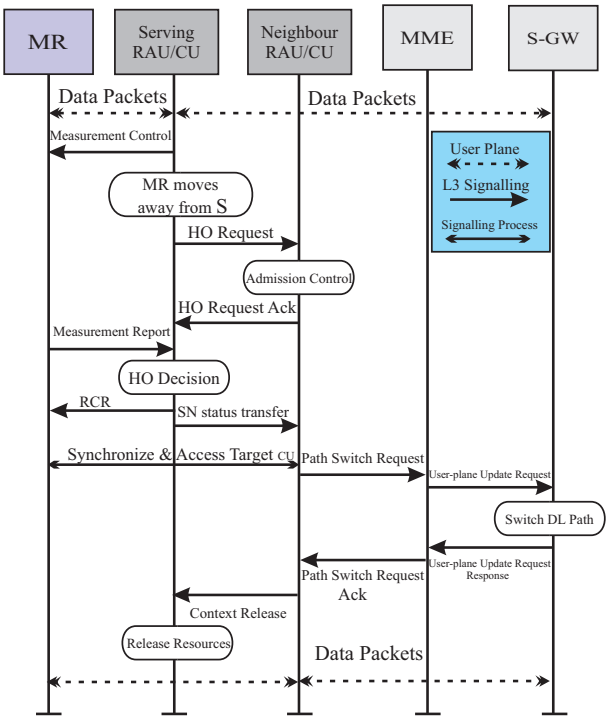

Figure 3.3: Proposed Central unit-central unit Handover.

3.3.2 Handover Triggering Conditions

As Fig. 3.1 shown, CU_j performs handoff to neighbour RAU which belongs to CU_{j+1} if the RSQ of the neighbour is above a predefined threshold for the TTT (assumed to be zero ms herein). As long as the above condition is satisfied, the MR triggers the measurement report to CU_j for evaluation, and CU_j will decide whether to handover. The hysteresis parameter is not included in the above condition as the ping-pong effect [87] in this architecture will be eliminated since CU_j has a list of the current and target RAUs, and the train is moving linearly at a high-speed as at any time there is only one possible candidate to camp on. In this way, a fast triggering condition that fits HSR speed as well as the RAU's small coverage area can be achieved.

Since railway is usually constructed in wide rural or viaduct areas, where a multipath effect could be neglected most of the time, the main path signal is only considered [88]. With equal power allocation among RAUs, the received power of the MR from RAU k $\in\{S, T\}$ at the ith time interval is denoted by P_i^k, which can be calculated as

$$P_i^k[dBm] = P_t[dBm] - P_{L_i}^k[dB], \tag{3.1}$$

where P_t is the transmitted power per RAU and it can be found as

$$P_t[dBm] = 10\log_{10}\left(\frac{P_T/N}{M}\right), \tag{3.2}$$

where P_T is the total transmitted power of CU_j, N is the total number of RAUs under CU_j control, and M is the total number of subcarriers.

$P_{L_i}^k$ in (3.1) refers to the large scale fading between S/T and the MR. According to D2a scenario of WINNER II model [89], $P_{L_i}^k$ can be given by

$$\begin{aligned} P_{L_i}^k[dB] &= 44.2 + 20\log_{10} d_i^k + 20\log_{10}(f[GHz]/5) \\ &\quad + 10\log_{10} g_i^k, \qquad 10m < d_i^k < d_{BR}, \end{aligned} \tag{3.3}$$

where d_i^k is the distance between the MR and the kth RAU, d_i^T is given by $(\sqrt{(D-x_i)^2+(d_v)^2})$, d_i^S is given by $(\sqrt{(x_i)^2+(d_v)^2})$ [3], which is a 2-dimensional model used by most of the current literature. $d_{BR} = 4h_R h_T f/c$ is the breaking point distance. Shadowing at the ith time interval is represented by $10\log_{10} g_i^k \sim \mathcal{N}\ (0,\ (\sigma_i^k)^2)$ that

follows a Gaussian distribution with a zero mean and a standard deviation σ_i^k. Now, let $A[dBm] = 10\log_{10}\left(\frac{P_T/N}{M}\right) - 44.2 - 20\log_{10}(f[GHz]/5)$. Then, equality (3.1) can be rewritten as

$$P_i^k[dBm] = A - 20\log_{10}(d_i^k) - 10\log_{10} g_i^k. \tag{3.4}$$

Then, the received signal quality at the MR is represented by

$$\omega_i^k = \frac{10^{P_i^k/10}}{(\Delta \cdot 10^{P_i^k/10}) + \sigma_o^2}, \tag{3.5}$$

where $\Delta = 1 - \int_{-1}^{1}(1-|x|)J_0(2\pi f_D T_s x)dx$ is the tight upper bound of the ICI power of orthogonal frequency division multiplexing (OFDM) system [90], as LTE-A is employed here which uses OFDM as a radio interface in the downlink. $J_0(.)$ is the zeroth-order Bessel function of the first kind. $f_D = (v \cdot f)/c$ is the maximum Doppler frequency shift, f is the carrier frequency, v is the MR's/train's speed, $c = 3 \times 10^8$ m/s is the speed of light in vacuum, and T_s is the symbol duration. σ_o^2 denotes the noise power. The received signal to noise ratio with a normalized noise power can be then calculated as

$$\omega_i^k = \frac{10^{P_i^k/10}/\sigma_o^2}{(\Delta \cdot 10^{P_i^k/10})/\sigma_o^2 + 1}, \tag{3.6}$$

Accordingly, the received signal quality can be obtained in dB as

$$\Omega_i^k[dB] = A - 20\log_{10}(d_i^k) - 10\log_{10} g_i^k - 10\log_{10}\sigma_o^2 - I_i^k[dBm], \tag{3.7}$$

where I_i^k denotes the normalized noise and ICI power, I_i^k can be derived as

$$I_i^k[dBm] = 10\log_{10}\left[\frac{(10^{\frac{(P_t[dBm]-P_{L_i}^k[dB])}{10}}) \cdot \Delta}{\sigma_o^2} + 1\right], \tag{3.8}$$

3.4 Performance Evaluation

3.4.1 Handover Probability

The HO probability is the probability that the HO is triggered at a position x_i. According to the HO scheme this probability can be obtained as follows

$$\begin{aligned}
\mathbf{P}_{trigg} &= \mathbf{P}\left\{\Omega_i^T \geqslant \beta\right\}, \\
&= \mathbf{P}\left\{A - 20\log_{10} d_i^T - 10\log_{10}\sigma_o^2 - I_i^T - 10\log_{10} g_i^T \geqslant \beta\right\}, \\
&= \mathbf{P}\left\{10\log_{10} g_i^T \leqslant A - \beta - 20\log_{10}(d_i^T) - 10\log_{10}\sigma_o^2 - I_i^T\right\}, \\
&= 1 - \mathbf{Q}\left(10\,\frac{A - \beta - 20\log_{10}(d_i^T) - 10\log_{10}\sigma_o^2 - I_i^T}{10\cdot\sigma_i^T}\right),
\end{aligned} \tag{3.9}$$

where β is the triggering threshold and $Q(x) = \frac{1}{\sqrt{2\pi}}\int_x^\infty e^{\frac{-t^2}{2}}dt$ represents the Q-function. (3.9) also applies for the HO probability for the conventional HO scheme case. According to (3.9), when the MR is located at a position x_i, the HO process can be triggered if and only if the detected signal quality is equal to or better than β.

3.4.2 Handover Failure Probability

HO probability represents the probability of HO triggering occurrence which might not end up with conducting the whole HO procedures. In order to obtain a successful HO all the negotiated messages through the air interface should be recovered correctly through the intended receivers. If one of the negotiated messages is lost, the transmitter will submit the same message again until it is successfully received, or reaching the maximum retransmission times. If the allowed maximum retransmission times have been reached, a radio link failure (RLF) is declared. In general, the MR negotiates five messages through the air. Two of them are with CU_j (measurement report, RCR) and the others are with CU_{j+1} (random access (RA), RA response (RAR), and RCR complete). Each message has a maximum number of retransmission trials specified by the standard. However, those maximum trial numbers might not be reached as the HSR might pass the overlapping area so quickly that the MR is not able to finish the HO process successfully within the

overlapping area, as the standard specifications are optimized for low-to-medium-speeds. This is also because of the HSR harsh communication environment, i.e., the RSQ is timely distorted due to Doppler frequency shift. Also, the large UE numbers that request to HO simultaneously could considerably increase the HO failure probability (when there are a large number of MRs or the UEs are communicating directly with the RAUs) compared to low-to-medium speed scenarios. To calculate the total failure probability of the HO process, first we will calculate the maximum number of trials associated with CU_j side (RCR maximum trials count) of the traditional HO scheme

$$\delta = \frac{\rho \cdot \chi - v \cdot T_{dec}}{v \cdot T_{RCR}}, \tag{3.10}$$

where ρ is the percentage of the overlapping area dedicated to recover the RCR correctly. χ is the overlapping area, T_{dec}, and T_{RCR} are the HO preparation time of the traditional HO scheme, and the time required to recover RCR successfully, respectively (see Table 3.1). While the maximum number of trials associated with CU_j side (RCR maximum trials count) of the proposed HO scheme can be found as

$$\delta^{prop} = \frac{\rho \cdot \chi - v \cdot T_{dec}^{prop}}{v \cdot T_{RCR}}, \tag{3.11}$$

where T_{dec}^{prop} denotes the HO preparation time of the proposed HO scheme, see Table 3.1. To calculate the maximum possible number of trials associated with the target cell, this can be obtained as follows

$$\gamma = \frac{(1-\rho) \cdot \chi}{3 \times v \times T_o}, \tag{3.12}$$

where T_o is the time required for performing one of the target access procedures which is assumed to be 8 ms. $(3 \cdot T_o \cdot \gamma)$ should not exceed T_{304}, where T_{304} is the access process expiry timer associated with CU_{j+1}, due to the following formula

$$\chi = v \cdot (T_{dec} + \delta \cdot T_{RCR} + T_{304}), \tag{3.13}$$

Assuming that the HO preparation phase is to be initiated at the overlapping area beginning point. However, T_{304} value was proposed by the standard with variable values for different overlapping area distances for a user's mobility in the range of fixed-to-nomadic speed. Therefore, this is not suitable for high-speed trains where the channel

quality/condition is worse than the traditional case. Thus, the MR will require more retransmissions to reach the same performance of a lower system speed. As a result, we will not consider the T_{304} as the maximum retransmission limit. Otherwise, we will use the overlapping area as the main retransmissions limit. In terms of real world implementation, this issue can be avoided by optimizing the system parameters according to the HSR highest speed which normally cannot be exceeded. Hence, the selection of overlapping area length along with the overlapping area percentage dedicated for each process can be optimized for this particular speed. (3.10) implies that γ increases by either increasing χ or ρ or decreasing the speed v assuming a fixed time of the operation in the denominator T_o. Our proposed scheme can decrease the failure probability since it reduces T_{dec}, i.e., the time required to perform the HO decision algorithm, by expediting the RCR triggering process which results in increasing δ due to reducing T_{dec} and triggering RCR in an earlier position with a better signal quality. More specifically, the RCR command is ready to be transmitted to the MR once the measurement report is received, so there is no need to send HO request and wait for CU_{j+1} response which might delay the process. So the failure probability of RCR command reception of the traditional HO scheme can be found in (3.14) which do not consider the retransmission attempts, and (3.15) refers to the final RCR command reception failure probability which considers the retransmission case.

$$\begin{aligned}
\mathbf{P}_f^{RCR} &= \mathbf{P}\left\{\Omega_i^S < U\right\}, \\
&= \mathbf{P}\left\{A - 20\log_{10} d_i^S - 10\log_{10}\sigma_o^2 - I_i^S - 10\log_{10} g_i^S < U\right\}, \\
\mathbf{P}_f^{RCR} &= \mathbf{Q}\left(10\,\frac{A - 20\log_{10}(d_i^S) - 10\log_{10}\sigma_o^2 - I_i^S - U}{10\cdot\sigma_i^S}\right), \qquad (3.14)\\
\mathbf{P}_{f_T}^{RCR} &= \prod_{z=1}^{\delta}\left[\mathbf{Q}\left(10\,\frac{A - 20\log_{10}(d_{i,z}^S) - 10\log_{10}\sigma_o^2 - I_{i,z}^S - U}{10\cdot\sigma_i^S}\right)\right], \qquad (3.15)
\end{aligned}$$

where $I_{i,z}^S$ denotes the normalized noise and ICI power for the retransmission trial z between the serving RAU and the MR. The failure probability of the proposed HO scheme can be found in the same way as in (3.14) and (3.15) for one and multiple transmission trials, respectively, by substituting δ^{prop} instead of δ in (3.15). While the failure probability

of the whole HO scheme of the traditional HO scheme which includes the RCR and RA procedure for only one and multi transmission trials can be found respectively as in (3.16) and (3.17).

$$\mathbf{P}_f^h = \left[\mathbf{P}_f^{RCR} + (1 - \mathbf{P}_f^{RCR}) \cdot \left[\mathbf{P}_{f_{tar}}\right]\right], \tag{3.16}$$

$$\mathbf{P}_{f_T}^h = \left[\mathbf{P}_{f_T}^{RCR} + (1 - \mathbf{P}_{f_T}^{RCR}) \cdot \left[\prod_{z=1}^{\gamma} \mathbf{P}_{f_{tar_z}}\right]\right]. \tag{3.17}$$

where $\mathbf{P}_{f_{tar}}$ is the failure probability associated with the target RAU T and it can be calculated as

$$\mathbf{P}_{f_{tar}} = \left[\mathbf{P}_{f_c} + (1 - \mathbf{P}_{f_c}) \cdot \mathbf{P}_{f_c} + (1 - \mathbf{P}_{f_c}) \cdot (1 - \mathbf{P}_{f_c}) \cdot \mathbf{P}_{f_c}\right], \tag{3.18}$$

where $\mathbf{P}_{f_c} = \mathbf{P}\left\{\Omega_i^T < U\right\} = \left[Q\left(10\,\dfrac{A - 20\log_{10}(d_i^T) - 10\log_{10}\sigma_o^2 - I_i^T - U}{10 \cdot \sigma_i^T}\right)\right]$ denotes the command failure probability of either RA, RAR, or RCR complete, as failing to receive any of them leads to a failure event of accessing the target. Again the total failure probability of the proposed HO scheme can be found by substituting δ^{prop} instead of δ when calculating $\mathbf{P}_f^{RCR}$ in (3.17).

The most crucial part of the HO scheme is the reception of the RCR command in an expeditious manner. Since the train is moving away from the current RAU to target RAU which implies a continuous degradation in the signal quality of the serving RAU. Failing to recover RCR might lead to increased delay (due to retransmission attempts) or even a RLF situation which wastes the resources and interrupt the users' services. Therefore, receiving RCR with the best possible signal quality is very critical to finish the HO scheme successfully. Once the MR receives RCR successfully, the MR tries to synchronize and access the target RAU by negotiating RA, RAR, and RCR complete commands. These command should have a lower failure probability than RCR command, since the train is moving towards the target at a high speed, so the signal quality of the target is getting better and better.

Table 3.1: Success Handover Latency Analysis.

HO Phases	Conventional	Proposed
HO decision (T_{dec}, T_{dec}^{prop})	14 ms	5 ms
HO command (T_{RCR})	8 ms	8 ms
Synchronization (one trial only)	8 ms	8 ms
Path Switch	13 ms	13 ms
Total Latency (T_s)	85 ms	76 ms

3.4.3 Overlapping Area

The overlapping area between successive RAUs is a crucial factor which decides the overall system performance. Increasing the overlapping area guarantees a successful HO. Therefore, obtaining a sufficient overlapping area is a decisive factor to ensure a stable system performance.

3.4.4 Upper Bound Average Latency

HO latency is another decisive performance metric when it comes to user experience and the provided QoS. The total average latency can be found as

$$\mathbf{T} = (1 - \mathbf{P}_{f_T}^h) \cdot T_s + \mathbf{P}_{f_T}^h \cdot T_{rec}, \tag{3.19}$$

where T_s and T_{rec} ($T_{rec} = T311 + T301$ see Table 3.2) are the HO latencies in case of a successful and failure situations, respectively. Table 3.1 shows the HO latency of each scenario for a successful HO case. The proposed scheme shrinks the HO decision phase up to 64.286%, thus giving the system a better chance to finish HO successfully with a lower latency. Note that Table 3.1 calculations are based on [7, 91, 92].

Table 3.2: Default Simulation Parameters.

Parameter	Value
Carrier Frequency f	2 GHz
Speed of light in vacuum c	3 x 10^8 m/s
Symbol Duration T_s	1/14 ms
Bandwidth of Subcarrier	15 kHz
Total Transmit Power P_T	43 dBm
Power Density of Background Noise	-111 dBm/Hz
number of subcarriers M	1000
Shadow Fading Deviation σ_i	4 dB
Triggering Threshold β	1.44 dB
Total RAUs in each cell N	4
Cell radius	105 m
Overlap	10 m
Length of Train	400 m
Distance between RAU and Track d_v	10 m
T304, T301, T311 in ms, respectively	50, 100, 1000

3.5 Results and Discussion

In this section, by means of simulation, the performance of the proposed expedited predictive HO scheme is investigated and compared with the traditional HO scheme in terms of the aforementioned metrics. The default system parameters used to obtain the results of this chapter are presented in Table 3.2.

First, the average RSQ of the serving RAU S and the target RAU T is shown in Fig. 3.4 as a function of the MR location. As it can be seen, the received signal quality of the serving RAU S is decreasing as the MR is moving away towards the target RAU T. In contrast to the received signal strength of the target RAU T which is increased as the MR is moving from the serving towards the target RAU T.

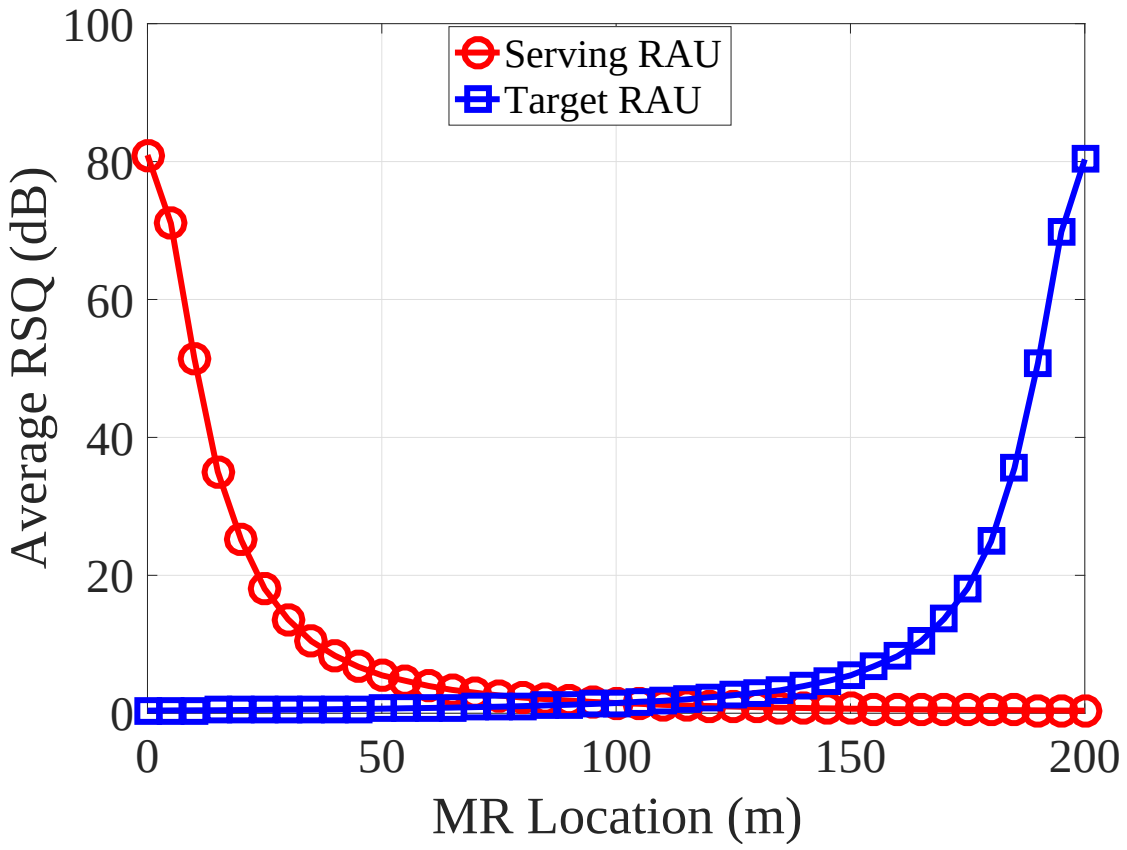

Figure 3.4: The average MR's received signal quality as a function of the MR location of both the serving and the target RAUs under a train speed of 100 m/s.

Second, the triggering probability as a function of the MR location is investigated under different triggering condition as shown in Fig. 3.5. As it can be seen, the higher the triggering condition value, the lower the triggering probability. This is due to the fact that the triggering probability is based on the received signal quality of the target RAU which is increasing as the MR is moving towards the target RAU T, this is also why the triggering condition is increasing as the MR approaches the target RAU T under varying triggering conditions. Selecting a suitable triggering condition is crucial in having a successful HO scheme, since the HO scheme encounters commands negotiation with both serving and target RAU. For instant, choosing an early triggering condition i.e., Ω_i^S =0, means that the HO process will be triggered early than it should which can result in HO failure event. Thus, the triggering condition should be chosen so that Ω_i^S and Ω_i^T are higher or equal to U until finishing the HO scheme.

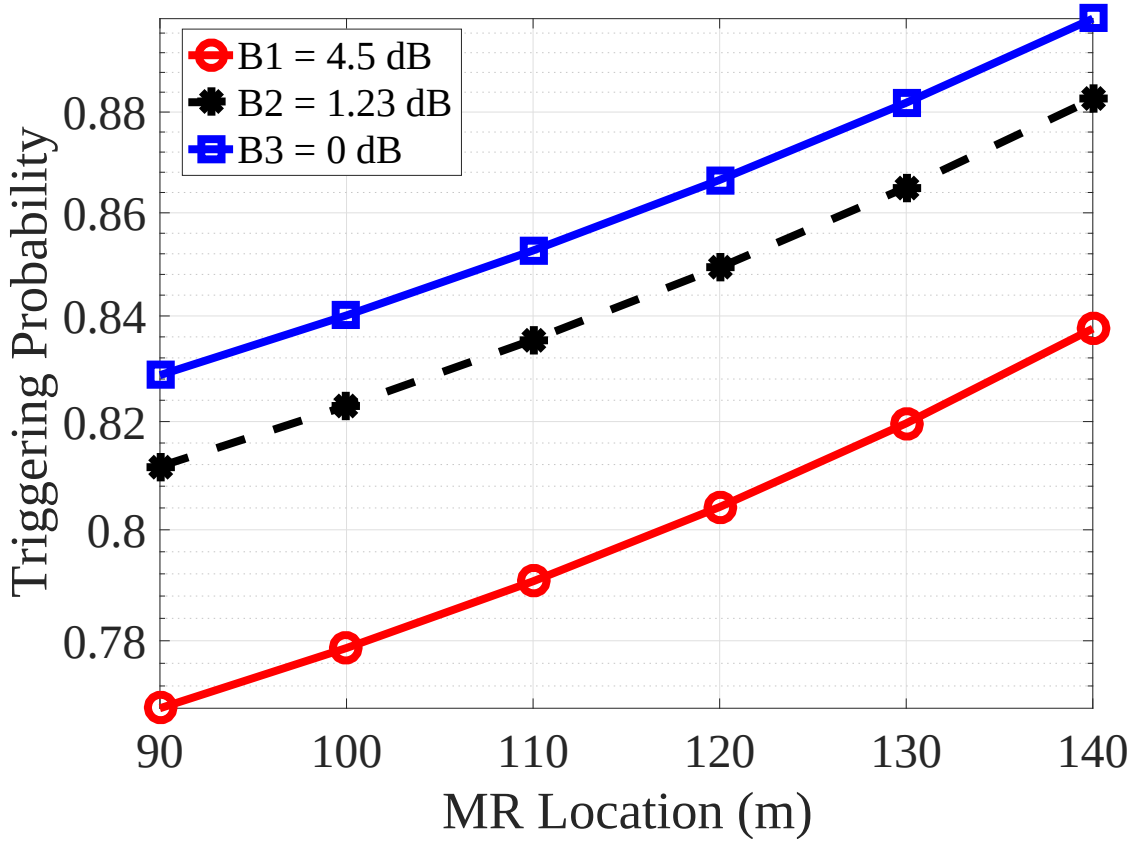

Figure 3.5: Triggering probability as a function of the MR location for different triggering conditions under a train speed of 100 m/s.

Next, in Fig. 3.6, the relationship between a general failure probability of a command associated with either the serving or the target RAU is investigated as a function of the minimum required RSQ to recover a command successfully (U) under multiple transmission trials. As it can be seen, for a single transmission trial, the lower the U value, the lower the failure probability. This is due to the fact that a lower U value means that Ω_i^S and Ω_i^T values used to transmit the command on are higher compared with the U value. This eventually can result in a higher achievable success probability. A superior Ω_i^K value used to send a command on means necessarily a lower failure probability. In addition to that, the higher the retransmission trials, the lower the failure probability especially with small U values i.e., U =-4, -3, -2, -1, and 0. As the U value is increasing the effect of the retransmission trial on the failure probability is reduced and becomes less compared with lower U values. This means that sending a command with superior/stronger Ω_i^K value is

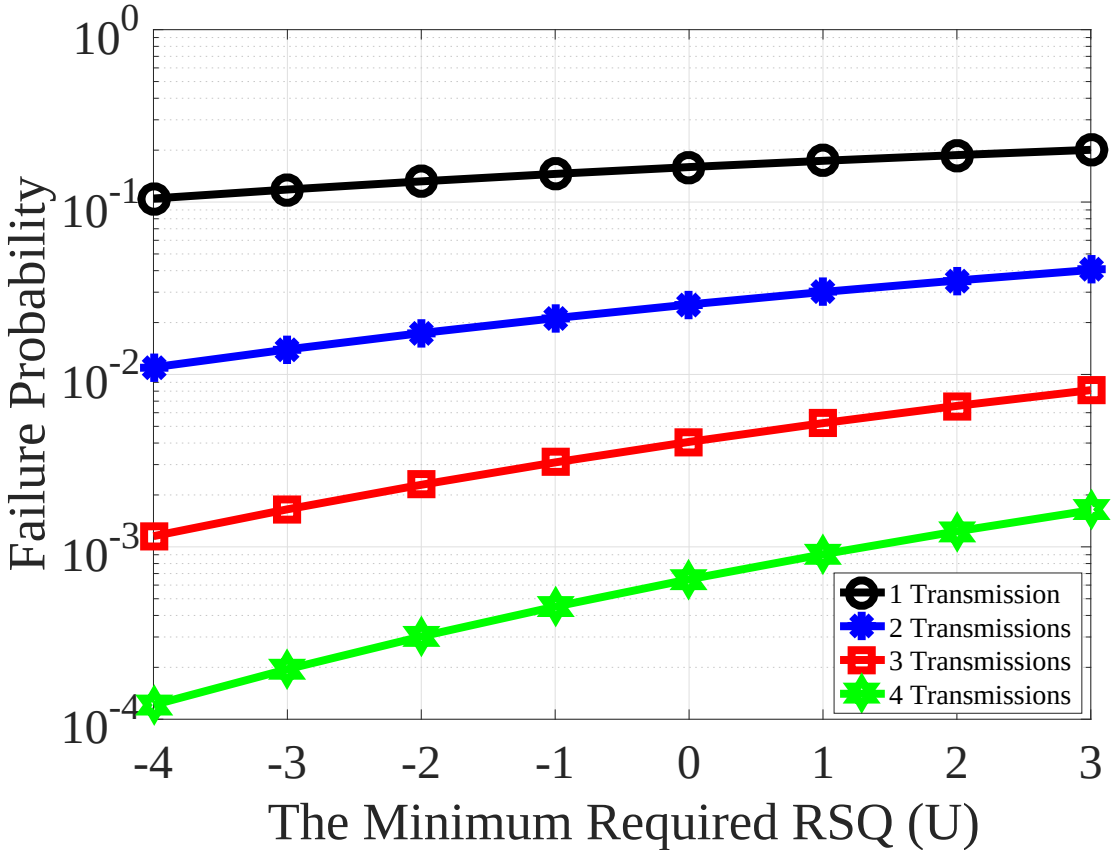

Figure 3.6: Failure probability versus the minimum required RSQ (U) needed to recover a HO command successfully under a speed of 100 m/s, evaluated at $x_i = 100$m.

better than trying to transmit it more, not to mention the effect of retransmission latency resulted from these trials as we will see in the upcoming chapters. Moreover, it can be deduced that to achieve a certain failure probability, the better the RSQ, the lower the required retransmission trials to achieve that specific failure probability. For instant, for U = -4 dB, it requires 4 transmission trials to achieve a failure probability of 10^{-4}, while for the same transmission trials but with a higher minimum U value i.e., 1 dB, it can obtain a failure probability of 10^{-3}. This means for U = 1 dB, the system requires more than 4 trials to achieve a failure probability of 10^{-4}. So it can be concluded that the better the RSQ used to transmit a certain command on, the lower the required transmission trials required to recover that command successfully.

Fig. 3.7 shows the RCR failure probability. As it can be seen, as ρ (the percentage of the overlapping area dedicated to recover the RCR correctly) decreases, the RCR failure

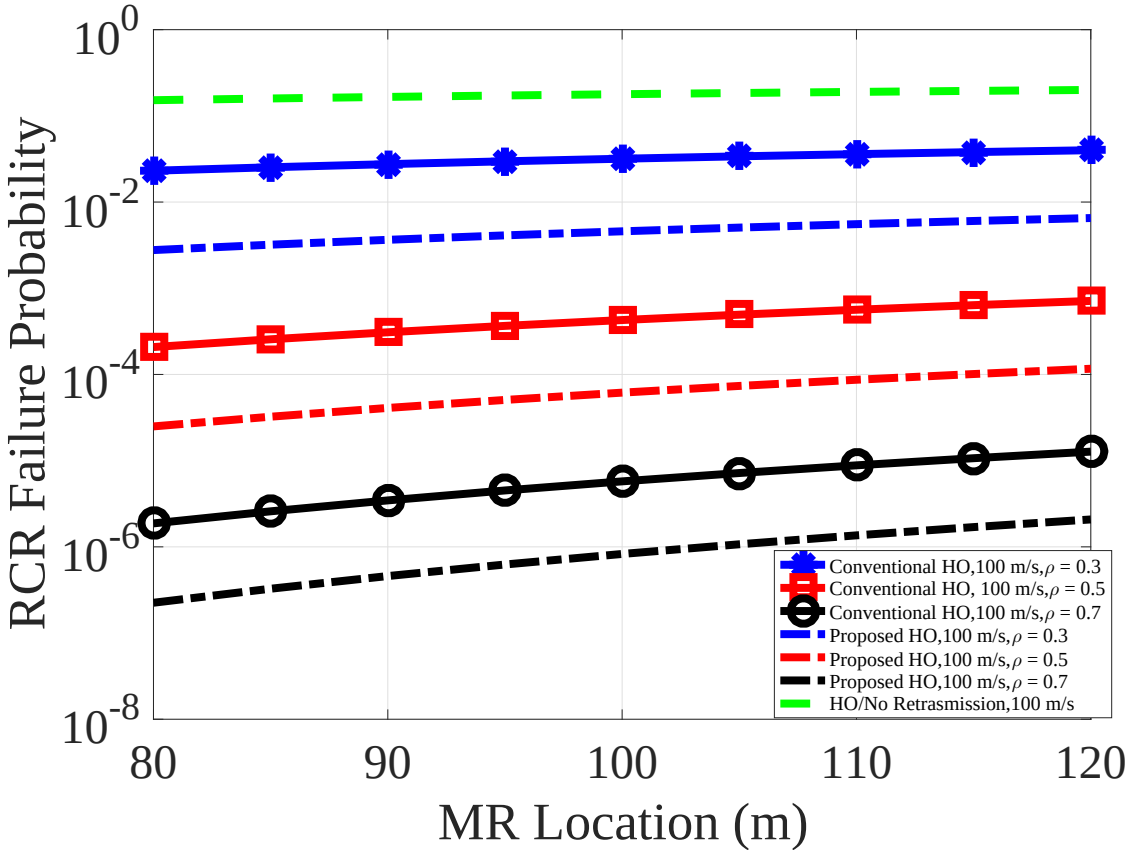

Figure 3.7: RCR failure probability versus the MR location under $U = 1.33$ dB.

probability increases due to the lower retransmission trials for both the conventional and the proposed HO schemes associated with lower ρ values. Moreover, the proposed scheme shows a better performance compared with the conventional HO scheme, as the proposed scheme offers more retransmission trials compared with the conventional scheme. In addition, the RCR failure probability of no retransmissions case is shown in figure and compared with the retransmission case, the no retransmission case undoubtedly shows a higher failure probability. This means that the evaluation which does not consider the retransmission case will not necessary reflect the true system performance of the real world implementation. Furthermore, all the investigated cases show an increasing function in terms of the RCR failure probability as a function of the MR location. This is because as the MR is moving away from the serving RAU, the RSQ of the serving RAU is decreasing resulting in this increasing behaviour in the failure probability, as the RCR command should be recovered successfully by the serving RAU.

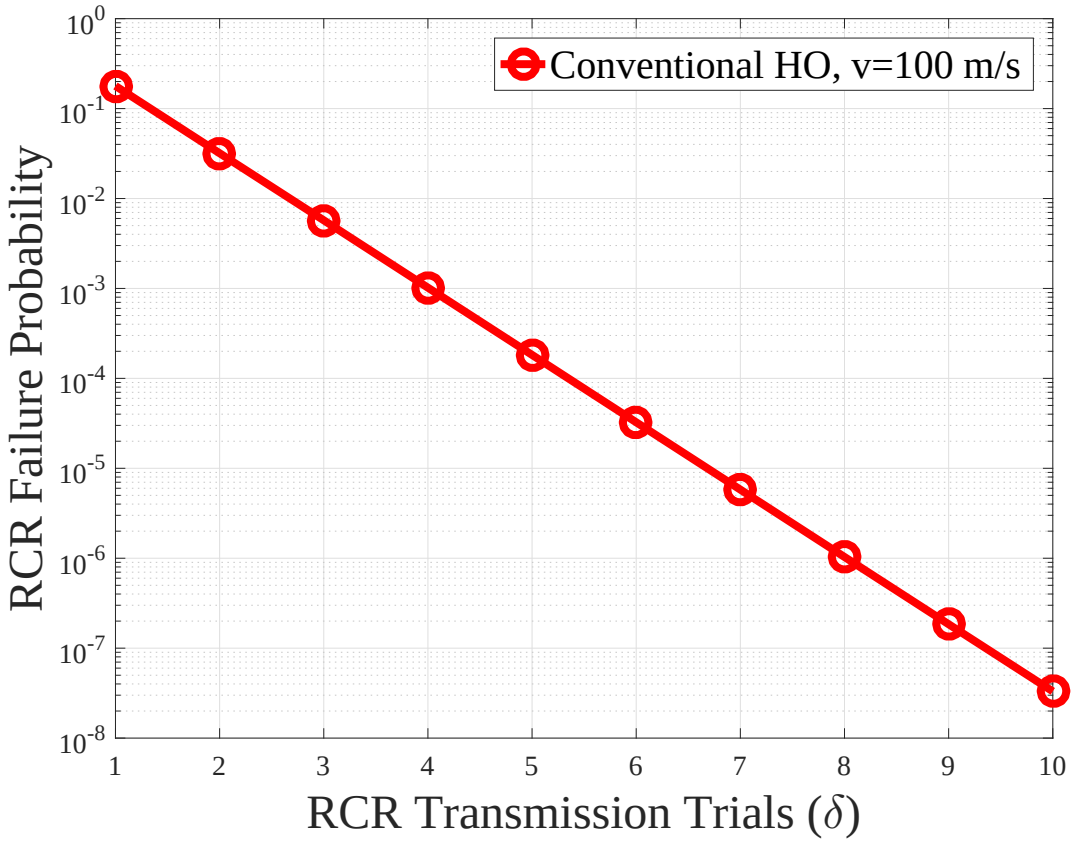

Figure 3.8: RCR failure probability as a function of retransmission trials δ under $U = 1.33$ dB, evaluated at $x_i = 100$m.

RCR failure probability of the conventional HO scheme as a function of δ is shown in Fig. 3.8. As it can be seen, the RCR failure probability decreases as δ increases. The more retransmission trials, the lower the RCR failure probability; this can eventually improve the user's QoS considerably by avoiding a failure scenario. Also, we can observe that every extra retransmission trial improves the RCR failure probability by almost 0.1 percent. For example, retransmission trial number four shown in the same figure improves the RCR failure probability from 10^{-2} to almost 10^{-3}.

Further, Fig. 3.9 shows the total HO failure probability as a function of the MR location for both the proposed and conventional HO schemes for single and multiple retransmission trials. As it can be seen, the proposed HO scheme shows a better performance compared with the conventional HO scheme. The investigated schemes show almost the same performance inside the overlapping area 95-105m. After passing the

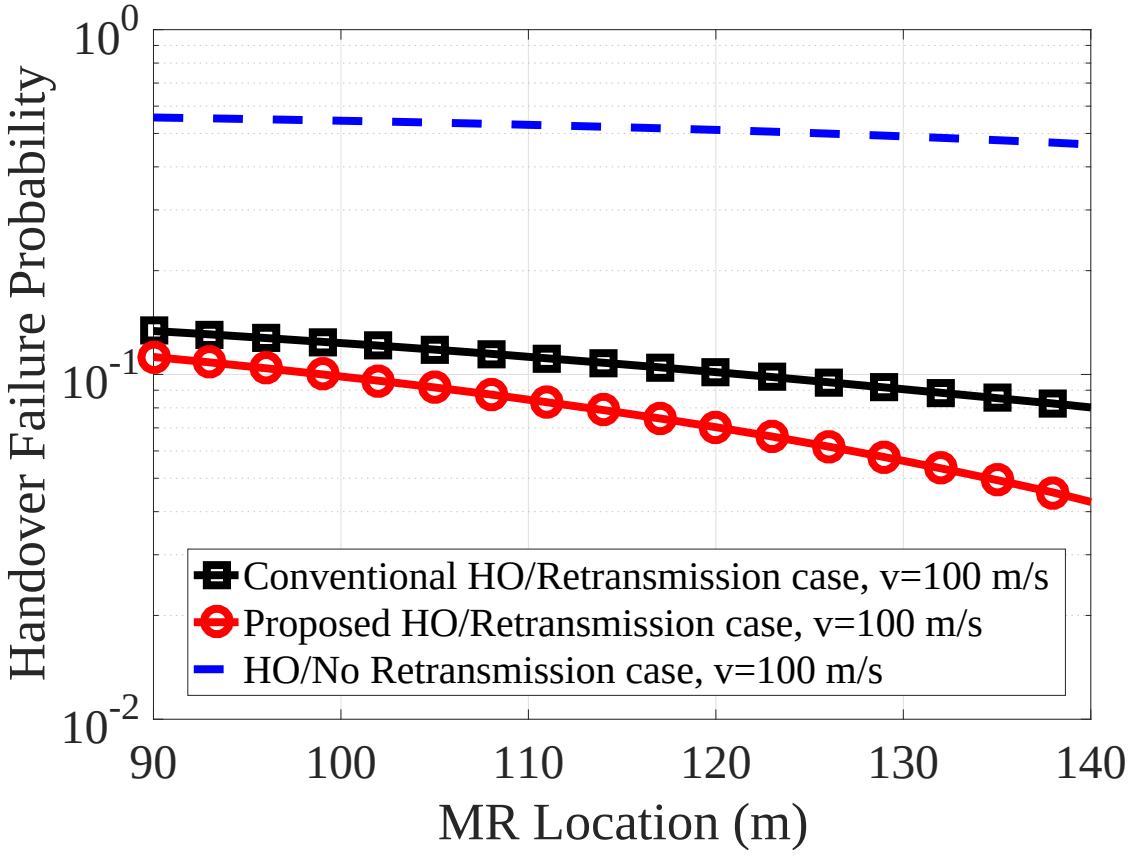

Figure 3.9: HOF probability versus the MR location under $U = 1.33$ dB and ρ =0.3.

overlapping area, the HO failure probability decreases for all the investigated schemes, this is due to the fact that the failure probability is more correlated with the target RAU since three commands are negotiated between the MR and the target RAU. Thus, as the MR moves towards the target RAU, this results in enhancing the RSQ of the target RAU and consequently a lower failure probability can be obtained. Moreover, the HO with no retransmission case shows the worst performance in comparison to the retransmission case.

Fig. 3.10 shows the HOF probability for the conventional and the proposed HO schemes as a function of the overlapping area. It can be noted that the proposed HO scheme exhibits an enhanced performance compared with the conventional HO scheme, as it requires less overlapping area to achieve the same failure probability of the conventional HO scheme. Furthermore, the lower the speed, the lower the failure probability, this is due to the stronger RSQ of lower speeds compared with higher speeds steam from

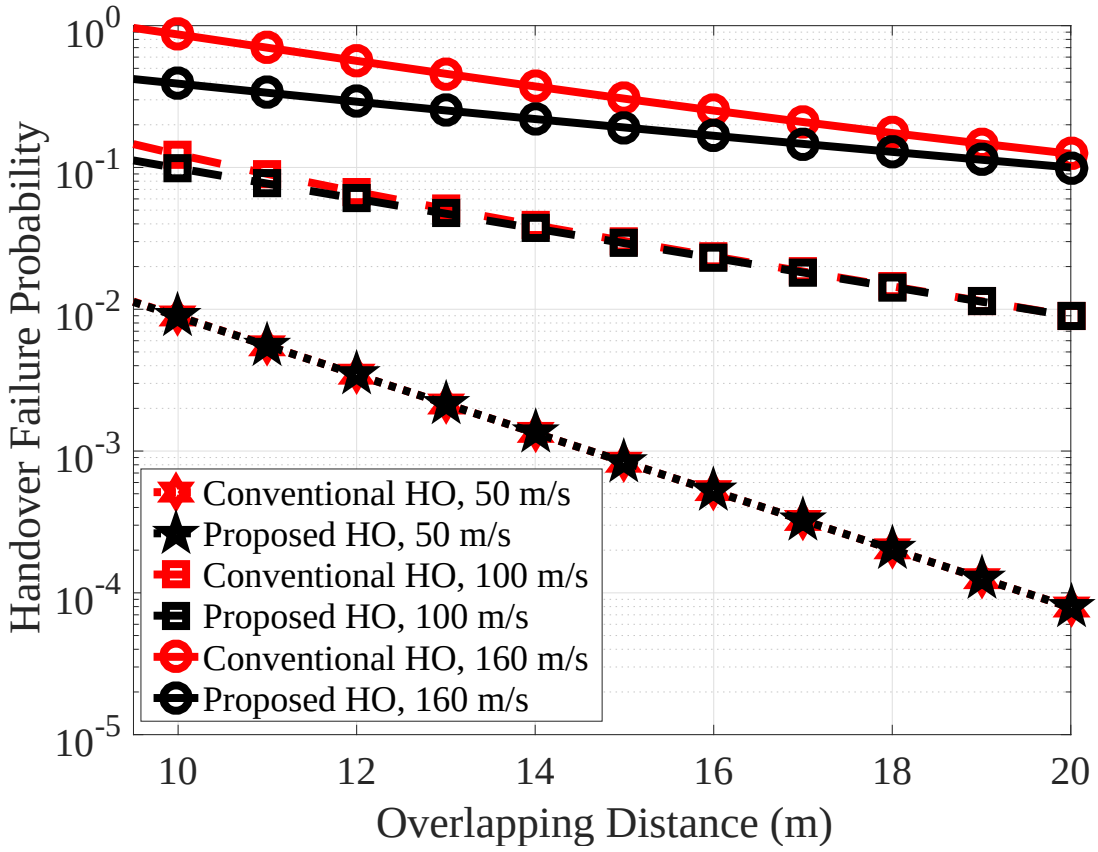

Figure 3.10: HOF probability versus the overlapping area length under U = 1.33 dB and ρ =0.3.

the effect of the ICI effect and also due to the higher retransmission trials associated with lower speed which leads to a higher success probability and consequently a lower required overlapping area compared with higher speeds. Additionally, as the overlapping area increases, the failure probability decreases due to the more achievable retransmission trials. For example, twenty meters are sufficient to reduces a failure probability of almost 0.4 to be less than 0.1 at a system speed of 160 m/s for the proposed case. Finally, the higher the speed, the more advantageous our scheme, as a higher speed results in a higher failure probability and the proposed scheme supports a lower failure probability compared to the conventional scheme by offering more transmission trial. While at a lower speed, for example at v= 50 m/s, the proposed scheme required less overlapping area compared with the conventional scheme before reaching an overlapping area of 6m. After 6m, both schemes show the same performance, as the failure probability is already very small.

Fig. 3.11 shows the average HO latencies for the investigated cases versus different

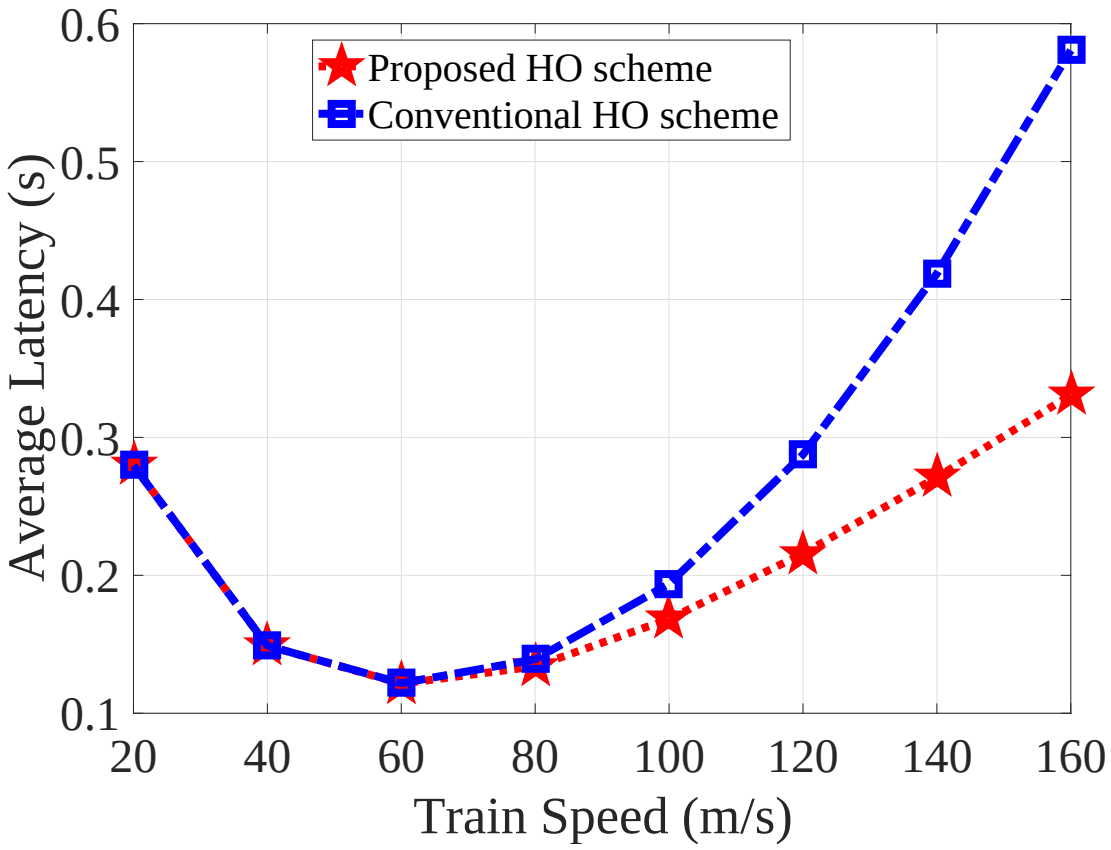

Figure 3.11: Handover average latency as a function of varying train's speed evaluated at the MR location of 100 m under $U = 1.33$ dB and $\rho = 0.3$

train's speed. On one hand, for speeds in the range of lower than or equal to 60 m/s, the proposed HO scheme and the conventional HO scheme have approximately the same average latency, despite the fact that the proposed scheme increases the retransmission trials. Nonetheless, approximately the same average latencies can be obtained due to the higher success probability that the proposed scheme provides. On the other hand, for speeds in the range of higher than or equal to 60 m/s, the proposed HO scheme shows a lower average latency than the conventional HO scheme. This is due to the fact that at high speeds, the failure probability increases. However, our proposed scheme performs better in terms of the failure probability, which resulted in a better performance in terms of latency. Additionally, we can see that the average latency of both schemes have almost a U shape curves for the examined speeds. As the speed increases from 20 m/s to 60 m/s, the latency decreases. This is because lower speed has the opportunity to retransmit more

trials compared with higher speed. After a speed of 60 m/s, the average latency starts to increase again due to increasing the failure probability. Therefore, and as shown in the figure, 60 m/s speed represents the optimal point which reduces the retransmission trials to the level which does not affect the failure probability. As a result, a trade-off between reliability and latency can be drawn, as increasing the reliability comes at the cost of increasing the latency which directly relates to the user's QoS. Thus, a careful balance is required to preserve the reliability given an acceptable latency level.

3.6 Summary

This chapter has provided the full details of our proposed predictive HO scheme when moving between RAUs belong to two neighbouring CUs. This scheme is enabled thanks to the HSR linear one-dimensional cell layout, where there is only one possible candidate to camp on. As a result, the serving CU can infer the upcoming need to HO so the serving CU can perform part of the preparation phase in advance so that when the actual HO triggering condition is met, the MR sends the measurement report and accordingly the serving CU can respond with an immediate HO command. Therefore, when the serving CU receives the measurement report it will not be needed to perform either HO request, HO request ACK, or admission control as these operations have been already performed earlier. Hence, this gives the serving CU the opportunity to transmit the HO command with a stronger RSQ, and it also gives the serving CU the chance to transmit more trials compared with the traditional HO scheme, so that a lower failure probability can be achieved.

Furthermore, a number of points can be drawn from the this chapter and as follows. First, a careful selection of the triggering threshold should be taken into consideration to prevent an early or late triggering which leads to increase the HO rate as well as increasing the failure probability. Second, sending the command on a stronger RSQ is more efficient in reducing the failure probability compared with increasing the transmission trials not to mention that the latter reduces the failure probability at the cost of increasing the total latency. Moreover, the better the RSQ used to transmit a certain command, the lower the

required transmission trials needed to recover that command successfully. The analytical analysis which have been verified using simulation results further prove that the predictive scheme support a lower failure probability due to the lower failure probability of the RCR command of the predictive HO scheme compared with the conventional HO scheme. Moreover, the required overlap between cells was studied as well, and it has been shown that the predictive scheme requires less overlap to achieve the same performance of the conventional HO scheme. Finally, the average latency of both schemes were also investigated, and it has been verified that the predictive scheme shows a better performance especially at higher speeds compared with the conventional HO scheme.

CHAPTER 4

SEAMLESS MOBILITY UNDER A DEDICATED DISTRIBUTED ANTENNA SYSTEM FOR HIGH-SPEED RAIL NETWORKS

4.1 Introduction

There are growing demands for users to have an instant and fast Internet access whether they are fixed or on the move. Long term evolution (LTE) and its developing successors i.e., LTE-Advanced is a fourth-generation mobile technology which is expected to meet the ever-increasing service demands by providing data rates of 1 Gbps and 100 Mbps for slow and high mobility users, respectively [93]. 4G networks can support communication with a user speed up to 250 km/h, while 5G networks promise to support communication for user speeds up to 500 km/h or more.

Lately, there has been an increasing interest from both industry and academia in high speed railway (HSR) wireless mobile communications to provide high Internet access quality-of-services (QoSs) [80] to attract travellers, as today's wireless communication system exhibits the best performance only for low-to-medium-mobility situations.

A novel dedicated wireless network for HSR system is necessarily required to satisfy the users demands [84, 94–101]. Therefore, distributed antenna system (DAS) is now considered as a very promising candidate architecture for future 5G HSR wireless commu-

nication systems thanks to its ground-breaking capabilities. In such networks, a plethora of remote antenna units (RAUs) are scattered linearly along the rail track and are linked to a central unit (CU) via optical fibres. CU can include one or multiple BSs/BBUs assigned to a fixed single or multiple RAUs under the control of the same CU, thereby, increasing the overall system capacity and spectrum efficiency.

In such an architecture, if the CU includes only one BS/BBU, the same set of communication resources, i.e. the same frequency and time slot will be used within the CU's coverage area, and as a result a soft HO is only needed between RAUs under the control of the same CU. However, intra CU HO becomes a certain necessity if the CU holds multiple BSs/BBUs since each BS/BBU and its associated RAUs use a different set of communication resources. Yet, the need for hard HO can be eliminated by exploiting the moving frequency concept (MFC) [21] or the frequency switch (FSW) scheme [102], by which, there are no fixed group of RAUs associated with a single BS/BBU within the CU control any longer, instead CU can dynamically associate the same RAU with multiple BSs/BBUs under the control of the same CU. More specifically, a frequency pattern in each RAU moves/switches along with the train's movement instead of a train moving along with a fixed repeated frequency pattern, so that the train is always served by the same frequency.

Thus, the frequent HO issue within the coverage of one CU can be then totally avoided by employing DAS architecture along with FSW scheme as each CU can control RAUs up to 20-40 km [1] (where the main limitation factor of the separation distance between CU and RAU comes from the delay requirement associated with hybrid automatic repeat request (HARQ) scheme [1]). As a result, less HO frequency will take place. However, a HO is still needed when moving between RAUs controlled by different CUs. In this context, we propose an enhanced fast HO scheme based on a dedicated linear one-dimensional cell layout to alleviate the effect of the HO process. Hence, DAS can be deemed as the most effective remedy to tackle the HO issue in future HSR mobile communications.

Despite the fact that there are considerable amount of researches regrading the HO issue in HSR environment, very limited researches have been done under a DAS architecture as a solution to mitigate the HO issue. For example, DAS architecture has been

proposed in [10, 21, 82, 103] for HSR. Specifically, [30] proposes a HO scheme based on antenna selection to enhance the received signal strength (RSS) so that the overall system performance is improved. Whereas, [10, 21, 103] have investigated a MFC, based on the train's location, to mitigate the frequent HO issue. Nonetheless, they have not provided neither satisfactory technical details nor performance analysis which necessarily reflects the scheme performance. In our previous work [102], a FSW scheme has been discussed roughly and also a HO scheme was proposed in [104] (presented in the previous chapter) to allow the serving BS estimating whether the MR is moving away, so that the serving BS can perform part of the preparation phase in advance and the serving cell can respond to the MR's measurement report with an immediate RCR command.

Based on the aforementioned research work, motivated by attaining a low latency, a high system capacity, an ultra transmission reliability, and consequently a superior mobile wireless communication QoS for commuters on HSR, this chapter utilizes the DAS along with the two-hop architecture and proposes a new mechanism, known as the FSW scheme to supplant the conventional HO between RAUs under the control of the same CU by applying the MFC into CU. In this mechanism, a frequency switch is triggered based on satisfying a predefined threshold. Therefore, the MR triggers a measurement report back to CU via the current associated RAU. This scheme aims to deliver a fast and robust mobility signalling which ensures a lower failure probability than the traditional HO scheme. And then between RAUs linked with different CUs a simplified HO scheme is offered through utilizing a dedicated one-dimensional DAS network architecture which provides more degree of freedom to optimize the HO scheme for high mobility users. Since a HO process generally occurs when the MR moves from one RAU's coverage area linked to the serving CU to another RAU's coverage area linked to the target CU under a dedicated DAS architecture deployment, the target CU could be known in advance as it will be the only possible candidate that the MR will eventually be handed over to, so that the HO command/RCR can be triggered in advance to assure an improved system performance. Moreover, this chapter also considers the ICI effect on the overall system performance. This chapter further considers the retransmission trials times and their effect on the overall system performance. Finally, closed-form expressions for triggering probability, HO

command failure probability, the total failure probability, average latency, overlapping area distance are derived through theoretical analyses.

The remainder of this chapter is structured as follows. Section 4.2 describes the traditional HO scheme. The proposed schemes along with the system architecture are presented in Section 4.3. Section 4.4 develops an analytical model for traditional and proposed schemes. Finally, the schemes' performance evaluation based on numerical results are introduced and discussed in Section 4.5.

4.2 Traditional Handover Scheme

Traditionally, the HO scheme is divided into handover preparation phase, handover execution phase, and handover completion phase as illustrated in Fig. 4.1. The details of each phase are as follows.

Phase I: Handover Preparation,

1. First, the BS prepares the measurement control to be sent to the MR. The measurement control contains the RFs to be measured and their associated physical cell identification (PCI). Those RFs are known as the measurement objects. Second, the BS sets up a list of reporting configurations. Any report configuration includes the reporting criteria about whether it is a periodic or an event-based as well as the reporting format which sets the reporting entities that should be reported by the UE, e.g., how many cell should be reported. It also includes the required measurement quantities type, namely, RSS, and/or reference signal received power/quality (RSRP/RSRQ). Further, a measurement ID is used to link one measurement object to its reporting configuration. Its worth noting that this chapter assumes the RSQ to be the metric to trigger both FSW and HO schemes. Also, an event based reporting configuration are adopted as the periodical type might delay the process. The measurement control contents are shown in Table 4.1 for the last RAU (RAU N).

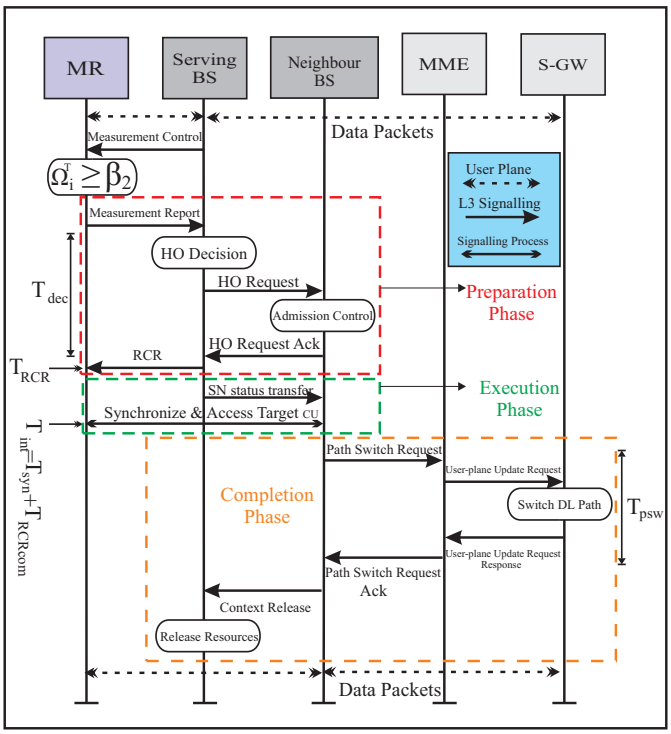

Figure 4.1: Traditional CU-CU handover.

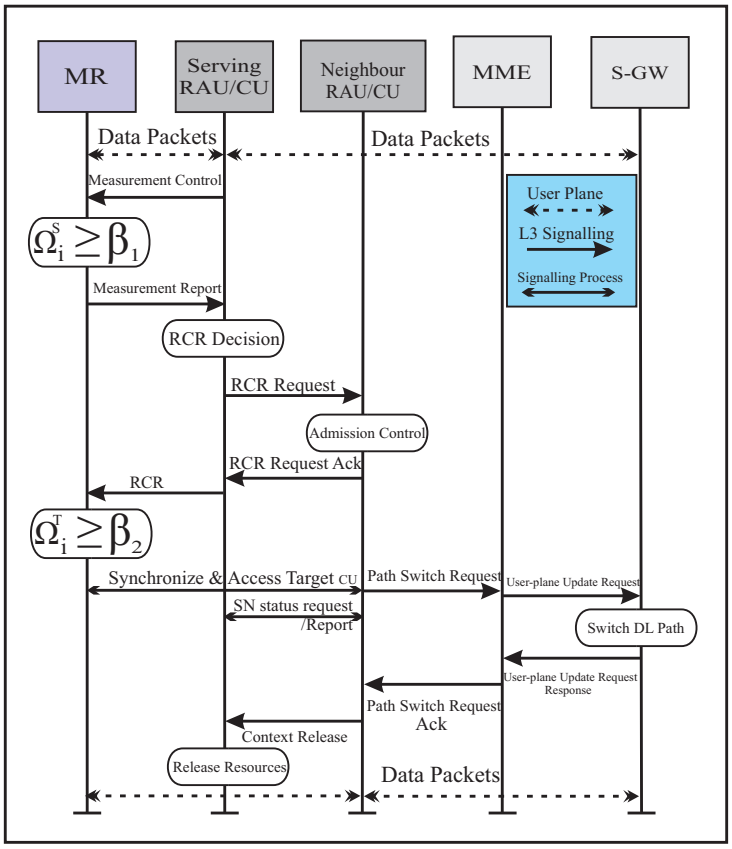

Figure 4.2: Proposed CU-CU handover.

Table 4.1: Measurement control of traditional HO (FSW) scheme for RAU N $(N-1)$.

Measurement Object	Object ID
LTE Target Carrier Frequency, Measurement BW, Offset Frequency, Physical Cell ID (PCI)	1

Object ID	Measurement ID	Report ID
1	1	1

Report ID	Report Configuration
1	Event A4 ($\Omega_i^T \geqslant \beta_2$), TTT, Threshold ($\beta_2$), Triggering Quantity (RSRP and/or RSRQ), Reporting Quantity (e.g., RSRP), Maximum Report Cell

2. As shown in Fig. 4.1, the MR should initially recover the measurement control from the serving BS in order to set the triggering configuration. After recovering the triggering configurations, and once the triggering condition i.e., the RSQ of target, denoted by Ω_i^T (in dB), is higher than or equal to a predefined threshold (β_2) (A4 event triggering condition type in LTE-A), holds true for a time-to-trigger (TTT) value. The MR issues the measurement report which contains the PCI that satisfies the triggering condition back to the serving BS. The contents of the measurement report are illustrated in Table 4.2.

3. The serving BS immediately performs the HO decision algorithm once it recovers the measurement report successfully to determine whether to hand over. The serving BS then issues a HO request to the target BS. The target BS then performs the admission control algorithm to reserve the requested resources, and then responds with a HO request acknowledgement (ACK) which mainly contains the HO command to be transferred transparently to the serving BS along with the admitted E-UTRAN radio access bearer (E-RAB) list. Next, the serving BS issues the RCR command to the MR, the command includes a new cell radio network temporary identifier (C-RNTI), dedicated random access channel (RACH) preamble, RACH response window size needed to access target cell, and the target BS security algorithm identifiers. It may also include the master information block (MIB) as well as the system information blocks (SIBs) required to access the target BS. At the meantime, the serving BS sends packet data convergence protocol (PDCP) sequence number (SN) information to the target BS in a SN status transfer message. This is

Table 4.2: Measurement report content.

Serving CU m Enhanced Fast HO Scheme	Measurement ID (1), RSRQ ($\Omega_i^S \leqslant \beta 1$) Measurement ID (2), RSRQ ($\Omega_i^T \geqslant \beta_2$), PCI, Measurement Quantity (RSRQ)
BS (Serving CU m) Traditional HO (FSW) Scheme	Measurement ID (1), RSRQ ($\Omega_i^T \geqslant \beta_2$), PCI, Measurement Quantity (RSRQ)

crucial to avoid missing or duplicate packets during the HO process.

Phase II: Handover Execution,

4. If the MR is able to recover RCR command successfully, then the MR is immediately detached from the serving and try to synchronize and access the target. If the access procedures finished successfully by receiving RCR complete command from the MR, the completion phase is initialized, and the MR can now transmit and receive via the target BS.

   Phase III: Handover Completion,

5. At this stage, the target BS sends a path switch request to the mobility management entity (MME) which in turn will send a user plane update request to the serving gateway (S-GW) to switch the downlink path from the serving to the target BS. The S-GW then sends a user plane update response to MME. Finally, MME responds with a path switch request ACK to target BS which in turns sends a UE contest release to the serving BS.

Traditional HO scheme was designed and optimized originally for the two-dimensional cell layout, where the MR might have multiple candidate BSs to scan and measure continuously. In this context, the target cell can not be known in advance. As a result, HO commands such as the measurement report, RCR, synchronize and RCR complete, all of which were sent/performed at the cell edge where the channel might experience poor conditions which might in turn increase the failure probability. Failure event consequently causes a longer interruption time during which all of the packets of the unacknowledged type will be lost, which will considerably decease the system throughput.

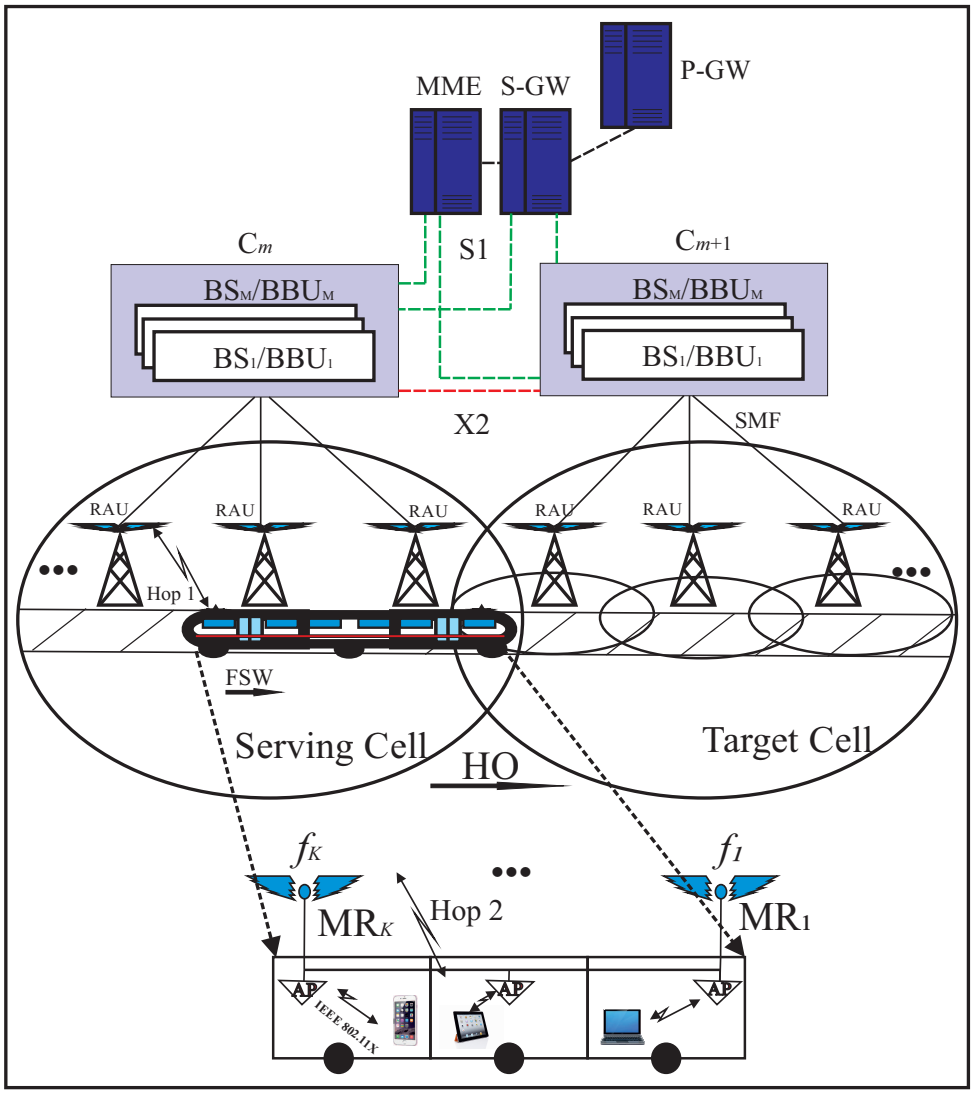

Figure 4.3: DAS LTE-A system architecture entities.

4.3 Proposed Schemes

In this chapter, by utilizing the two-hop architecture, with the target of providing low-latency and ultra-reliability, the MR is envisioned to perform two-schemes. First is the FSW scheme exploited to shift the serving frequency between two RAUs under the control of the same CU when the MR runs from one RAU to the other RAU. When the MR moves to a neighbouring RAU belonging to another CU, a HO scheme will be initiated. Both strategies are designed based on the 3GPP specification [105]. Before explaining the two schemes, the details of the system architecture are explained as follows.

4.3.1 System Architecture

A carefully designed system architecture is a vital key to provide multi-objective solutions delivering low-latency, high data rates, ultra-reliable transmission links, and a seamless mobility to preserve high QoS to end users. For that purpose, this chapter proposes a DAS network infrastructure based two-hop architecture as shown in Fig. 4.3.

In such networks, there is no need for a HO between adjacent RAUs under the control of the same CU even though multiple radio frequencies (RFs) (multiple BSs/BBUs under the control of the same CU) might be used within the control of a specific CU, by exploiting FSW scheme which will be explained in details in Section 4.3.2. Avoiding the need for HO under the control of the same CU coverage area, which could be extended to 40 km [1], means that the HO rate could be greatly reduced. Therefore, a better QoS experience could be achieved. Further, in order to have a smooth and simple synchronous switching process, the train could be split into a couple of non-interfering RF zones which are connected to their own corresponding RAUs communicating utilizing the same RFs. This means that RAU footprint is directly pertinent to the train carriages physical length. Specifically, each RF zone creates a small cell in the range of 200 m or even smaller than that. Moreover, deploying RAUs in a linear one-dimensional layout provides the ability to simplify/optimize the HO scheme for such a network topology. In such a topology, the target CU/RAU can be known early enough to trigger part of the mechanism in advance, namely triggering the HO scheme earlier so that the MR is able to recover the HO command with a lower failure probability than the traditional scheme as there is only one possible target RAU to camp on. This improves the overall system performance as provided in Section 4.6.

Furthermore, the core network contains a MME and a S-GW along with a packet gateway (P-GW). Having one MME, S-GW, and P-GW entities controlling multiple CUs further reduces the HO rates due to either MME or S-GW/P-GW HO/relocation [106] which incurs more delay and signalling overhead cost that might otherwise affect the user's QoS.

4.3.2 Frequency Switch Scheme

Herein, a FSW scheme is proposed and composed of three-phases: switching preparation, switching execution, and switching completion. Fig. 4.4 shows the FSW decision algorithm performed by the serving CU (m). In the following, without loss of generality, the FSW process of the first MR is described. The details are as follows.

Phase I: Switching Preparation,

1. After recovering the measurement control (shown in Table 4.1) from the serving RAU (S) triggered by the serving CU m, the MR will be able to distinguish the RFs to be measured and their associated PCIs.

2. Once the triggering condition ($\Omega_i^T \geqslant \beta_2$) sustains for a TTT value, the MR triggers the measurement report (shown in Table 4.2) including PCI, which fulfils the triggering condition, back to CU m. The MR should be pre-configured not to expect to receive RCR command when moving between RAUs belongs to the same CU, instead it expects to receive a measurement control to update the MR with the new associated frequencies along with their corresponding PCIs. Note that at each time an FSW scheme is performed, CU m should send a measurement control to update the MR with the new list of frequencies and their associated PCIs.

3. CU m immediately performs the FSW decision algorithm (see Fig. 4.4) after recovering the measurement report successfully to determine whether to switch. Note that the preparation phase of the FSW scheme does not need to carry out the admission control algorithm when switches between RAUs belongs to the same CU, as the switching process does not encounter CU change.

Phase II: Switching Execution,

4. In case CU m decides to switch the MR from S to neighbour RAU (T). Immediately, CU m switches all the MR's packets from RAU S to RAU T by modulating the intended stream with the same frequency f but this time for RAU T. During the FSW process the only occurred interruption is the contribution of the optical switcher switching time. Thus, the FSW scheme interruption time is equivalent to the optical switcher capability. Throughout this period, CU m buffers the packets intended for this particular MR until the switching process performed successfully.

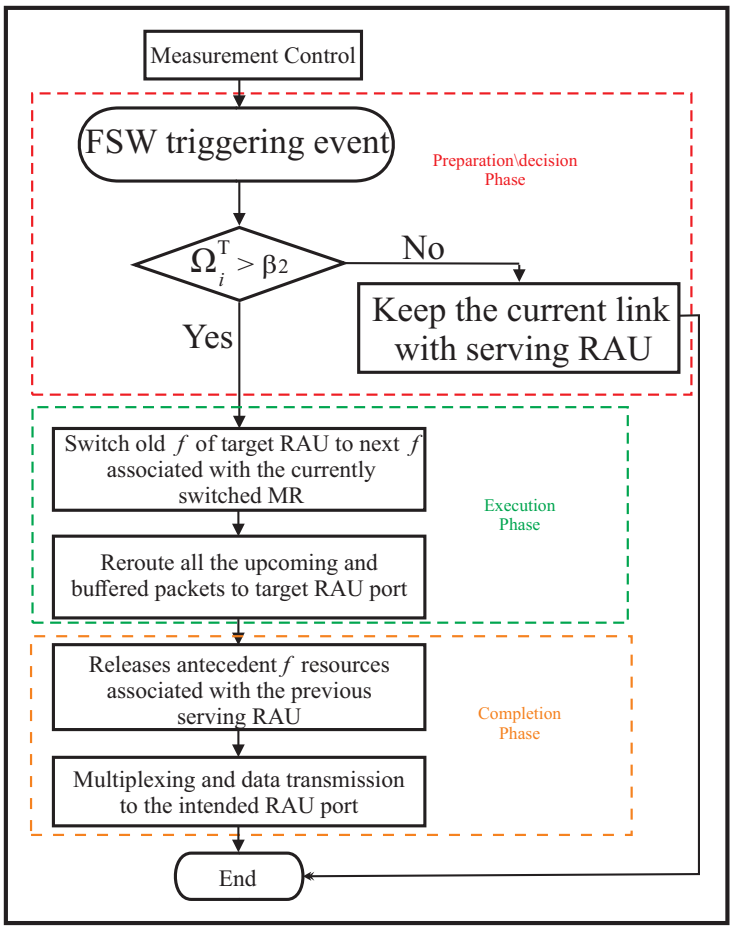

Figure 4.4: Frequency switch scheme algorithm.

Since, the switching process happens within the control of the same CU, then, the switching scheme does not require to perform either bi-casting [107] or data forwarding [105]. Consequently, all the incurred overhead associated with such processes will not take place herein whether the delay or the associated signalling overhead. Because the switching is timely very brief, and both RAU S and RAU T are under the control of the same CU m, hence CU m is capable of buffering the packets until a successful switching takes place. Thereby, this scheme can provide a lossless communication during the switching process. Moreover, there will be no need for the MR to detach from RAU S and perform a synchronization (neither frequency nor downlink synchronizations is needed) to RAU T, as they will be using the same time-frequency set to communicate, and they are controlled by the same CU m as well. Furthermore, there will be no RACH preamble or access parameters negotia-

tion, as it is already uplink synchronized, and the MR is connected and linked to the same CU m. Therefore, there is no need to send neither RCR nor RCR complete commands as the CU is internally controlling the switching process, enabling the MR to be linked to RAU with the best available signal quality. From the moving MR point of view, at a particular moment it is transmitting/receiving to/from RAU S, after awhile it will be transmitting/receiving to/from RAU T with a considerable small interruption time. As a result, the proposed scheme is fully controlled and executed by the network instead of the MR as in the traditional HO scheme. Since, all the above mentioned operations are not needed by the FSW mechanism, consequently their associated negotiating messages are not needed either. As a result, FSW scheme is able to provide a fast and reliable scheme compared with the traditional HO when moving between RAUs belongs to the same CU.

Phase III: Switching Completion,

5. Once CU m finishes the switching scheme successfully for the first MR, the old RAU S releases the antecedent f and associates with another frequency to connect with the upcoming MR (if already has been requested). Afterwards, a multiplexing process and transmission of the streams to the intended RAUs will take place.

For the FSW scheme, traditional HO procedures including SN status transfer, path switch, and UE context release will not be performed as CU m is the same. Also, there is no need for tracking area update as the S-GW is not changed.

4.3.3 Proposed Enhanced Fast CU-CU Handover

Based on a dedicated linear one-dimensional DAS architecture shown in Fig. 4.3, this chapter proposes a simplified HO scheme by which the MR triggers a measurement report back to the serving cell based on a predefined condition satisfaction which in turn will respond with a RCR command. It is worth mentioning that the proposed scheme is not practical to be used in the traditional hexagonal deployment shown in Fig. 4.5, as the MR will be measuring multiple RSQ associated with multiple candidate BSs, and therefore can not decide which one is the best to camp on until the MR is already at the cell edge. Triggering an early RCR command aims to enhance RCR success probability and

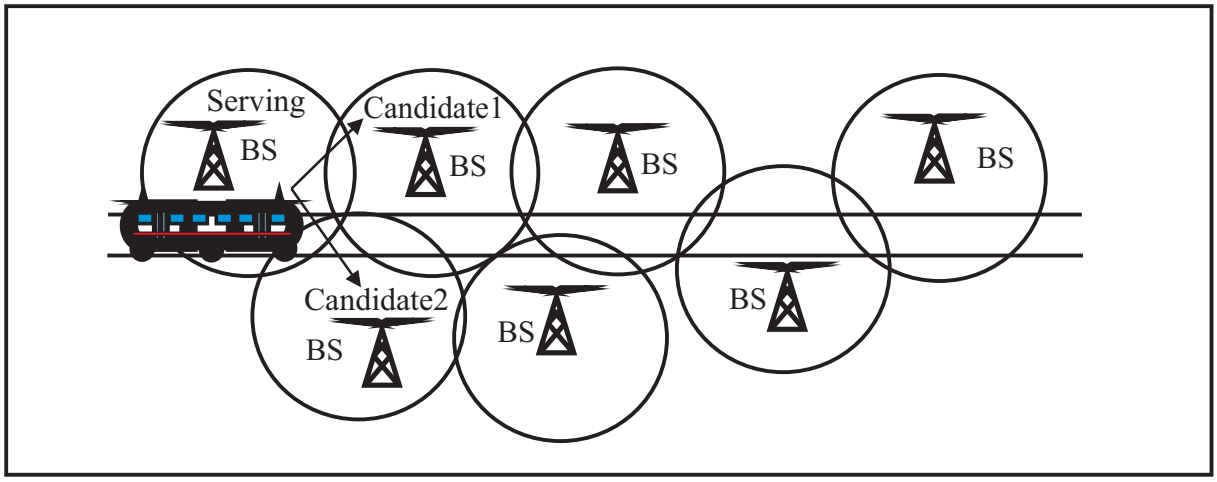

Figure 4.5: Traditional two-dimensional cell layout.

consequently to avoid the long service interruption time associated with a HOF event. The proposed scheme consists of three-phases: handover preparation, handover execution, and handover completion. Fig. 4.2 illustrates the signalling flow of the proposed scheme. The details are as follows.

Phase I: Handover Preparation,

1. Once the MR detects the need to trigger FSW process upon FSW triggering condition satisfaction, the MR triggers a measurement report back to CU m. The measurement report includes PCI that has the highest RSQ. Once received by CU m, CU m observes that the RAU requested to be switched to the last controlled RAU, then CU m perceives that the MR will request to hand over soon. Therefore, CU m issues another measurement control to set the triggering condition of the HO scheme, as shown in Table 4.3.

2. According to the predefined configuration provided by CU m to the MR via the measurement control, the MR triggers a measurement report upon satisfying the triggering condition for a TTT value. The triggering condition sets for this event is that the RSQ of RAU S $\Omega_i^S \leqslant \beta_1$. The predefined threshold is chosen so that measurement report and the corresponding response (RCR command) may have the highest transmission success probability throughout RAU S coverage area. Accordingly, the set threshold should be the highest RSQ that can be achieved under the

Table 4.3: Measurement control of the proposed enhanced fast HO scheme sent through the last RAU (N).

Measurement Object	Object ID
LTE Serving Carrier Frequency, Measurement BW, Offset Frequency, Physical Cell ID (PCI)	1
LTE Target Carrier Frequency, Measurement BW, Offset Frequency, Physical Cell ID (PCI)	2

Object ID	Measurement ID	Report ID
1	1	1
2	2	2

Report ID	Report Configuration
1	Event A2 ($\Omega_i^S \leqslant \beta_1$), TTT, Threshold ($\beta_1$), Triggering Quantity (RSRP and/or RSRQ), Reporting Quantity (e.g., RSRP), Maximum Report Cell
2	Event A4 ($\Omega_i^T \geqslant \beta_2$), TTT, Threshold ($\beta_2$), Triggering Quantity (RSRP and/or RSRQ), Reporting Quantity (e.g., RSRP), Maximum Report Cell

coverage area of RAU S, which should be obtained near RAU S location (typically when the MR reaches the middle point of RAU S coverage area).

3. Upon reception of measurement report by CU m via RAU S, CU m then performs a HO decision algorithm to check if the RSQ is higher than or equal to the threshold, if CU m decides to do so. Next, CU m sends a HO request to CU $m+1$. Subsequently, CU $m+1$ performs the admission control algorithm to determine whether to accept the request or not. If the target CU $(m+1)$ is capable of providing the requested resources, consequently, CU $m+1$ sends a HO request ACK back to CU m. Afterwards, CU m transmits the HO/RCR command immediately to the MR.

4. As soon as the MR recovers RCR command successfully, the MR keeps the command for a later use and maintains the current link with RAU S.

   Phase II: Handover Execution,

5. Thereafter, the MR waits for the complementary HO triggering condition to be satisfied ($\Omega_i^T \geqslant \beta_2$). When this condition is met, the MR can then (follows one of two-approaches either) sends a measurement report to notify CU m that the HO process will be performed immediately. If the initial measurement report was failed to be recovered, the MR can try to send the maximum allowed retransmission trials. If the MR did not receive the corresponding ACK, (or) the MR can detach (immediately) from CU m and try to access CU $m+1$ by performing step 6. While

If CU m successfully recovers it, then it stops sending the MR packets and sends SN status transfer. MR detaches from CU m and uses RCR command content to access CU $m+1$. The MR then performs access procedure with CU $m+1$ and the rest is the same as the traditional HO scheme.

6. Immediately upon CU $m+1$ perceives that the MR is trying to access it (any packet received from the MR via the target RAU T will initiate the upcoming procedure), it sends a SN status request back to CU m, CU m responds with a SN status report back to CU $m+1$. At the moment of SN status request reception, CU m realizes that the MR has been detached from it and currently performing HO. Accordingly, CU m stops sending packets to the detached MR, and then responds with a SN status report back to CU $m+1$ to ensure a lossless HO process. It should be pointed out that the HO completion phase is identical to LTE/LTE-A standard.

To conclude, the proposed scheme avoids the loss/failure to recover both measurement report and/or RCR messages as the proposed scheme enables an early transmission of both commands in which the failure probability is trivial due to the high RSQ which has been used to send the commands on. In contrast, measurement report and especially RCR command might be susceptible to transmission failure (which leads to either retransmission attempts which hinder the HO process or a HOF event) in the traditional HO scheme. This is due to the fact that the MR receives RCR at the cell edge where the RSQ is deteriorated (i.e., the MR is moving away from RAU S) and the interference level in some situation might be high as well, not to mention the Doppler effect which makes HSR scenario a challenging environment.

4.4 Analytical Model

As stated earlier, once the MR detects that the triggering condition is met for a TTT period, it sends a measurement report back to CU_m for evaluation. Then, CU_m performs the FSW/HO decision algorithm to decide whether to switch/handover the MR to the next RAU. The main criteria in deciding the need for switching/handing over is the value of the received signal quality, i.e. the received signal quality of the reference/pilot signals

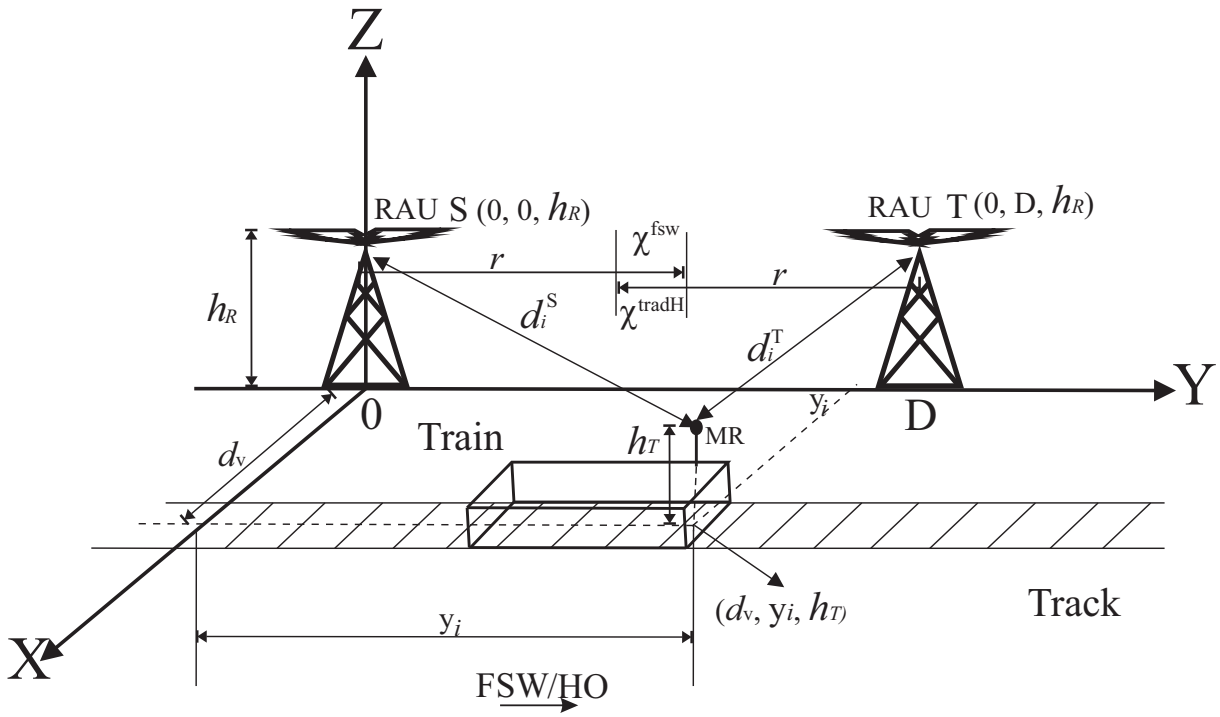

Figure 4.6: System model shows the parameters for both the HO and the FSW case.

sent by the serving RAU S or the target RAU T. Because railway tracks are generally constructed in a wide rural area and/or in a viaduct area, where multipath effect could be ignored most of the time [5, 30, 88], only the large scale fading is considered in the analysis. Thus, the same system model of the previous chapter is used here except for the large scale fading and the distance model associated with it. According to WINNER II model, specifically, D2a rural moving networks scenario [89], $P_{L_i}^k$ can be given by

$$P_{L_i}^k[dB] = \begin{cases} 44.2 + 20\log_{10}(d_i^k) + 20\log_{10}(f[GHz]/5) + 10\log_{10} g_i^k, & 10m < d_i^k < d_{BR}, \\ 10.5 + 40\log_{10}(d_i^k) + 1.5\log_{10}(f[GHz]/5) - 18.5\log_{10}(h_R) & \\ -18.5\log_{10}(h_T) + 10\log_{10} g_i^k, & d_{BR} < d_i^k < 10km, \end{cases} \tag{4.1}$$

where d_i^k is the distance between the MR and RAU $k \in \{S, T\}$. As shown in Fig. 4.6, d_i^T and d_i^S can be obtained as

$$d_i^T = \sqrt{(d_v)^2 + (D - y_i)^2 + (h_R - h_T)^2}, \tag{4.2}$$

and

$$d_i^S = \sqrt{(d_v)^2 + (y_i)^2 + (h_R - h_T)^2}, \tag{4.3}$$

respectively, where D is the inter-RAU distance between two successive RAUs, y_i is the MR's current location, and d_v is the distance between the RAU and the track. h_R and h_T are the heights of RAU and train, respectively. In contrast to the previous chapter we employ a more accurate 3-dimensional model to represent the distance between RAU k and the MR. $d_{BR} = 4h_R h_T f/c$ is the breaking point distance. Since the distance from the MR to the RAU satisfies $10m < (d_i^k) < d_{BR}$, the first sub-domain of (5.3) is employed in this chapter to model the large scale fading.[1]. Then, the rest system model is the same as the previous chapter[2].

4.5 Performance Evaluation

To investigate the effectiveness of the proposed schemes, in this section, triggering probability and failure probability will be analysed and compared with that of the traditional HO scheme. Further, a crucial key performance metric of QoS, i.e., the total average HO latency, will be investigated to verify the system ability to support low-latency services. Furthermore, the required overlapping area length of each scheme will be studied.

4.5.1 Triggering Probability

1. Traditional HO Scheme

   For traditional HO case, the HO process is triggered if and only if the triggering condition ($\Omega_i^T \geq \beta_2$) is satisfied. Consequently, the HO triggering probability for

[1]By assuming h_R and h_T are 4m and 32m, respectively, we have $d_{BR} = 4h_R h_T f/c = 32 \times 32 \times 10^9/(3 \times 10^8) = 3413.3$m. The maximum d_i^T is $\sqrt{(10)^2 + (200)^2 + (4-32)^2} = 202.1979$m, and the maximum d_i^S is $\sqrt{(10)^2 + (0)^2 + (4-32)^2} = 29.732$m. Then, we have $10m < (d_i^k) < d_{BR}$, and therefore the first sub-domain of (5.3) is used to model P_L.

[2]Without loss of generality a single MR is considered in the analysis, as the others achieve the same results.

the traditional case can be found as

$$\begin{aligned}\mathbf{P}_{trigg}^{tradH} &= \mathbf{P}\left\{\Omega_i^T \geqslant \beta_2\right\}, \\ &= \mathbf{P}\left\{A - 20\log_{10} d_i^T - 10\log_{10} g_i^T - 10\log_{10}\sigma_o^2 - I_i^T \geqslant \beta_2\right\}, \\ &= \mathbf{P}\left\{10\log_{10} g_i^T \leqslant A - \beta_2 - 20\log_{10}(d_i^T) - 10\log_{10}\sigma_o^2 - I_i^T\right\}, \\ &= 1 - Q\left(10^{\dfrac{A - \beta_2 - 20\log_{10}(d_i^T) - 10\log_{10}\sigma_o^2 - I_i^T}{10\cdot\sigma_i^T}}\right), \end{aligned} \tag{4.4}$$

where $Q(x) = \frac{1}{\sqrt{2\pi}}\int_x^\infty e^{\frac{-t^2}{2}}dt$ is the Q-function.

2. Frequency Switch Scheme

   The proposed FSW scheme triggers a measurement report to RAU S if the MR detects $\Omega_i^T \geqslant \beta_2$ for a TTT period. Let $\mathbf{P}_{trigg}^{fsw}$ denotes the FSW triggering probability. Similarly, $\mathbf{P}_{trigg}^{fsw}$ can be derived as equality (4.4). For the FSW scheme, once the MR triggers the report back to CU m and it has been recovered correctly, a successful FSW process is achieved, as the other procedures are conducted at the CU side and there are no further command messages to be exchanged between CU m and the MR, which might be susceptible to losses and retransmission events.

3. Enhanced Fast HO Scheme

   For the proposed scheme, the triggering probability consists of two parts. The first part is related to trigger the measurement report back to CU m to initiate the early HO request whenever the predefined condition is fulfilled ($\Omega_i^S \leq \beta_1$). The second part is associated with accessing CU $m+1$ once the predefined condition ($\Omega_i^T \geq \beta_2$) is satisfied. Therefore, the HO triggering probability for the proposed enhanced fast

HO scheme can be derived as

$$\begin{aligned}
\mathbf{P}_{trigg}^{efH} &= \Big[\mathbf{P}\left\{\Omega_i^S \leqslant \beta_1\right\}\Big] \cdot \mathbf{P}\left\{\Omega_i^T \geqslant \beta_2\right\}, \\
&= \Big[\mathbf{P}\left\{A - 20\log_{10} d_i^S - 10\log_{10} g_i^S - 10\log_{10}\sigma_o^2 - I_i^S \leqslant \beta_1\right\}\Big] \cdot \\
&\quad \Big[1 - Q\left(10\,\frac{A - \beta_2 - 20\log_{10}(d_i^T) - 10\log_{10}\sigma_o^2 - I_i^T}{10\cdot\sigma_i^T}\right)\Big], \\
&= \Big[\mathbf{P}\left\{10\log_{10} g_i^S \geqslant A - \beta_1 - 20\log_{10}(d_i^S) - 10\log_{10}\sigma_o^2 - I_i^S\right\}\Big] \cdot \\
&\quad \Big[1 - Q\left(10\,\frac{A - \beta_2 - 20\log_{10}(d_i^T) - 10\log_{10}\sigma_o^2 - I_i^T}{10\cdot\sigma_i^T}\right)\Big], \\
&= \Big[Q\left(10\,\frac{A - \beta_1 - 20\log_{10}(d_i^S) - 10\log_{10}\sigma_o^2 - I_i^S}{10\cdot\sigma_i^S}\right)\Big] \cdot \\
&\quad \Big[1 - Q\left(10\,\frac{A - \beta_2 - 20\log_{10}(d_i^T) - 10\log_{10}\sigma_o^2 - I_i^T}{10\cdot\sigma_i^T}\right)\Big]. \qquad (4.5)
\end{aligned}$$

For the first triggering event and since the serving RSQ has the same RSQ behavior before and after crossing the RAU origin point (periodic nature). Then, the first condition might be satisfied sooner than it should. To prevent that form happening, the MR can use the Doppler shift properties to infer if the MR is approaching the RAU or moving away. That is, if the MR observes a negative Doppler shift, then the MR is moving away from the RAU and thats when the MR can trigger a measurement report back to the serving RAU upon the triggering condition satisfaction.

4.5.2 Failure Probability

1. Traditional HO Scheme

   For the traditional HO scheme, the MR is required to negotiate commands with both CU m and CU $m+1$ in order to have a successful HO. Specifically, the MR should recover RCR sent by CU m, and then synchronize with CU $m+1$ by sending the RACH preamble thereafter receiving the response from CU $m+1$. Finally, the MR sends a RCR complete command back to CU $m+1$ to finalize the HO scheme

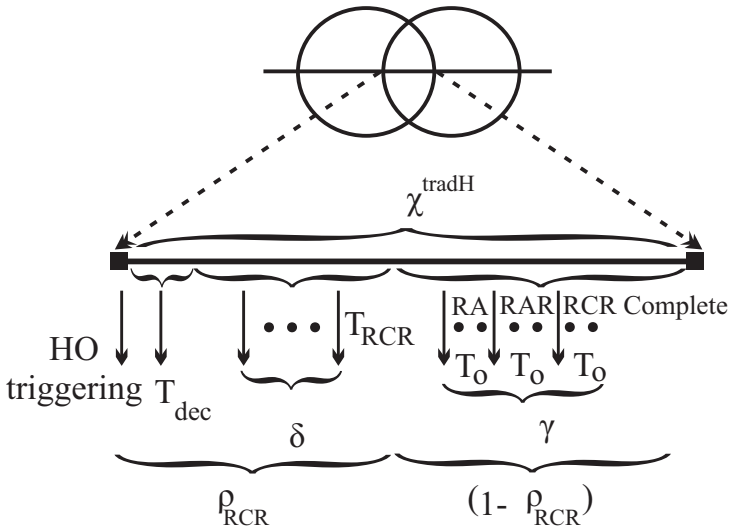

Figure 4.7: System model depicts the operations performed within the overlapping area associated with the traditional HO scheme.

successfully. It can be seen that both Ω_i^S and Ω_i^T should be larger than or equal to U which is the minimum signal threshold required to recover the commands successfully. Generally, failure events happen due to either a HO command reception failure or a target access failure. As RCR failure event is the main reason behind most of the HOF events as mentioned in [85], we only consider RCR failure in our analysis for the failure probability associated with CU m. RCR is traditionally sent over the cell edge within the overlapping area where Ω_i^S might be deteriorated. Losses of these commands will result in HOF events. To increase the success probability of the HO process, retransmission attempts are allowed at the cost of increased signalling overhead as well as HO latency. To obtain the maximum possible number of RCR trials, the HO preparation phase is assumed to be triggered at the beginning point of the overlapping area. Subsequently, the maximum number of retransmissions for the RCR command can be obtained as

$$\delta = \left\lfloor \frac{\rho_{RCR} \cdot \chi^{tradH} - v \cdot T_{dec}}{v \cdot T_{RCR}} \right\rfloor, \tag{4.6}$$

where $\lfloor \cdot \rfloor$ denotes the floor function. χ^{tradH} is the overlapping area associated with the traditional HO, v denotes the train's speed. T_{RCR} and T_{dec} are RCR transmission time and the time required to perform the HO decision algorithm, respectively. ρ_{RCR} is the overlapping area percentage dedicated to perform HO algorithm decision and

to recover RCR command. As a result, the RCR failure probability denoted as $\mathbf{P}_{f_{RCR}}^{tradH}$ for multiple retransmissions can be obtained as in equality (3.15). While γ denotes the maximum number of retransmission trials associated with the target access procedures, given by

$$\gamma = \left\lfloor \frac{(1-\rho_{RCR})\chi^{tradH}}{3 \times v \times T_o} \right\rfloor, \tag{4.7}$$

where T_o is the time cost of transmitting a one command message of the three-commands associated with the target access procedures. Unlike previous chapter, we adopt $\lfloor \cdot \rfloor$ to calculate the retransmission trials and consequently can obtain a more accurate failure probability associated with each retransmission trials type. Now, since a HOF event happens due to either failing to recover RCR command or failing to access the target RAU T, the HOF probability can be expressed as

$$\mathbf{P}_{f}^{tradH} = \left[\mathbf{P}_{f_{RCR}}^{tradH} + (1 - \mathbf{P}_{f_{RCR}}^{tradH}) \cdot \underbrace{\left[\prod_{z=1}^{\gamma} \mathbf{P}_{f_{tar_z}} \right]}_{(\mathbf{P}_{f_{tar}}^{tradH})} \right]. \tag{4.8}$$

where $\mathbf{P}_{f_{tar}}$ is the failure probability associated with the target RAU T and it can be calculated as in equality (3.18). Note that (4.8) applies for the no retransmission case when $\delta = 1$ and γ =1. Fig. 4.7 clarifies the HO operations performed within the overlapping area for the traditional case. Note that χ^{tradH} can be calculated as in equality (3.13). where $T_{304} = 50$ ms is the maximum time allowed to finalize the target access procedure as stated by the standard [92]. As a result, T_{304} can be obtained as

$$T_{304} = \gamma \cdot [(3 \times T_o)], \tag{4.9}$$

The value of T_{304} is optimized for nomadic-to-medium mobility speed, so we did not consider it here for the high-speed train as a sufficient number of retransmissions should be allowed to reduce the probability of a failure event.

2. Frequency Switch Scheme

   After the triggering condition is satisfied, the MR will issue the report back to the serving RAU S. If the serving RAU S cannot recover the command successfully,

the MR retransmits the command again until the command is successfully received or a failure event occurs. The maximum possible transmission trials for recovering the measurement report can be then found as

$$\alpha = \left\lfloor \frac{\chi^{fsw} - v \cdot T_{dec}^{fsw}}{v \cdot T_{mr}^{fsw}} \right\rfloor, \tag{4.10}$$

where χ^{fsw} is the total FSW overlapping area. T_{mr}^{fsw} and T_{dec}^{fsw} are a one-time transmission delay to recover the measurement report and the time required to perform the FSW scheme decision algorithm, respectively. Accordingly, the measurement report failure probability, $\mathbf{P}_{f_{mr}}^{fsw}$, and the failure probability of the FSW scheme per RAU, $\mathbf{P}_{f}^{fsw}$, considering retransmissions can be obtained as

$$\begin{aligned} \mathbf{P}_{f}^{fsw} = \mathbf{P}_{f_{mr}}^{fsw} &= \prod_{z=1}^{\alpha} \left[\mathbf{P} \left\{ \Omega_{i,z}^{S} < U \right\} \right] \\ &= \prod_{z=1}^{\alpha} \left[Q \left(10 \frac{A - 20\log_{10}(d_{i,z}^{S}) - 10\log_{10}\sigma_{o}^{2} - I_{i,z}^{S} - U}{10 \cdot \sigma_{i}^{S}} \right) \right], \end{aligned} \tag{4.11}$$

respectively. Note that (4.11) applies for the no retransmission case when $\alpha = 1$.

3. Enhanced Fast HO Scheme

   The proposed fast HO scheme can trigger RCR command earlier, thanks to the unique possible candidate cell to attach to. The singular target RAU T is enabled as a result of using a dedicated one-dimensional cell layout deployed along the rail track. Thence, to obtain the maximum number of retransmission trials associated with RCR for the enhanced fast HO scheme, and since the preparation phase as well as RCR command can be performed and received in advance outside the overlapping area with a high probability, the maximum retransmission trials count can be then given by

$$\vartheta = \left\lfloor \frac{(r - \chi^{efH}) - v \cdot T_{dec}}{v \cdot T_{RCR}} \right\rfloor, \tag{4.12}$$

   where r and χ^{efH} are the RAU radius and the overlapping area length associated with the proposed HO scheme, respectively. Similarly, the maximum retransmission

trials associated with the target access procedures can be calculated as follows

$$\xi = \left\lfloor \frac{\chi^{efH}}{3 \times v \times T_o} \right\rfloor. \tag{4.13}$$

Therefore, the RCR failure probability $\mathbf{P}^{efH}_{f_{RCR}}$ and the HOF probability $\mathbf{P}^{efH}_{f}$ of the proposed scheme can be obtained as

$$\mathbf{P}^{efH}_{f_{RCR}} = \prod_{z=1}^{\vartheta} \left[\mathbf{P}\left\{ \Omega^{S}_{i_z} < U \right\} \right] = \prod_{z=1}^{\vartheta} \left[Q\left(10 \, \frac{A - 20\log_{10}(d^{S}_{i,z}) - 10\log_{10}\sigma^2_o - I^{S}_{i,z} - U}{10 \cdot \sigma^{S}_{i}} \right) \right]. \tag{4.14}$$

and

$$\mathbf{P}^{efH}_{f} = \Bigg[\mathbf{P}^{efH}_{f_{RCR}} + (1 - \mathbf{P}^{efH}_{f_{RCR}}) \cdot \underbrace{\cdot \Big[\prod_{z=1}^{\xi} \mathbf{P}_{f_{tar_z}} \Big]}_{(\mathbf{P}^{efH}_{f_{tar}}) \text{ Proposed target access failure probability}} \Bigg]. \tag{4.15}$$

respectively. Note that (4.14) and (4.15) apply for the no retransmission case when $\vartheta = 1$ and ξ =1.

4.5.3 Average Latency

The average latency associated with transferring an ongoing session from cell to cell is a critical metric of evaluating a HO scheme. Such a latency is directly related to the negotiated signalling messages during the scheme. Less negotiated messages lead to a more seamless process. This latency can be categorized into two types according to the outcome whether it results in a success or a failure event.[3]

1. Average Success Latency

   The HO (FSW) success latency is defined as the time epoch from the moment the serving CU m recovers (the MR triggers) the measurement report to the moment the S-GW (serving CU m) switches the path to the target CU $m+1$ (RAU T).

   A) Handover Scheme

   As Fig. 4.1 depicts, HO decision, RCR, RA, RAR, RCR completion, and path switch

[3]As we aim to investigate the efficiency of the HO/FSW schemes, the fibre, processing, and uplink grant latencies are not considered in the latency analysis for simplicity.

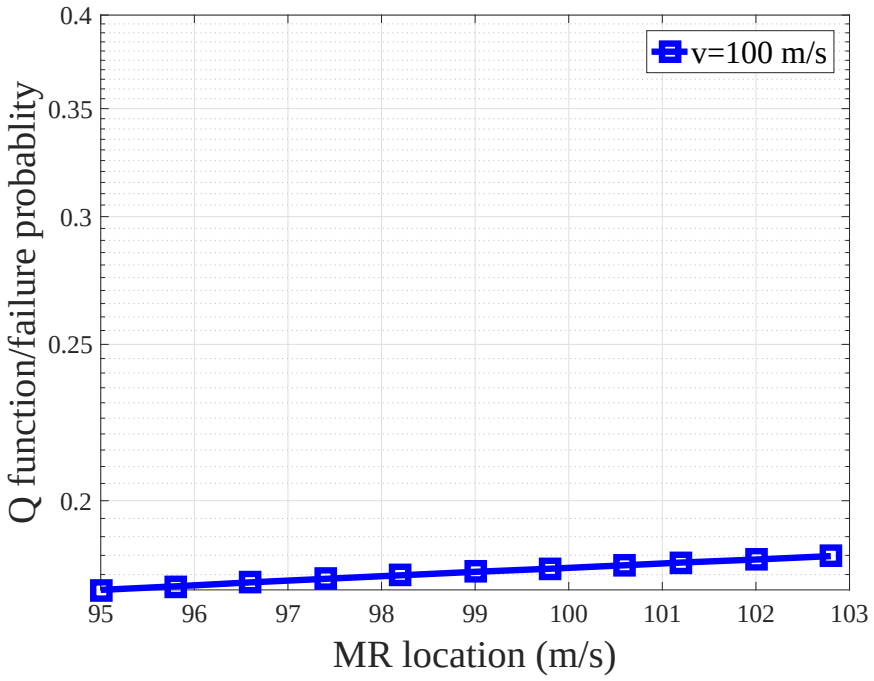

Figure 4.8: The failure probability of a single transmission versus the MR location under a train's speed of 100 m/s.

are messages/processes that contribute to the success HO latency. Therefore, the average success HO latency for the traditional HO scheme can be found as

$$T_{succ}^{tradH} = T_{dec} + \overline{\delta_s} \cdot T_{RCR} + \overline{\gamma_s} \cdot (3 \times T_o) + T_{psw}, \tag{4.16}$$

where T_{psw} is the path switch process latency. $\overline{\delta_s}$ denotes the average number of RCR retransmissions. We will assume that the probability of failure of various retransmission trials are independent. This assumption is reasonable assuming a train's speed of 100 m/s and retransmission time of 8 ms. Fig. 4.8 plots the probability of failure for a single transmission starting from 95m to 102.8m in increasing steps of 0.8m. As can be seen, the probabilities are monotonically increasing from 0.1761 to 0.1848 which represents an increase gain of only 4.43% for ten retransmissions. Thus, the failure probabilities of the retransmission trials can be assumed fixed, as the changing in the failure probabilities is trivial. As a result, the failure probability

of the RCR command can be then represented as

$$\mathbf{P}_{f_{RCR}}^{tradH} = \left[\mathbf{Q}\left(10\,\frac{A - 20\log_{10}(d_i^S) - 10\log_{10}\sigma_o^2 - I_i^S - U}{10\cdot\sigma_i^S}\right)\right]^{\delta},$$

The same concept applies for other cases, therefore $\overline{\delta_s}$ can be obtained as

$$\overline{\delta_s} = \left\lfloor \sum_{n=1}^{\delta} n\cdot\mathbf{P}\left\{\delta_s = n|\text{RCR is successful}\right\}\right\rfloor = \left\lfloor \frac{1}{(1-\mathbf{P}_{f_{RCR}}^{tradH})}\sum_{n=1}^{\delta} n\cdot\mathbf{P}\left\{\delta_s = n\right\}\right\rfloor \tag{4.17}$$

and

$$\mathbf{P}\left\{\delta_s = n\right\} = \Big[\mathbf{P}\left\{\Omega_i^S < U\right\}\Big]^{n-1}\cdot\Big[(1-\mathbf{P}\left\{\Omega_i^S < U\right\})\Big]. \tag{4.18}$$

Then,

$$\overline{\delta_s} = \left\lfloor \frac{1}{(1-\mathbf{P}_{f_{RCR}}^{tradH})}\sum_{n=1}^{\delta} n\cdot\Big[\mathbf{P}\left\{\Omega_i^S < U\right\}\Big]^{n-1}\cdot\Big[(1-\mathbf{P}\left\{\Omega_i^S < U\right\})\Big]\right\rfloor. \tag{4.19}$$

The term $\sum_{n=1}^{\delta} n\cdot\Big[\mathbf{P}\left\{\Omega_i^S < U\right\}\Big]^{n-1}$ can be simplified further as follows

$$\frac{(\delta\cdot\Big[\mathbf{P}\left\{\Omega_i^S < U\right\}\Big]^{\delta+1} - (\delta+1)\cdot\mathbf{P}_{f_{RCR}}^{tradH} + 1)}{\Big[\mathbf{P}\left\{\Omega_i^S < U\right\} - 1\Big]^2}. \tag{4.20}$$

Please refer to the proof in the Appendix Section. Furthermore, $\overline{\gamma_s}$ denotes the average number of the target access retransmissions and this can be calculated as

$$\begin{aligned}\overline{\gamma_s} &= \left\lfloor \sum_{n=1}^{\gamma} n\cdot\mathbf{P}\left\{\gamma_s = n|\text{target access is successful}\right\}\right\rfloor \\ &= \left\lfloor \frac{1}{(1-\mathbf{P}_{f_{tar}}^{tradH})}\sum_{n=1}^{\gamma} n\cdot\mathbf{P}\left\{\gamma_s = n\right\}\right\rfloor\end{aligned} \tag{4.21}$$

and

$$\mathbf{P}\left\{\gamma_s = n\right\} = \Big[\mathbf{P}\left\{\Omega_i^S < U\right\}\Big]^{n-1}\cdot\Big[(1-\mathbf{P}\left\{\Omega_i^S < U\right\})\Big]. \tag{4.22}$$

In the same way, $\sum_{n=1}^{\gamma} n\cdot\Big[\mathbf{P}\left\{P_i^T < U\right\}\Big]^{n-1}$ can be simplified further to get the following

$$\frac{(\gamma\cdot\Big[\mathbf{P}\left\{\Omega_i^T < U\right\}\Big]^{\gamma+1} - (\gamma+1)\cdot\mathbf{P}_{f_{tar}}^{tradH} + 1)}{\Big[\mathbf{P}\left\{\Omega_i^T < U\right\} - 1\Big]^2}. \tag{4.23}$$

T_{dec} is the latency associated with the HO decision process and can be given by

$$T_{dec} = T_{alg} + T_{req} + T_{req/ACK} + T_{adm}, \tag{4.24}$$

where T_{req} and $T_{req/ACK}$ are the latencies for a HO request and a HO request ACK, respectively. T_{alg} and T_{adm} are the latencies associated with performing the HO and the admission control decision algorithms, respectively. By contrast, for the enhanced proposed scheme, since the HO decision along with the RCR command transmission are performed before the triggering condition satisfaction $\Omega_i^T \geq \beta_2$, the HO success latency can be calculated as

$$T_{succ}^{efH} = \overline{\xi_s} \cdot (3 \times T_o) + T_{psw}, \tag{4.25}$$

where

$$\overline{\xi_s} = \left\lfloor \frac{1}{(1 - \mathbf{P}_{f_{tar}}^{efH})} \sum_{n=1}^{\xi} n \cdot \mathbf{P}\left\{\xi_s = n\right\} \right\rfloor, \tag{4.26}$$

And $\overline{\xi_s}$ denotes the average number of retransmissions till successful reception and this can be get as

$$\mathbf{P}(\xi_s = n) = \left[\mathbf{P}\left\{\Omega_i^T < U\right\}\right]^{n-1} \cdot \left[(1 - \mathbf{P}\left\{\Omega_i^T < U\right\})\right]. \tag{4.27}$$

Again, $\sum_{n=1}^{\xi} n \cdot \left[\mathbf{P}\left\{\Omega_i^T < U\right\}\right]^{n-1}$ can be simplified as

$$\frac{(\xi \cdot \left[\mathbf{P}\left\{\Omega_i^T < U\right\}\right]^{\xi+1} - (\xi + 1) \cdot \mathbf{P}_{f_{tar}}^{efH} + 1)}{\left[\mathbf{P}\left\{\Omega_i^S < T\right\} - 1\right]^2}. \tag{4.28}$$

Another type of latency which is part of the success latency called the average interruption time during which no packet transmission is performed, and this can be expressed for the traditional and the enhanced fast schemes as

$$T_{int}^{tradH} = \overline{\gamma_s} \cdot (3 \times T_o). \tag{4.29}$$

and

$$T_{int}^{efH} = \overline{\xi_s} \cdot (3 \times T_o). \tag{4.30}$$

respectively.

B) Frequency Switch Scheme

For the FSW scheme, the success latency is the contribution of recovering the measurement report, the FSW decision algorithm, and the optical switch latency, which can be obtained as

$$T_{succ}^{fsw} = \overline{\alpha_s} \cdot T_{mr}^{fsw} + T_{dec}^{fsw} + T_{os}^{fsw}, \tag{4.31}$$

where T_{mr}^{fsw} and T_{os}^{fsw} are the measurement report transmission and the optical switch latencies, respectively. $\overline{\alpha_s}$ is the expected value of the random variable α_s and this can be derived as

$$\overline{\alpha_s} = \left\lfloor \frac{1}{(1 - \mathbf{P}_{f_{mr}}^{fsw})} \sum_{n=1}^{\alpha} n \cdot \mathbf{P}\left\{\alpha_s = n\right\} \right\rfloor, \tag{4.32}$$

where

$$\mathbf{P}(\alpha_s = n) = \left[\mathbf{P}\left\{\Omega_i^S < U\right\}\right]^{n-1} \cdot \left[(1 - \mathbf{P}\left\{\Omega_i^S < U\right\})\right]. \tag{4.33}$$

The term $\sum_{n=1}^{\alpha} n \cdot \left[\mathbf{P}\left\{\Omega_i^S < U\right\}\right]^{n-1}$ can be simplified further to

$$\frac{(\alpha \cdot \left[\mathbf{P}\left\{\Omega_i^S < U\right\}\right]^{\alpha+1} - (\alpha+1) \cdot \mathbf{P}_{f_{mr}}^{fsw} + 1)}{\left[\mathbf{P}\left\{\Omega_i^S < U\right\} - 1\right]^2}. \tag{4.34}$$

$T_{dec.}^{fsw}$ is the FSW decision algorithm latency which can be found as

$$T_{dec}^{fsw} = T_{alg}^{fsw}. \tag{4.35}$$

The interruption time for this scheme is simply equaled to the optical switch time and can be expressed as

$$T_{int}^{fsw} = T_{os}^{fsw}. \tag{4.36}$$

which could be neglected as the semiconductor optical amplifier (SOA) switching time is 1ns [108].

2. Average Failure Latency

This chapter defines the average failure latency as the time interval between the

instant of a failure event declaration to the instant of a link reconnection. The average failure latency associated with each scheme can be found as follows.

A) Handover Scheme

Traditionally, a HOF occurs as a result of either the RCR reception failure after reaching the maximum retransmission attempts, or because of the target access procedure failure. However, sending the RCR in advance would greatly eliminate the chance to have a failure event as a result of RCR reception failure. Therefore, the proposed enhanced fast scheme can only fail as a result of the target access procedure failure. Since the resulted latencies from the target access failure are the same for both the traditional and the proposed schemes, a comparison will be made between the failure latencies of both schemes with regards to the RCR reception failure.

Note that, once a radio link failure RLF is declared after a RCR reception failure, the MR starts the timer T_{311} for a cell reselection. In this case without receiving the RCR command, the MR will not be aware of the serving cell selected target. As a result, the MR has to scan all the possible frequencies and then selects the best one. Once the MR selects a suitable cell, it starts reading all the required system information blocks (SIBs) to access the selected cell that is the neighbouring cell in the HSR case. If the needed SIBs are successfully acquired, the MR stops the timer T_{311} and starts the timer T_{301} in order to begin the connection re-establishment with the selected cell by sending RRC connection re-establishment request. The re-establishment procedure succeeds only if the MR selects a prepared cell with the UE context. Therefore, re-establishment latency of the traditional scheme in case of RCR reception failure can be found as

$$T_{rec}^{w/o[RCR]} = T_{311}^{w/o[RCR]} + T_{301}, \tag{4.37}$$

where $T_{311}^{w/o[RCR]}$ is the cell reselection timer in case of failure without recovering RCR command and can be calculated as

$$T_{311}^{w/o[RCR]}[ms] = 50 + N_{freq}^{w/o[RCR]} \cdot T_{search} + T_{SI}^{w/o[RCR]}, \tag{4.38}$$

where $N_{freq}^{w/o[RCR]}$ and T_{search} are the total number of frequencies to be scanned and the time required to search for them, respectively. $T_{SI}^{w/o[RCR]}$ is the time required for receiving all the relevant SIBs.

If a HOF event is declared upon the target access failure, the MR is already aware of the target as it has been informed earlier by RCR command. Accordingly the MR will not need to scan all the possible surrounded frequencies. Instead, it will only scan for the preselected target frequency. Later, the MR needs only to acquire SIB1 in order to detect if the system information has changed [32]. If not, the MR commences the re-establishment process by initiating T_{301} timer; otherwise, the MR has to acquire all the related SIBs. If successfully concluded, the MR stops T_{301} and starts transmitting/receiving from/to the target. Thus, the re-establishment latency for this case, that can be consequently considered as the enhanced scheme re-establishment latency, can be calculated as

$$T_{rec}^{w[RCR]} = T_{311}^{w[RCR]} + T_{301}, \tag{4.39}$$

where

$$T_{311}^{w[RCR]}[ms] = 50 + N_{freq}^{w[RCR]} \cdot T_{search} + T_{SI}^{w[RCR]}. \tag{4.40}$$

The interruption time resulted from the recovery process is equivalent to $T_{rec}^{w/o[RCR]}$ in case of RCR failure case for the traditional HO scheme. With our proposed enhanced fast scheme, the interruption time is $T_{rec}^{w[RCR]}$. Finally, the total average latency of the traditional and the proposed scheme can be obtained as

$$T_{avg}^{tradH} = T_{succ}^{tradH} \cdot (1 - \mathbf{P}_f^{tradH}) + T_{rec}^{w/o[RCR]} \cdot \mathbf{P}_f^{tradH}, \tag{4.41}$$

and

$$T_{avg}^{efH} = T_{succ}^{efH} \cdot (1 - \mathbf{P}_f^{efH}) + T_{rec}^{w[RCR]} \cdot \mathbf{P}_f^{efH}. \tag{4.42}$$

respectively. In the same way, the average interruption latency for the traditional HO scheme and for the proposed enhanced HO scheme can be found as

$$\overline{T_{int}^{tradH}} = T_{int}^{tradH} \cdot (1 - \mathbf{P}_f^{tradH}) + T_{rec}^{w/o[RCR]} \cdot \mathbf{P}_f^{tradH}, \tag{4.43}$$

and

$$\overline{T_{int}^{efH}} = T_{int}^{efH} \cdot (1 - \mathbf{P}_f^{efH}) + T_{rec}^{w[RCR]} \cdot \mathbf{P}_f^{efH}. \tag{4.44}$$

respectively.

B) Frequency Switch Scheme

For the FSW scheme case, a RLF event could happen due to the loss of the measurement report. The MR detects a RLF upon an indication that the maximum number of retransmission for the measurement report has been reached. Once the MR detects a RLF, it initiates T_{311} and follows the same procedure as in the case of recovery without receiving the RCR command. Here, the recovery time is also equivalent to the interruption time. As a result, the recovery time for the FSW case can be calculated as

$$T_{rec}^{fsw} = T_{311}^{w/o[RCR]} + T_{301}. \tag{4.45}$$

While the total average latency and the average interruption time are given by

$$T_{avg}^{fsw} = T_{succ}^{fsw} \cdot (1 - \mathbf{P}_f^{fsw}) + T_{rec}^{w/o[RCR]} \cdot \mathbf{P}_f^{fsw}. \tag{4.46}$$

and

$$\overline{T_{int}^{fsw}} = T_{int}^{fsw} \cdot (1 - \mathbf{P}_f^{fsw}) + T_{rec}^{w/o[RCR]} \cdot \mathbf{P}_f^{fsw}. \tag{4.47}$$

respectively.

4.5.4 Signalling Overhead Design Cost

Herein, the proposed FSW scheme signalling cost is obtained and compared with other HO schemes. This is a fair compression since FSW scheme eliminate the need for BBU-to-BBU HO, which can be equivalent to the traditional eNB-to-eNB HO. The signalling cost is calculated based on the account of each scheme negotiated signalling messages count. The FSW scheme switches the MR from one RAU to the next using only one negotiated message which is the measurement report, thereby reducing the failure probability and latency incurred by negotiating far fewer messages compared with other HO schemes. Further, this can reduce the extra incurred delays, signalling costs, and possible failure events resulting from the retransmission trials attempt of the negotiated messages through

Table 4.4: Comparison of Signalling messages along with Signalling Size for available schemes.

	LTE [3]	Tian [3]	Lee [8]	FSW
1. Measurement Report	4400	44	44	44
2. HO Request	24100	15982	241	-
3. HO Request/Ack	7000	2713	70	-
4. RCR	3600	36	36	-
5. RCR Complete	900	9	9	-
6. SN Status Transfer	7300	-	-	-
7. Path Switch Request	13600	5977	136	-
8. Path Switch Request/ACK	11700	8730	117	-
9. User-plane Update Request	16500	4521	165	-
10. User-plane Update Request/ACK	8000	4337	80	-
11. UE Context Release	3000	30	30	-
12. Bi-casting Request	-	2977	-	-
13. Bi-casting Request/ACK	-	3000	-	-
Total Number of Negotiated Messages	11	12	10	1
Total Signalling Size [Byte]	100100	48356	928	44

the air interface in case of transmission failure of the first attempt. As a result, the FSW scheme avoids service disruption with minimum signalling cost, and therefore a better QoS experience for the end users could be achieved compared with other schemes. The data in Table 4.4 have been obtained assuming 100 active users based on the calculation provided in [3] and [8], whom their schemes have been discussed earlier in the literature review section. Note that we have not compare with any other HO schemes as [3] and [8] are the only papers whom have compared their schemes in terms of signalling overhead count and size.

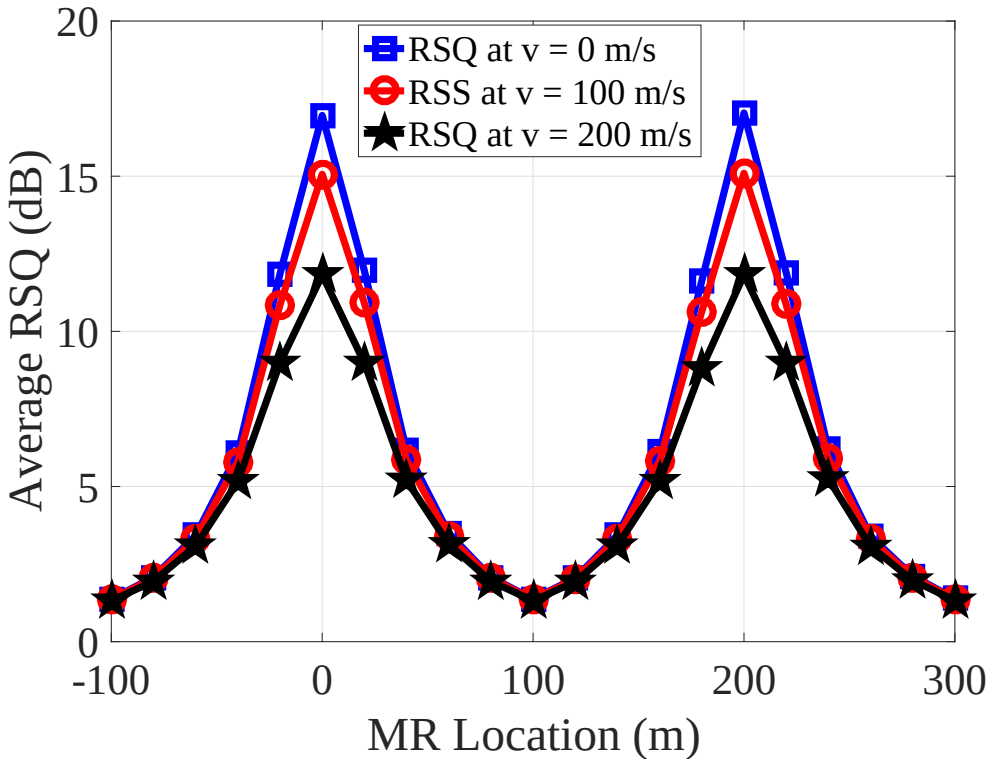

Figure 4.9: Average RSQs comparison under different MR/train speeds (0, 100, and 200) m/s versus the MR location.

4.5.5 Signalling Messages Size Overhead

In this subsection, we obtain the bandwidth consumption caused by the negotiated signalling size for each scheme. The related signalling size for the schemes of 100 UEs are given in Table 4.4 based on the calculation provided in [3] and [8].

4.6 Numerical Results and Discussions

In this section, numerical results are presented to show the performance of the proposed schemes. The traditional HO scheme consists of a serving cell and a target cell. For the proposed FSW/HO schemes, four RAUs are assumed under the control of each CU. For example, CU m controls RAUs with the coordinates of [0, 200, 400, 600]. When the MR moves between RAUs belonging to the same CU, a FSW scheme is performed; otherwise, a HO scheme is performed. For the purpose of a fair comparison, all cells have the same

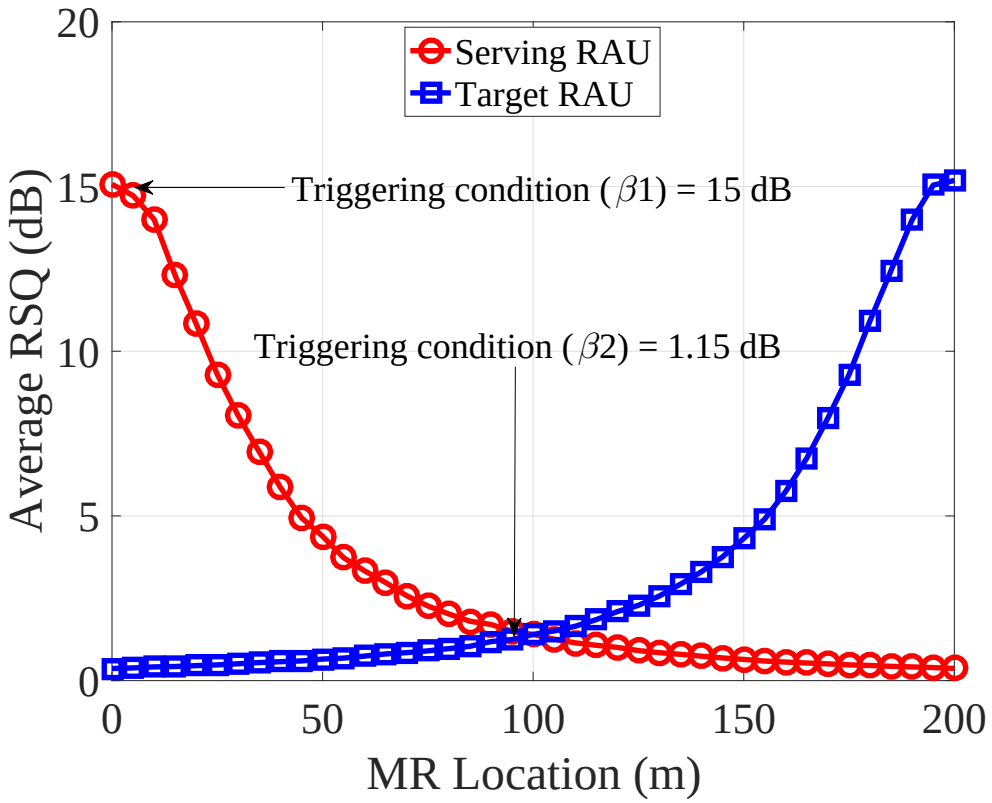

Figure 4.10: Average RSQs of the serving and the target RAUs as a function of the MR location under a train speed of 100 m/s.

coverage area and the same transmit power. Parameters used in this numerical analysis are given as follows: $f = 2$ GHz, $c = 3{\times}10^8$ m/s, $T_s = 1/14$ ms, $P_T = 43$ dBm, $\sigma_i^k = 4$ dB, $\beta_1 = 15$ dB, $\beta_2 = 1.15$ dB, U= 1.25 dB, $N = 4$, M=1000, $r = 105$ m, train's length $L = 400$ m, $d_v = 10$ m, $\chi^{efH} = \chi^{tradH} = \chi^{fsw} = 10$ m, $T_{RCR} = T_o = T_{mr}^{fsw} = 8$ ms (retransmission in case of FDD system) [109], $T_{dec} = 14$ ms, $T_{dec}^{fsw} = T_{alg} = T_{adm} = 5$ ms, $T_{psw} = 13$ ms, $T_{req} = T_{req/ACK} = 2$ ms [110], $T_{os}^{fsw} = 1$ ns, $T_{search} = 100$ ms, $N_{freq}^{w/o[RCR]} = N_{freq}^{w[RCR]} = 1$, $T_{SI}^{w/o[RCR]} = 80$ ms, and $T_{SI}^{w[RCR]} = 1280$ ms [32].

The RSQ is investigated as a function of the MR location under variable speeds as shown in Fig. 4.9. Near the RAU location, it can be seen that the higher the speed, the lower the RSQ due to the ICI effect on the received signal. However, as the MR moves towards the cell edges, the RSQ deteriorated and becomes the same regardless of the speed. At the cell edges, the noise dominated compared to ICI. Therefore, the performance difference becomes insignificant. In addition, in general, the RSQ decreases as the

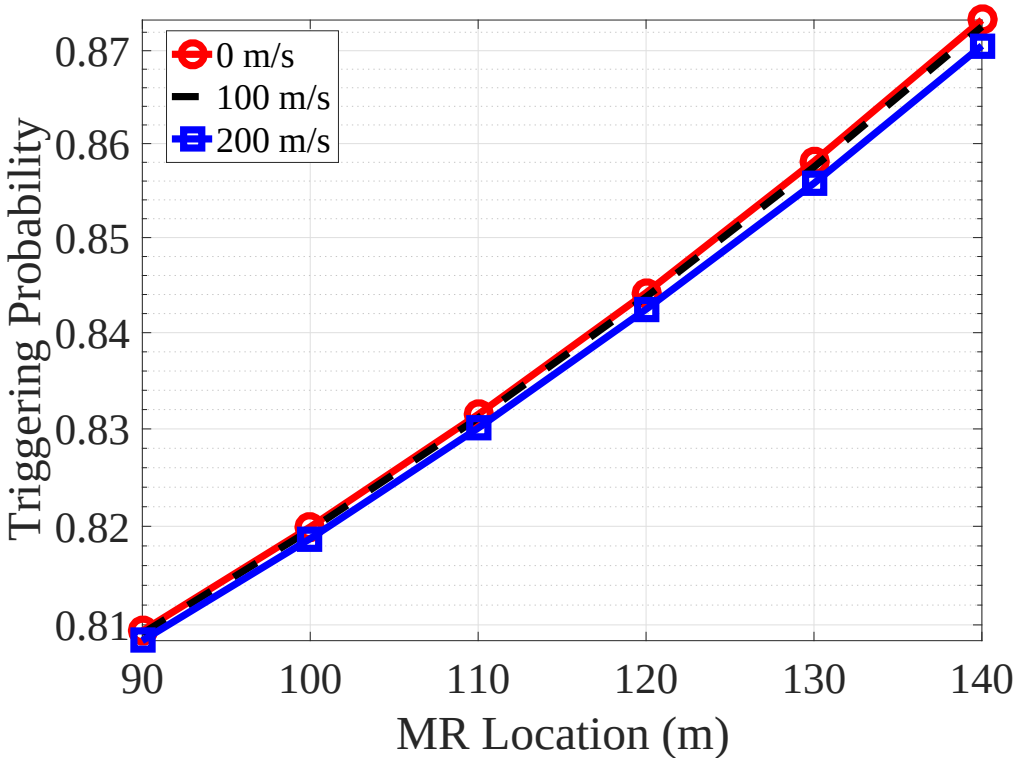

Figure 4.11: HO triggering probability versus the MR location under $\beta_2 = 1.15$ dB.

MR moves from the serving RAU towards the neighbouring RAU until it performs the FSW/HO scheme after which the RSQ becomes stronger and stronger.

Fig. 4.10 illustrates the RSQ of the serving and the target RAU along with the triggering conditions for both the traditional and the proposed schemes. It can be seen that the RSQ of the serving RAU is decreasing while the RSQ of the target RAU is increasing as the MR is moving away from the serving RAU. This fluctuation in the RSQs of the serving and the target RAUs necessarily reflects the real reason behind the HO purpose as a crucial process to preserve the user's QoS. Further, it can be clearly noticed that the proposed scheme triggers the HO command earlier ($\Omega_i^S \leqslant \beta_1$) than the traditional scheme ($\Omega_i^T \geqslant \beta_2$) as mentioned earlier in section 4.5.1, indicating that the proposed enhanced fast HO scheme ensures a better performance by reducing the possibility of a failure event due to either measurement report and/or HO command. The proposed FSW scheme is still envisioned to trigger the scheme at the RAU's cell edge, as the FSW scheme does not have many procedures that could deteriorate the signal quality following the triggering

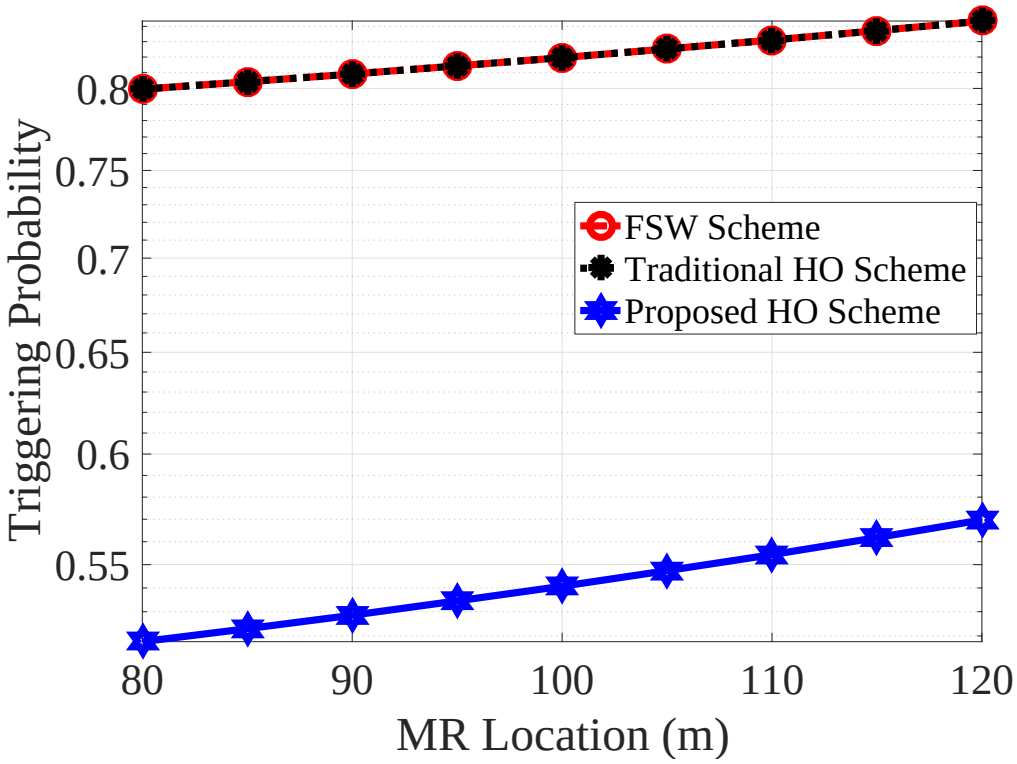

Figure 4.12: Triggering probability versus the MR location (β_1=15 dB and β_2=1.15 dB), under a speed of 100 m/s.

process. The following up procedures only include performing the decision algorithm and executing the switching process to the next RAU, neither of which exceed 5 ms approximately. Note that the overlapping area lies between 95-105 m.

The triggering probability under varying speeds are presented in Fig. 4.11 as a function of the MR's location. It can be observed that for different speeds the MR almost have the same triggering probability. This is due to the fact that at the cell edge no matter the speed, the signal quality is dominated by the noise resulting into almost the same triggering probability. Thus, no early or late triggering due to varying speeds.

Fig. 4.12 illustrates the relationship between the triggering probability of the investigated schemes and the MR's location. Clearly, the traditional HO and the proposed FSW schemes have the same triggering performance behaviour as they have the same triggering criteria. However, the proposed HO scheme is lower compared with that of the aforementioned schemes, as it has a different triggering condition.

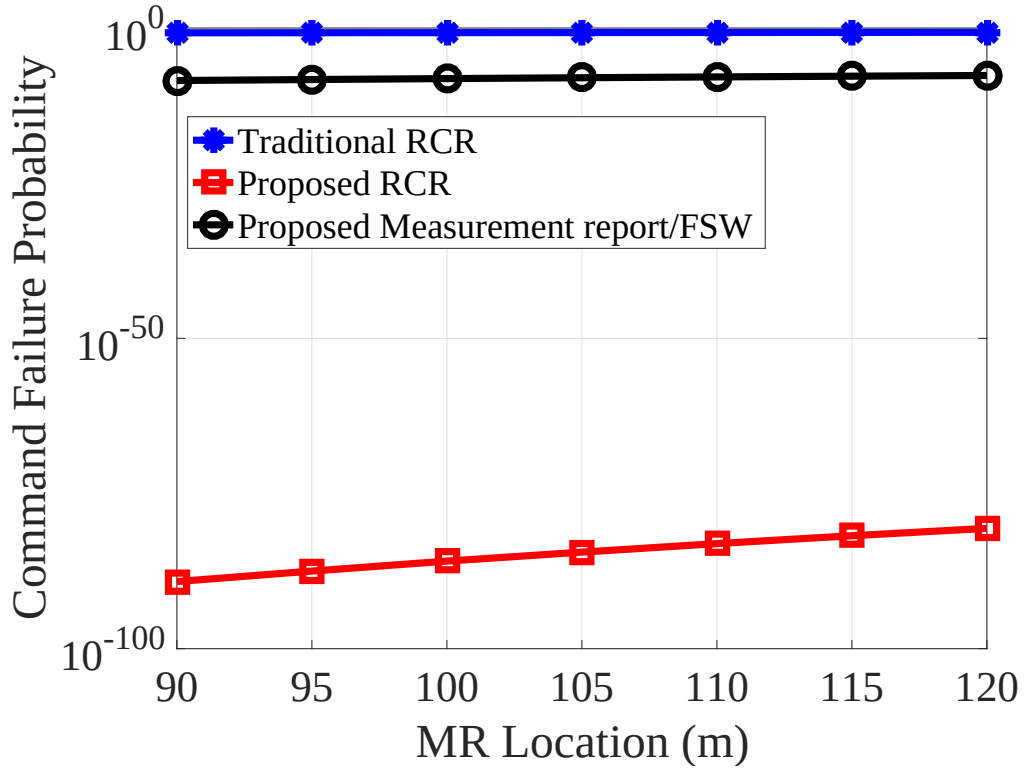

Figure 4.13: The HO commands and the measurement report failure probabilities for the HO schemes and the FSW scheme, respectively, as a function of the MR location, under a train's speed of 100 m/s when $\rho_{RCR} = 0.3$.

Fig. 4.13 shows the FSW's measurement report and the HO command failure probabilities versus the MR's location. It is shown that the proposed HO scheme achieves the lowest failure probability as the RCR is sent when the RSQ is at the highest level near the serving RAU location. And more retransmissions can be performed for the proposed HO scheme compared to FSW and traditional HO schemes, since the available distance to perform retransmissions is higher than that of other schemes. While the traditional HO scheme has a failure probability of 0.1 and increasing as the MR is moving towards the target RAU. For the FSW scheme, the measurement report failure probability is 10^{-8}, as almost the whole the overlapping area is dedicated for recovering the measurement report. Furthermore, the all the investigated failure probabilities are increasing as the MR is moving towards the target RAU, this is because these investigated commands are correlated with the serving RAU. These failure probabilities may also look very small especially the proposed schemes, since we have used the retransmission trials upper bound while in real

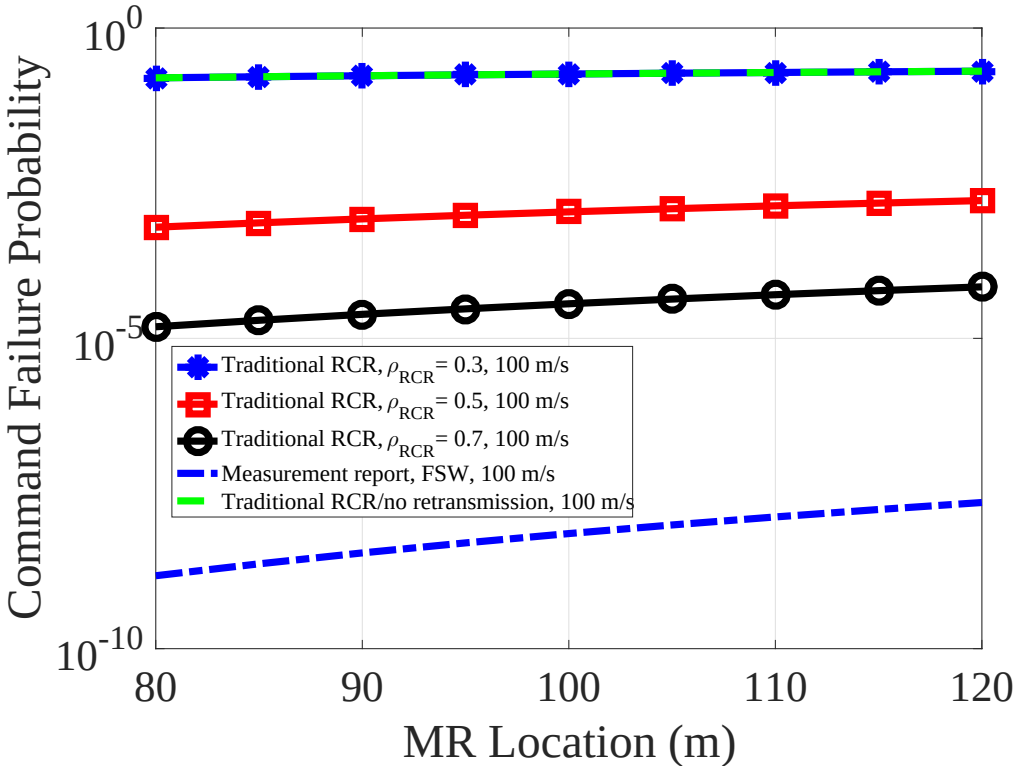

Figure 4.14: The HO command and the measurement report failure probabilities of the traditional HO scheme and the proposed FSW scheme, respectively, as a function of the MR location, under a train speed of 100 m/s.

world scenarios only a limited trial times is permitted. However, no optimization for the number of permitted trials is done for the HSR scenario and therefore we have considered the upper bounds. An optimization for the number of trials will be performed as a future work taking into account the latency trade-off.

Whereas, Fig. 4.14 presents the RCR and measurement report failure probabilities of the traditional HO and the FSW schemes, respectively, versus the MR's location under ρ_{RCR} =0.3, 0.5, and 0.7 for the traditional HO scheme. Undoubtedly, the measurement report has a lower failure probability compared with the RCR of traditional HO scheme due to the fact that the FSW decision algorithm time is lower than the HO decision algorithm time, $T_{dec}^{fsw} < T_{dec}$ and almost the entire χ^{fsw} is dedicated to retrieve the measurement report. Further, the higher ρ_{RCR}, the lower the failure probability as this results in more retransmission trials. Moreover, the traditional RCR failure probability which does not consider retransmissions is also shown and it performs the same as the traditional HO

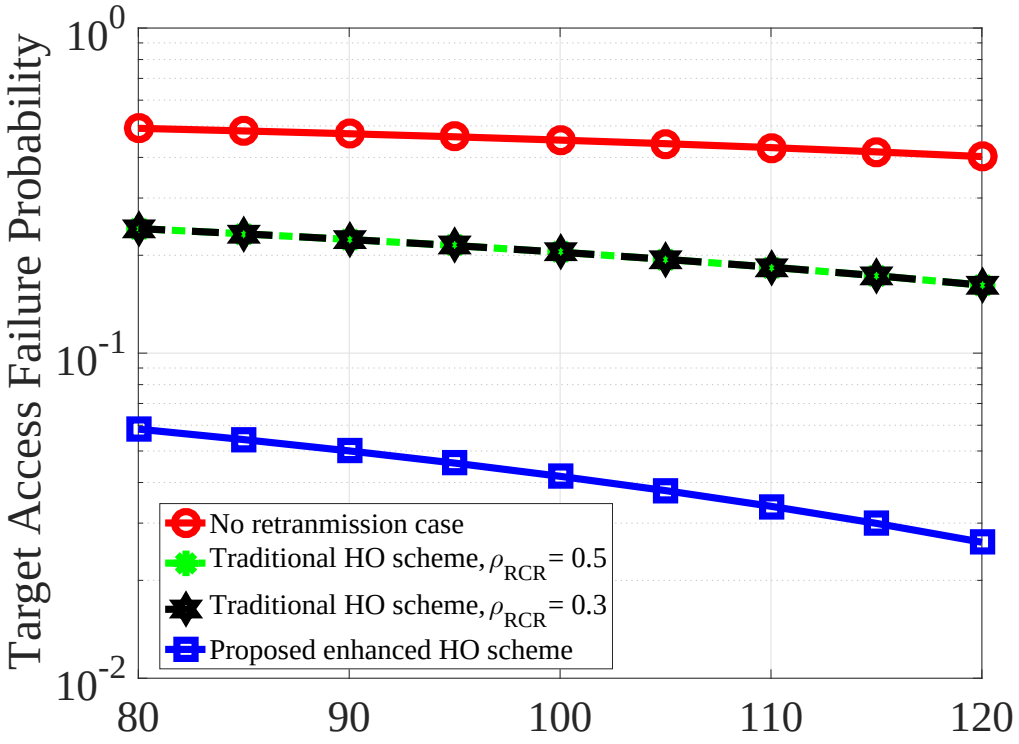

Figure 4.15: Access failure probabilities as a function of the MR location under a speed of 100m/s.

when ρ_{RCR} =0.3, this is due to using $\lfloor \cdot \rfloor$ in (4.6), and both perform the worst compared to others. Also, all failure probabilities increase as the MR moves away towards the target RAU. This is because the commands should be recovered successfully by the serving RAU, thus all commands are associated with the serving RAU in which the associated RSQ decreases as the MR moves away from the serving RAU.

While Fig. 4.15 shows the access failure probabilities of the traditional and the proposed HO schemes versus the MR location. As it can be seen, for the traditional HO case, the access failure probability is the same when ρ_{RCR} = 0.3 and 0.5. This is because of using $\lfloor \cdot \rfloor$ in (4.7), and also increasing the percentage of the overlapping area dedicated for the access procedures from 0.5 to 0.3 is not enough to reduce the failure probability further as the access procedures encounter $3 \times T_o$ instead of T_o. The traditional target access failure probability without retransmissions on the other hand shows the worst performance compared with other cases. Whereas, the proposed target access failure probability shows the best performance since the proposed enhanced HO scheme

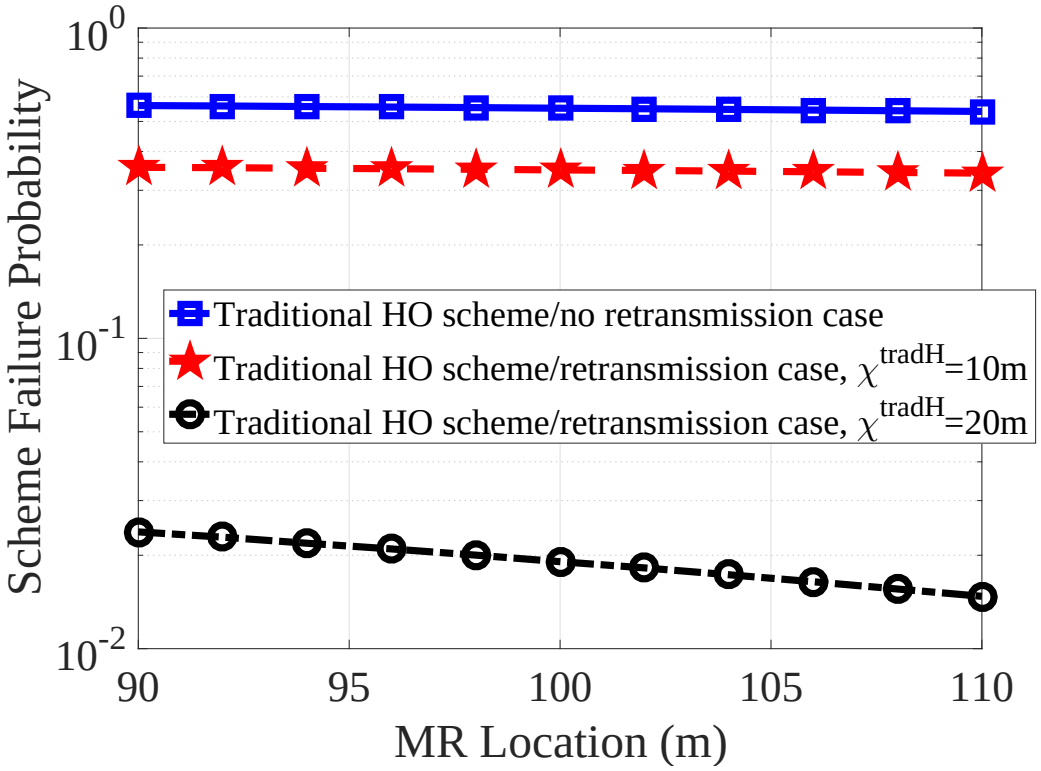

Figure 4.16: HO failure probabilities versus the MR location for a speed of 100 m/s when $\rho_{RCR} = 0.3$.

dedicate the whole overlapping area to retrieve the target access commands.

A comparison in terms of failure probability of the traditional HO scheme in case of considering retransmission trials and in case of no retransmission trials is shown in Fig. 4.16. As it can be seen, for the retransmission case, it has a lower failure probability than the one that does not consider the retransmissions scenario. Furthermore, for the traditional HO scheme/no retransmission case, the curve of the failure probability is decreasing as the MR moves away from the serving RAU towards the target RAU, this is due to the fact that the failure probability is more correlated with the target RAU since it negotiates three commands instead of one compared with the serving RAU. Also, we can observe that the more available overlapping area, the lower the failure probability, as more overlapping area means more retransmission trials. Therefore, considering the retransmissions in evaluating the failure probability gives us more realistic results which can reflect the intrinsic performance of the real-world deployed system and gives us a better insight into understanding each parameter and its effect on the system performance.

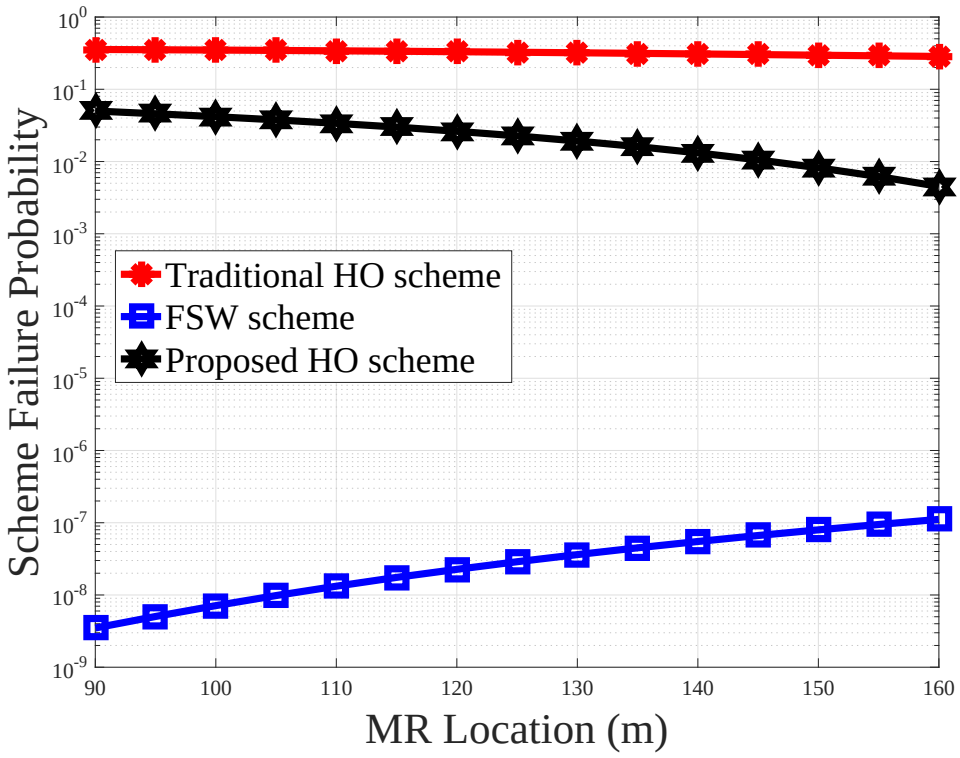

Figure 4.17: Schemes failure probabilities versus the MR location for a train speed of 100 m/s when $\rho_{RCR} = 0.3$.

It should be noted from Fig. 4.13, and Fig. 4.14 that some of the command failure probabilities of the proposed schemes are very low which might look unrealistic. This is because we have assumed unlimited retransmission trials which is governed only by the system speed and the available distances that the proposed schemes offer. In practical system scenario, the system will have a limited retransmission trials which upon expiry, the system fails and consequently follows the reestablishment procedures. Generally speaking, 3GPP standard assumes four transmission trials only. However, this value is optimized for slow-to-medium speeds only. As a result, we have assumed here the maximum number of trials that the schemes' can achieve, as the system with higher speeds should be given an enough number of transmissions in order to reduce the failure events.

The schemes failure probabilities as a function of the MR location are shown in Fig. 4.17. This Figure shows that the traditional HO scheme performs the worst compared with other schemes due to the restricted number of trials associated with the traditional HO scheme.

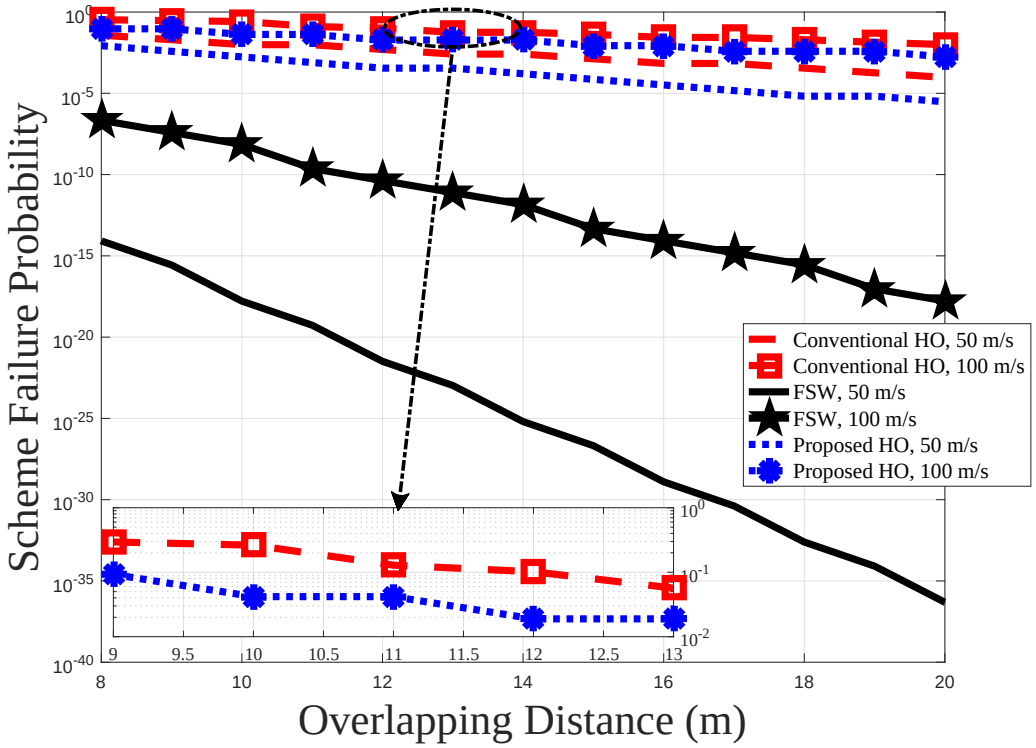

Figure 4.18: Scheme failure probability as a function of the overlapping area when $\rho_{RCR} = 0.3$ under different speed.

Moreover, the failure probability curve of the traditional HO scheme is monotonically decreasing because the traditional HO scheme procedures are associated with both the serving RAU as well as the target RAU but more with the target RAU as it needs to recover three commands with it. On one hand, the failure probability of the proposed enhanced scheme $\mathbf{P}_f^{efH}$ decreases when approaching the target, since the proposed HO scheme is highly correlated with the target (by performing the target access procedures) as the RCR is expected to be received with a very high success probability. On the other hand, the FSW scheme is highly correlated with the RSQ of the serving RAU since the measurement report needs to be recovered to have a successful scheme, resulting in an increase in the failure probability as the MR moves away from the serving cell. Based on the acquired results, the proposed schemes are able to deliver an ultra-reliable communication compared with the traditional HO scheme thanks to the relaxed versions of the proposed schemes compared with the traditional HO scheme.

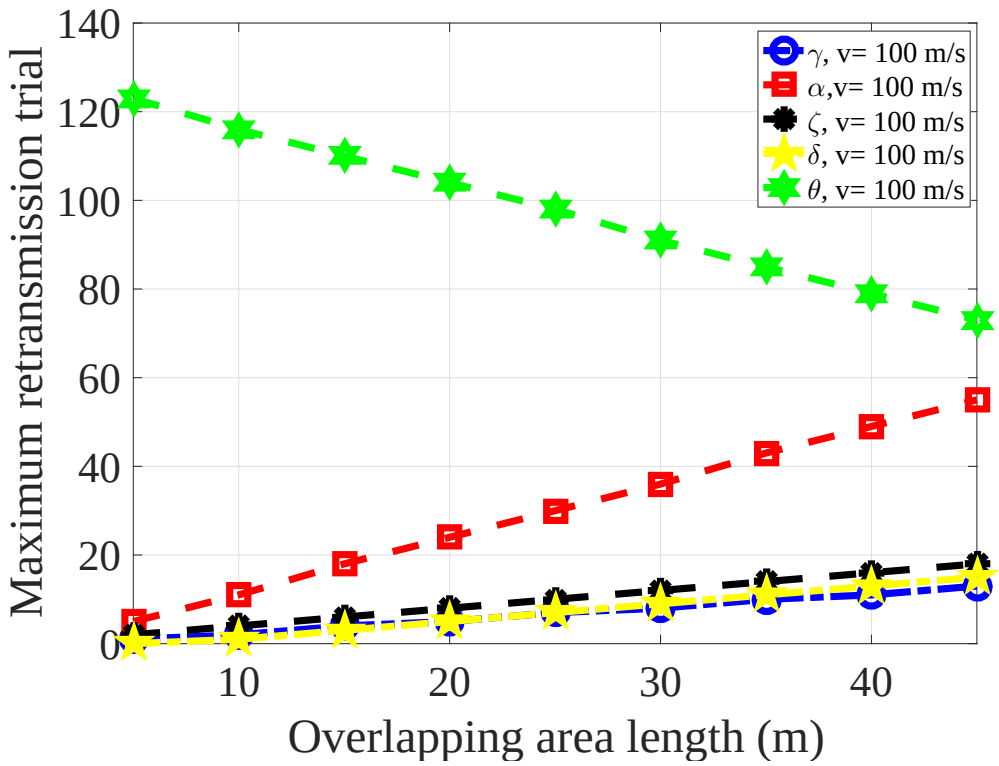

Figure 4.19: Maximum retransmission trials as a function of the overlapping area when $\rho_{RCR} = 0.3$ under a speed of 100 m/s.

Moreover, Fig. 4.18 illustrates the schemes' failure probabilities as a function of the overlapping area distance under different speeds. It can be clearly observed that the proposed HO/FSW schemes require less overlapping area to achieve the same failure performance compared with the traditional HO scheme. For instant, the traditional HO scheme requires 25m to reach a failure probability of 0.005 under a speed of 100 m/s. While the proposed FSW and HO schemes require 4m and 18m to reach a failure probability of 0.006 and 0.004 under a speed of 100 m/s, respectively. This means a reduction gain of 84% and 28% can be achieved for the proposed FSW and HO schemes, respectively. This reduction leads then to decrease the HO/FSW rate which ultimately leads to reduce the failure probability and improves the users QoS for the proposed schemes. Furthermore, the lower the speed, the lower the required overlapping distance, since lower speed means more retransmission attempts over the same traversed distance, as in the case of 50 m/s which represent twice trials of that of 100 m/s.

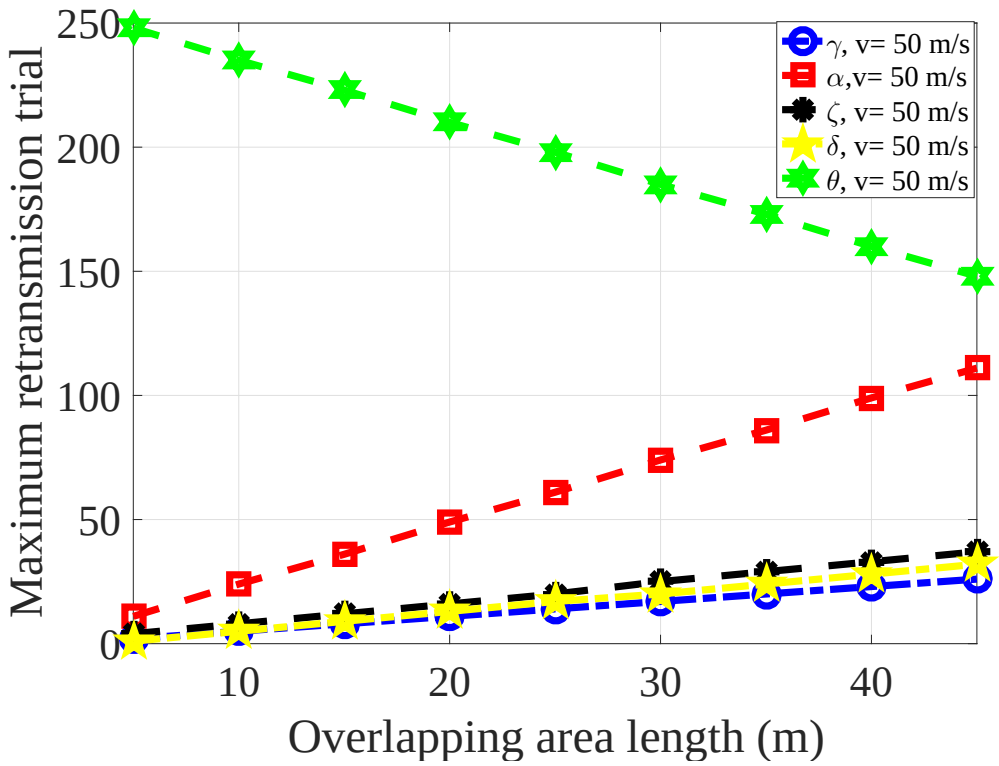

Figure 4.20: Maximum retransmission trials as a function of the overlapping area when $\rho_{RCR} = 0.3$ under a speed of 50 m/s.

The upper bound of the retransmission trials for each scheme is presented in Fig. 4.19 as a function of the overlapping area length. As it can be seen, the proposed schemes retransmissions, namely ϑ, ζ, and α are larger than the traditional HO scheme, namely δ, and γ. This is because the proposed schemes have the chance to retransmit more than the traditional HO scheme, due to the longer overlapping area distance available for the proposed schemes, as the proposed schemes are a relaxed version of the traditional HO scheme. Also, it can be noticed that the maximum retransmission trials are increasing as the overlapping area increased except for ϑ. This increment is due to the fact that the maximum retransmissions ζ, δ, γ, and α are directly proportional with the overlapping area length. While ϑ is inversely proportional with the overlapping area. For example, at the speed of 100 m/s and under the overlapping area of 10m, $\alpha = 11$, $\delta = 1$, $\gamma = 2$, $\zeta = 4$, and $\vartheta = 116$. This means that comparing the proposed scheme maximum retransmissions ϑ with the traditional maximum retransmissions δ, an increasing gain of 11500% can be

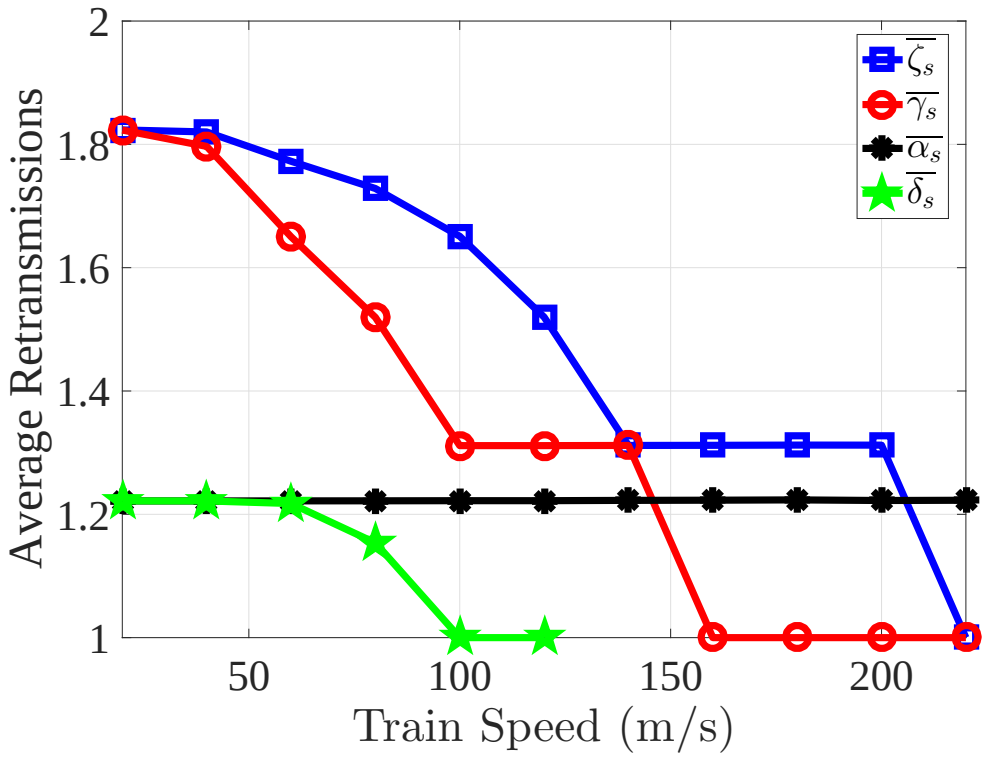

Figure 4.21: Average retransmissions as a function of the speed for ρ_{RCR} =0.3.

achieved for the same overlapping area. While if we compare γ with ζ an increasing gain of 100% can be obtained for the same overlapping area. Fig. 4.20 shows the maximum retransmissions under the speed of 50 m/s. As it can be clearly noticed that the trials are twice that of the speed of 100 m/s. This is reasonable since lower system speed means more possibility to retransmit assuming a fixed overlapping area.

Fig. 4.21 shows the average retransmission trials versus the train's speed obtained by removing $\lfloor \cdot \rfloor$ from their corresponding equalities. As it can be seen, the average retransmission trials associated with traditional HO scheme, namely $\overline{\gamma_s}$ decreases from 1.8 to almost 1.3 as a result of increasing the speed from 20 m/s to 100 m/s, respectively. This is reasonable since increasing the speed reduces the retransmission trials required to preserve the same performance given that there is an enough overlapping area to perform those trial. $\overline{\gamma_s}$ then is able to preserve the same average of 1.3 retransmissions for speeds in the range of (120-140) m/s. Beyond the speed of 140 m/s, the average retransmission trials $\overline{\gamma_s}$ reduce to one trial only as the dedicated overlapping area is not enough to per-

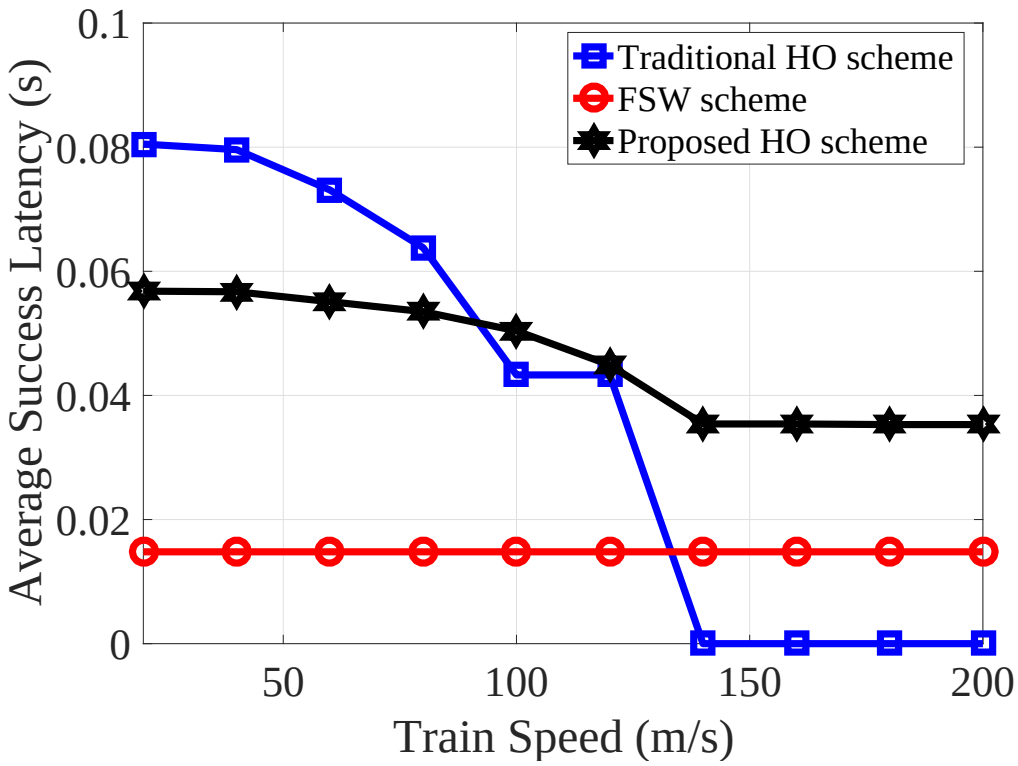

Figure 4.22: Schemes average success latency versus the train's speed when $\rho_{RCR} = 0.3$.

form more than that for speeds between (140-220) m/s. For the case of $\overline{\delta_s}$, and for speed in the range of (20-60) almost 1.2 trials can be performed and as the speed increases to 80 m/s the average reduces further until it reaches the range of (100-120) m/s where only one trial can be performed due to the limited overlapping area dedicated for it (ρ_{RCR} =0.3), whilst for speeds above that range, $\overline{\delta_s}$ value is not defined (NaN) for the same reason. While the average retransmission trials of the proposed FSW scheme, namely $\overline{\alpha_s}$, it keeps the same average regardless of the speed since the overlapping area is sufficient to support that average. $\overline{\zeta_s}$ on the other hand decreases from almost 1.8 to almost 1.3 as the speed increases from 20 m/s to 140 m/s, respectively. Yet, the decreasing rate is less compared to the traditional $\overline{\gamma_s}$. For example, the traditional HO scheme is able to support average trials of 1.3 for speed range of (100-140) m/s while the proposed HO scheme is able to support an average of 1.3 for speed range of (140-200) m/s. This means that the proposed HO scheme can support higher speed and have the same performance compared with the traditional HO scheme but for a lower range of speeds. After the speed of 220 the average

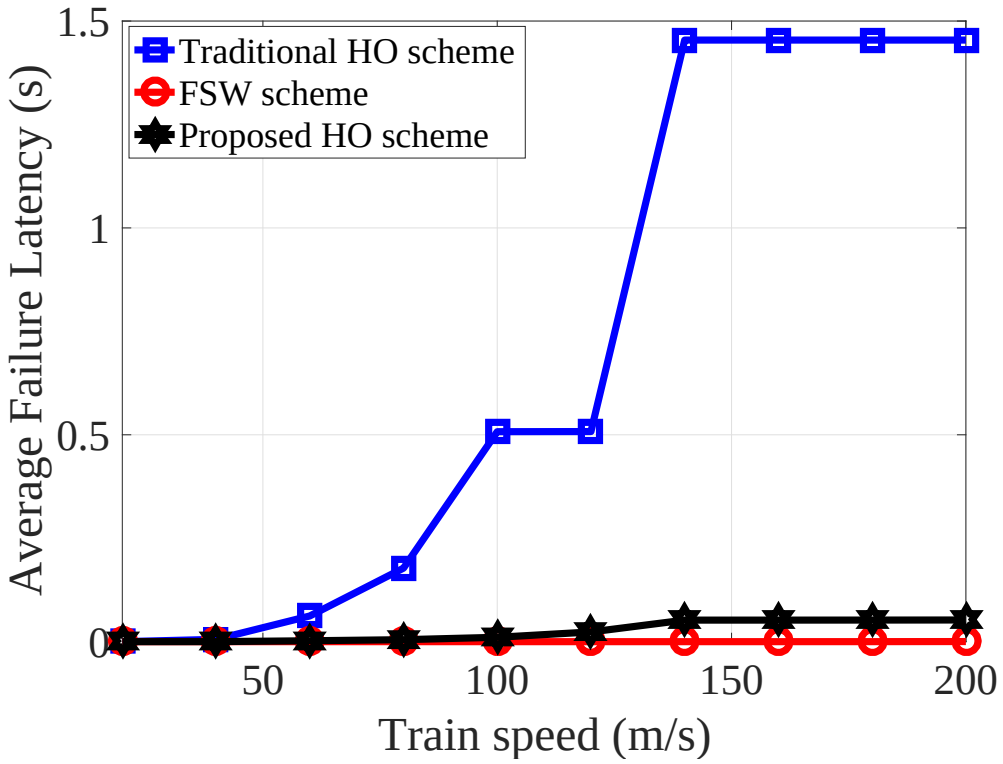

Figure 4.23: Schemes average failure latency versus the train's speed when $\rho_{RCR} = 0.3$.

transmission trials decreases to 1 trial only due to the overlapping area shortage at such a high-speed for a process which includes $3 \times T_o$. Lastly, the lower the average retransmission trials the higher the failure probability. This means that the proposed average retransmission trials $\overline{\zeta_s}$ and $\overline{\alpha_s}$ performs better than both $\overline{\gamma_s}$ and $\overline{\delta_s}$ and can support a higher speed compared with the traditional scheme.

The average success latency as a function of the speed is shown in Fig. 4.22. As can be noticed, FSW scheme shows the lowest latency compared with other schemes. Additionally, the proposed HO scheme performs better in comparison to the traditional HO scheme. Moreover, it can be seen that the traditional HO scheme start decreasing seriously after a speed of 60 m/s and keep decreasing until it reaches the speed of 140 m/s when it becomes zero due to reducing the success probability to zero due to increasing the failure probability to 1. This means that both HO scheme success probability start decreasing after 100 m/s and 120 m/s. However, the proposed HO scheme decreases slightly compared with the traditional HO scheme which decreases dramatically after the

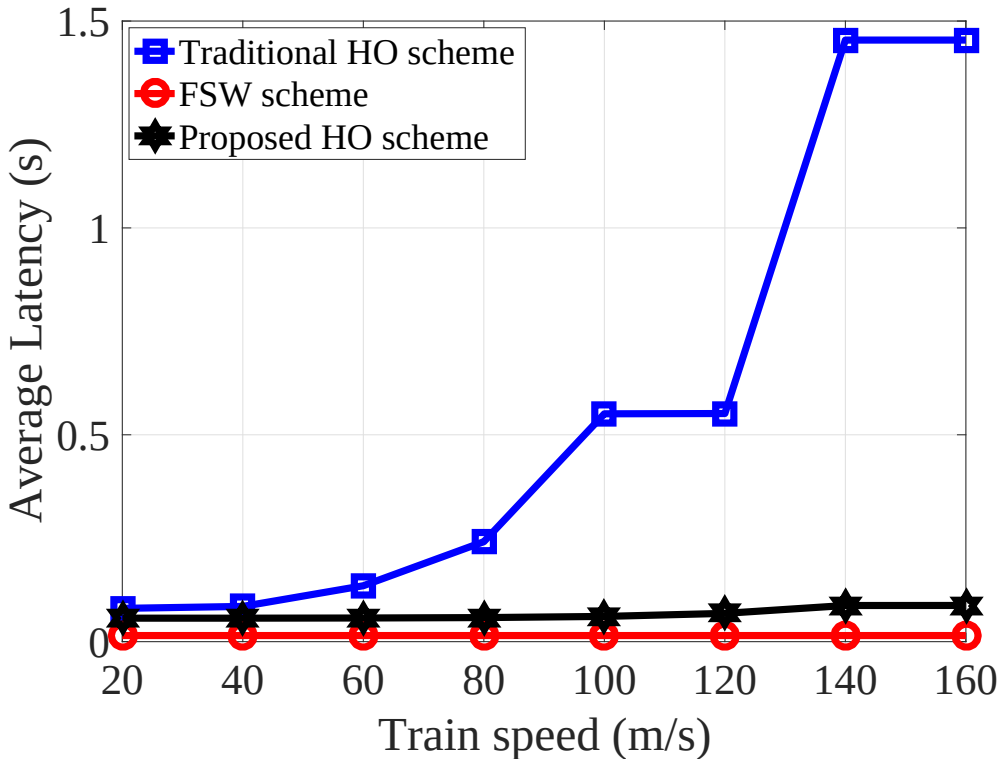

Figure 4.24: Schemes average latency versus the train's speed when $\rho_{RCR} = 0.3$.

speed of 140 m/s. In conclusion, the proposed FSW scheme can handle speeds up to 200 m/s without performance degradation and with slight degradation for the proposed HO scheme. Whilst the traditional HO scheme can handle speeds up to 120 m/s.

Fig. 4.23 depicts the average failure latency as a function of the speed. As it can be seen, both proposed schemes shows a very low latency compared with the traditional HO scheme under speeds up to 200 m/s. This is due to the fact that the proposed schemes failure probabilities are near zero. However, the traditional HO scheme failure latency starts to increase after the speed of 40 m/s and more after 100 m/s and finally after a speed of 140 m/s to reach a latency of approximately 1.5s.

Fig. 4.24 depicts the schemes' average latency as a function of the train's speed. For speeds between (20-60) m/s, the schemes' latency experience a comparable performance. However, for speeds higher than that, the gap between the proposed schemes FSW/HO and the traditional HO scheme increase. This is caused by the high failure probability which increases as the speeds increase specifically for the traditional HO scheme, as

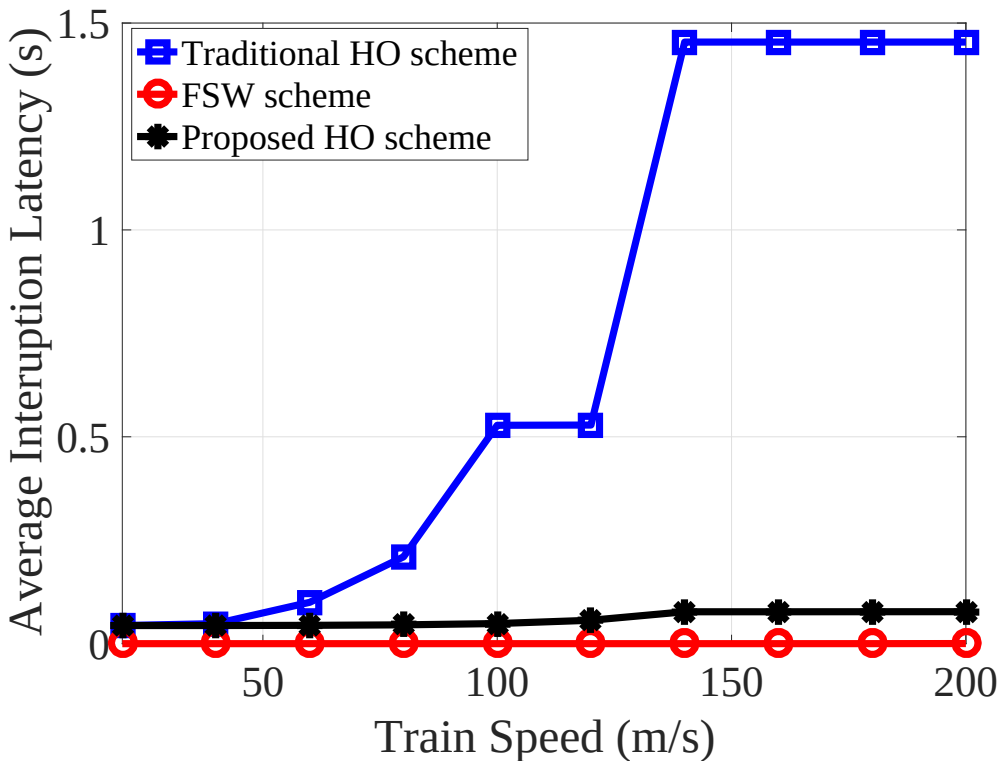

Figure 4.25: Schemes average latency versus the train's speed when $\rho_{RCR} = 0.3$.

higher speeds have very limited retransmission trials compared with lower speeds for the traditional HO scheme. Both proposed schemes show no/slight increasing in the average latency which means that the proposed schemes can counteract failure probability even for a very high-speed of 160 m/s, and therefore the long interruption time associated with it. Nevertheless, even in case of failure, the enhanced fast scheme reduces the interruption time from 1454 ms to 254 ms according to the equality of $T_{rec}^{w/o[RCR]}$ and $T_{rec}^{w[RCR]}$, respectively. This means that the proposed HO scheme offers a reduction gain of 82.53% in terms of interruption time in case of failure event. Further, the FSW scheme yields the lowest latency due to the scheme's relatively brief and more reliable procedures; whereas, the enhanced fast scheme delivers a considerable latency reduction compared with traditional HO scheme. Our proposed HO scheme relaxes the traditional HO procedures by triggering few of them in advance. This gives the proposed scheme the chance to retransmit more and therefore maintain a low failure probability, and consequently to obtain a lower average latency compared with the traditional scheme. It is worth emphasizing that

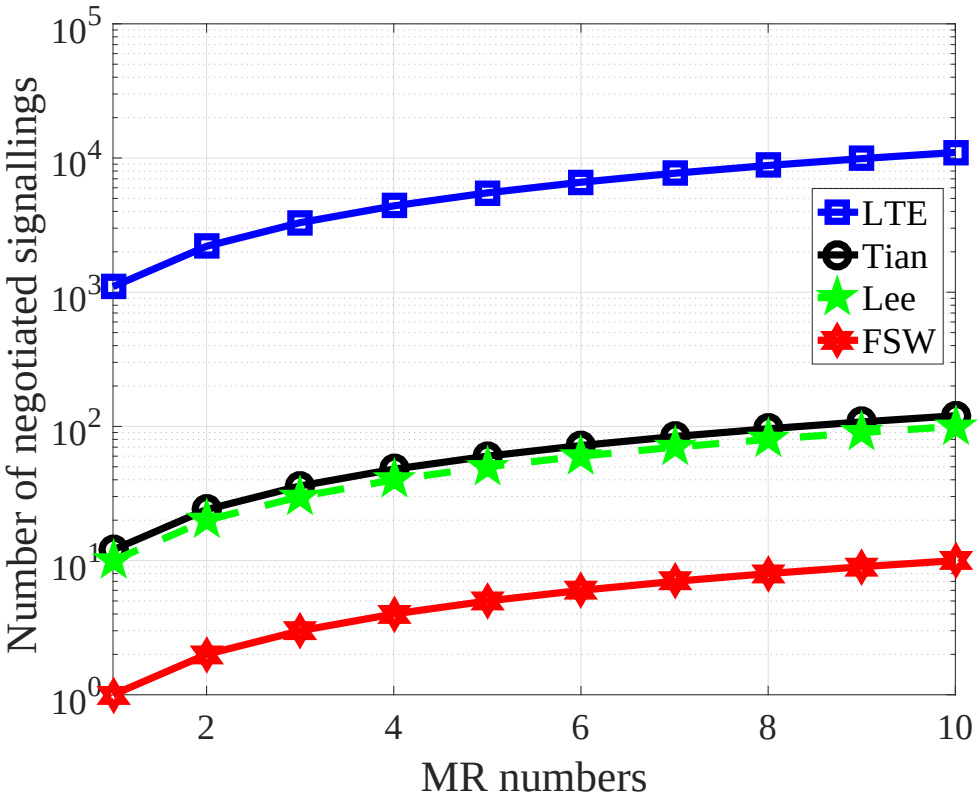

Figure 4.26: Signalling count comparison of the available solutions (LTE [3], Tian [3], and Lee [8]) to deal with recurrent HO issue.

the average success latency of FSW scheme does not involve any interruption time due to the transient optical switching time. Building on the above, the proposed schemes are able to support low-latency compared with the traditional HO scheme.

The average interruption time as a function of a speed is illustrated in Fig. 4.25. As it can be seen, the higher the speed, the higher the interruption latency specifically for the traditional HO scheme which interruption time begins to increase rapidly after the speed of 100 m/s to reach an interruption time of approximately 1.5s at the speed of 200 m/s. Yet, the proposed schemes are nearly the same, this is because the interruption time for the proposed schemes are the contribution of the success interruption time only since the failure probability of the proposed schemes are near zero.

Fig. 4.26 shows the signalling count of the required negotiated air interface commands for different schemes proposed to deal with the frequent HO issue in HSR scenario as a function of the MR number. As it can be seen, the FSW scheme performs the best com-

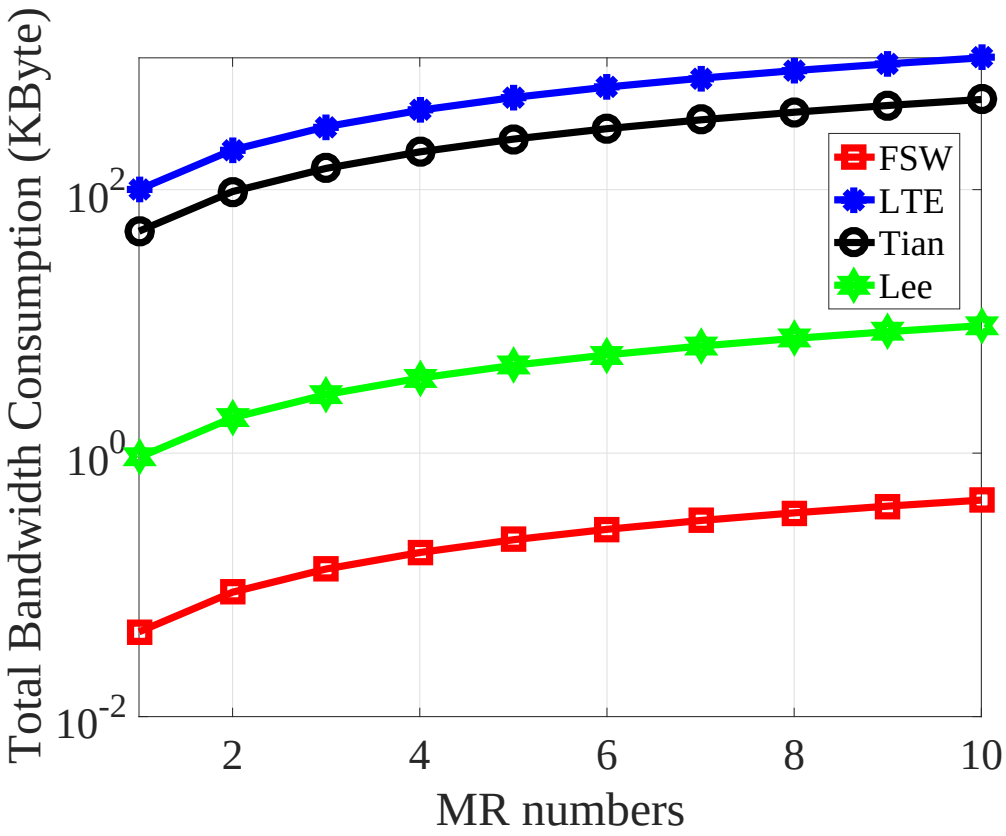

Figure 4.27: Signalling size cost comparison of the available HO schemes (LTE [3], Tian [3], and Lee [8]).

pared with other schemes as it only needs a measurement report command to finish the scheme successfully. In contrast, the traditional HO scheme (LTE) [3] performs the worst as it employs the direct communication approach instead of using a MR, while the other schemes proposed by Tian [3] and Lee [8] do or employ its equivalent. As a result, each UE executes the scheme independently in the case of the LTE scheme, which increases the negotiated signalling messages considerably consuming a huge network resources. Tian and Lee as well as the FSW scheme perform better compared to the traditional case as 100 UE are represented by one MR only. It should be noted that Table 4.4 and Fig. 4.26 do not reflect the retransmission trials case and the calculations are based on [3, 8, 111–113].

A comparison is given in Fig. 4.27 in terms of the bandwidth consumption of the signalling overhead . Consistent with the performance of the number of negotiated messages through the air interface, the bandwidth consumption of the signalling overhead shows a comparable performance. The FSW scheme and the traditional scheme perform the best and the worst, respectively, compared with other schemes. Additionally, the signalling

sizes increase as the number of the employed MRs increases. As mentioned earlier in chapter 1, we have not made a performance compression with other literature work except for the signalling overhead's count and size metrics. As these metrics depends only on the schemes itself and will not affected by either the analytical approach or the system assumption, which might be different among different literature works.

4.7 Summary

In this chapter, we have proposed two schemes to alleviate the effect of the frequent HO issue by proposing a FSW and an enhance fast handover scheme when moving between two RAUs belong to the same and different CUs, respectively. Both schemes provide a better reliability and a lower average latency compared with the traditional HO scheme. This has been achieved due to the FSW scheme less exchanged signalling messages and the more reliable process associated with the enhanced fast HO scheme (sending part of the scheme's signalling command in advance at a stronger RSQ along with given the system more trials in case the first transmission failed to be recovered) compared with the traditional HO scheme. In addition, both schemes provide more retransmission trials than the traditional HO scheme, as provided in the upper bound and the average retransmission trials analysis, which means a lower failure probability can be achieved compared with the traditional HO scheme.

Furthermore, the proposed FSW and the enhanced fast HO scheme require less overlapping area length than the traditional HO scheme which achieve a reduction gain of 84% and 28% for the proposed FSW and HO schemes, respectively. Again this is due to the FSW scheme less negotiated signalling overhead and due to perform part of the enhanced fast HO scheme in advance outside overlapping area resulting in a more relaxed HO scheme compared with the traditional HO scheme. Moreover, the average latency associated with the proposed schemes and the traditional HO scheme was studied, and it has been shown that the proposed schemes have a considerably lower average latency compared with the traditional HO case, More specifically, a reduction gain in the latency of 93.98% and 98.98% under a speed of 200 m/ was achieved for the proposed HO scheme

and the FSW scheme, respectively. Most importantly, the average interruption time was also investigated and a reduction gain of 94.68% and 99.98% was achieved under a speed of 200 m/s for the proposed HO scheme and the FSW scheme, respectively. This means a better throughput and QoS can be achieved for the proposed schemes. Further, the FSW scheme has been compared with other works in terms of the negotiated signalling overhead count and size, and the obtained results support our claim that the proposed FSW scheme reduces the burden on the core network due to the FSW scheme short procedure. Finally, varying speeds have the same triggering probability regardless of the ICI effect as the triggering probability normally takes place at the cell edge where the noise dominate over the ICI effect resulting eventually in the same triggering performance no matter the speed.

CHAPTER 5

ONBOARD SEAMLESS FREQUENCY SWITCH SCHEME ALONG DISTRIBUTED ANTENNA SYSTEM FOR HIGH-SPEED TRAIN

Due to the ever-increasing demand for mobile communications anytime anywhere, one possible solution is to increase the cell density so that user equipments (UEs) are closer to base stations (BSs), which increases the spectrum efficiency. Since high speed railway (HSR) could carry numerous number of users onboard who require an acceptable quality-of-service (QoS), small cell deployment is becoming an urgent necessity. In this context, distributed antenna system (DAS) is proposed and is heralded as the most promising candidate to deliver users' needs in terms of bandwidth demands and considerably reduce the power consumption as the UEs are closer to BSs. The HSR's DAS comprises a trackside central unit (TCU) [1] which is in control of many small cell remote antenna units (RAUs). TCU is also responsible for all the signal processing, while a RAU is a simplified radio head used to transmit/receive wireless signals from/to TCU/UE [84, 94–100].

However, to perceive the expected benefits regarding coverage and capacity, recent related issues have emerged such as, mobility management [114], and inter-cell interference

[1]Since this chapter assumes two CU to be coexist, one is located at the system core and the other is located onboard the train. As a result, to differentiate between the two CUs, the earlier will be called as the TCU while the latter will be called as the OCU.

coordination (ICIC) [115]. The mobility management is considered as the most pressing challenge. More specifically, handover (HO) is the most crucial issue. More deployed cells in conjunction with HSR system velocity means necessarily higher HO rate which eventually might lead to more HO failure (HOF) events. To handle this issue, we have previously proposed a frequency switch scheme (FSW) [102], referred to as the trackside FSW (TFSW) scheme in this chapter, to alleviate the effect of frequent HOs, thereby providing a better QoS. In such a scheme, RAUs are no longer associated with a fixed radio frequency (RF). Instead, an RF paradigm switches among RAUs according to the onboard antenna (OA)[2] measurements such that the OA is always linked to the same time-frequency set. The switching process is triggered by issuing a measurement report (MRT) from the OA to the TCU based on a predefined threshold satisfaction. Based on the recovered MRT, the TCU usually decides whether to switch the OA to the next RAU.

Note that, the MRT is exchanged at the cell edge and its associated failure probability increases as the system's speed increases assuming a fixed overlapping area length among cells (where HO/FSW usually takes place). Since the HSR system always tends to increase its speed, the failure probability of the TFSW scheme would become significant, which consequently leads to a high possibility of link loss with the serving RAU. Losing the link would impact the end user's QoS, since the link recovery procedure is very time consuming. However, failure probability can be reduced by increasing the retransmission trials at the cost of increasing the latency and necessarily expanding the length of the overlapping area, as the system optimization normally takes into account the signal levels across the cell coverage including the overlapping areas. So that the signal level should satisfy the minimum level of service across the whole cell, this means negotiating any command outside the overlapping areas may fail to be recovered successfully, as the signal level outside the cell might not satisfies the minimum required signal threshold to communicate. Increasing the overlapping area length eventually increases the HO rate which in turn increases the HO number per itinerary, as more RAUs need to be deployed to cover the same itinerary. As a result, this is not the optimal solution to deal with

[2]For convenience, this chapter employs an onboard antenna instead of the MR as in the previous chapters. As this chapter deals with multiple antennas instead of multiple MR. This chapter does not encounter any MR instead the onboard antennas linked directly to the onboard CU via optical links.

the necessity for frequent HO/switching, especially in the next generation mobile communication of the communication systems that aims to support ultra-reliable low-latency communications.

In this chapter, a simpler yet more reliable onboard FSW (OFSW) scheme is proposed, in which an OA is no longer associated with a fixed RF. The same concept of TFSW scheme is utilized, by using the optical switch to switch frequencies/streams among OAs according to the OAs' current measurements/locations. By doing so, the switching process is controlled by the onboard control unit (OCU) instead of TCU. Thus, there is no need to issue a MRT back to the TCU to start the process, as the switching process is performed onboard. Only the measurement control (MC) command is needed to be recovered to have a successful OFSW scheme. Moreover, the MC can be exchanged outside the overlapping area, hence the reliability of the proposed scheme can be improved by increasing the retransmission trials without increasing the overlapping region. This achieves a more seamlessly switching process since the proposed scheme does not encounter any command negotiation at the cell edge which might be further susceptible to retransmission trials or even failure events. Furthermore, increasing the scheme's reliability could avoid the long interruption associated with the link failure recovery process, due to the fact the failed OA will have to perform the reestablishment process with the RAU which has the best signal by scanning all the surrounded RAU.

Note that a typical partial interruption problem could take place when only part of the OAs request to switch, resulting in a loss of connection to part of the communicating frequencies due to using a single OA per a serving RAU. Therefore, this chapter proposes to employ multiple antennas on each carriage (depending on the number of the used RFs) so that if one antenna is switched to the next RAU, the other is still communicating with that RAU until. The extra antenna is proposed to be located on the middle of the carriage so that when the front antenna is near the cell edge with a poor signal quality, the middle antenna is linked with the serving RAU with the best possible signal quality. Because of the elaborately middle antenna location, the links can be always kept connected with at least one antenna without any loss. Subsequently, no communication interruption occurs at all. Additionally, employing multiple antennas per link not only

eliminates the possibility of link disruption but also reduces the required retransmission trials for achieving a given failure probability, and can thus support low-latency communications. This chapter provides comprehensive details of the proposed scheme as well as the required architecture. The proposed scheme is analysed and compared with the TFSW scheme. Both schemes are investigated in terms of triggering probability, failure probability, communication interruption probability, overlapping area length, and the average latency. The analytical results support our claim that the proposed OFSW scheme can deliver an ultra relaible low latency communications compared with TFSW scheme. More specifically, the OFSW scheme shows a reduction gain of 59.3% and 61.16% in the failure probability and the average latency, respectively, compared with TFSW scheme.

The remainder of this chapter is organised as follows. Section 5.1 reviewed the TFSW scheme. Section 5.2 introduces the system architecture and the proposed OFSW scheme. Section 5.3 presents the system model and Section 5.4 introduces the performance evaluation. Section 5.5 presents the results and discussion and finally the chapter is concluded in Section 5.6.

5.1 Traditional Switching Scheme

In this Section, comprehensive details of the motivation behind proposing a new scheme to replace the traditional one are given. Fig. 5.1 illustrates the trackside scheme and the details can be found in Section 4.3.2.

5.1.1 Trackside Scheme Inherent Flaws

Herein, some of the major trackside scheme drawbacks are presented and discussed, which form the fundamental motivation behind proposing a new FSW scheme. The details are as follows.

5.1.1.1 Signalling Overhead

The TFSW scheme needs the MC along with the MRT to be recovered successfully in order for the TFSW scheme to be finished successfully. However, high-speed movement

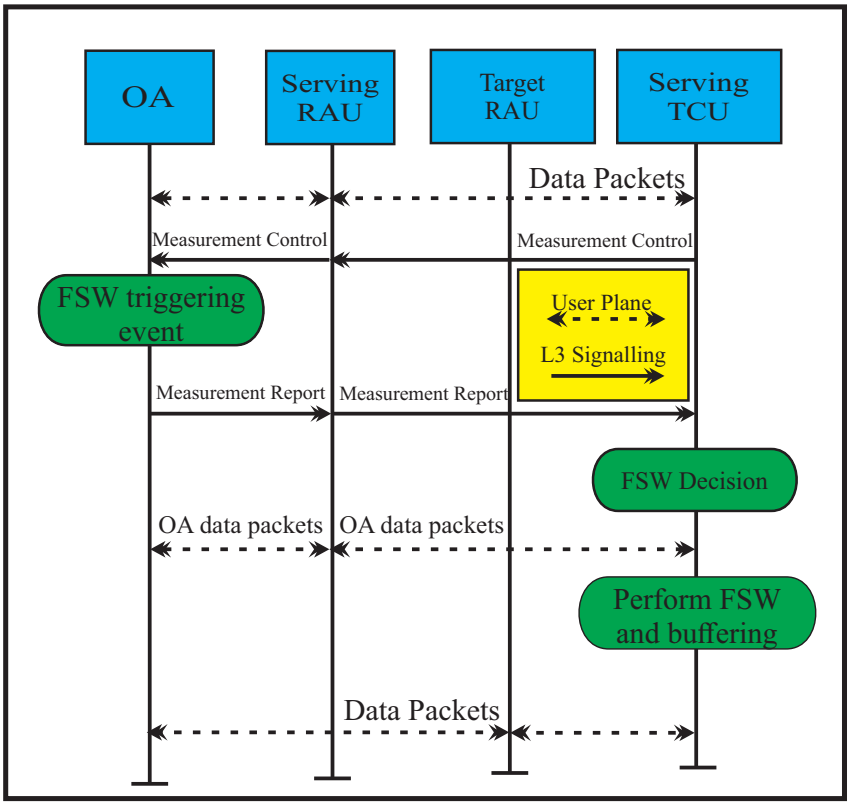

Figure 5.1: Trackside FSW scheme.

results in a Doppler shift. A severe Doppler shift has a serious impact on the system performance, as it can result in a carrier frequency offset to OFDM systems. The resulted frequency offset of the uplink is twice that of the downlink, which can be beyond the estimation capabilities of the BS, as Doppler shift of the HSR scenario is much higher compared with the cellular scenario.

Under each BS coverage area, the moving OA faces a rapid frequency offset transition from a positive to a negative Doppler shift when the OA approaches and crosses over the BS, respectively. Estimating and compensating for such a large and rapid Doppler fluctuation is intricate. Additionally, harsh frequency offset results in subcarriers nonorthogonality, consequently users might not be distinguished any more. Further, carrier frequency offsets may introduce an intercarrier interference (ICI) effect which might further deteriorate the link performance and the system capacity of HSR. Usually, to alleviate the Doppler shift effect, the vertical separation distance between BS and the track (d_s) can be increased, as shown in Fig. 5.2 and Fig. 5.3 in case of macro BS. Yet this solution might

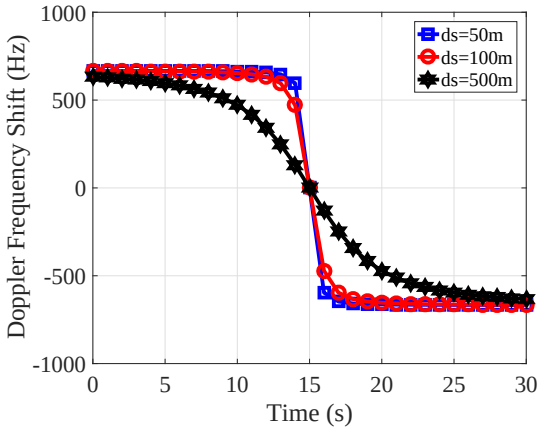

Figure 5.2: Doppler shift at 2GHz of a macro cell BS which has a coverage area = 3km under variable vertical distances.

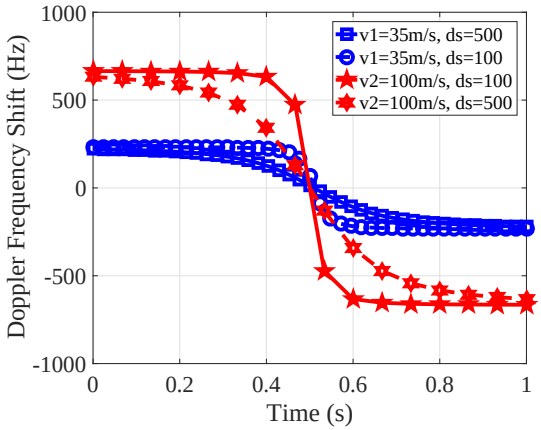

Figure 5.3: Doppler shift at 2GHz of a macro cell BS which has a coverage area of 3km under variable speeds and vertical distances.

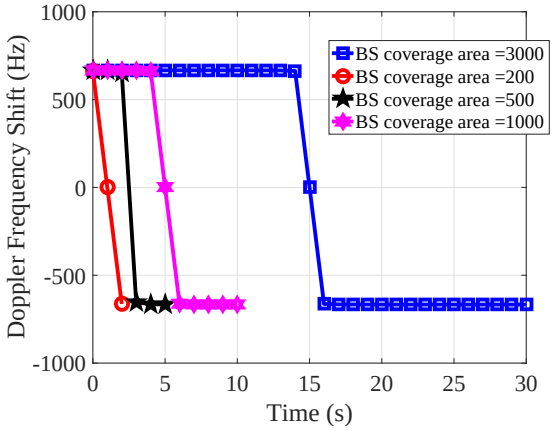

Figure 5.4: Doppler shift at 2GHz of variable BSs coverage area under a vertical distances of 10m and a speed = 100m/s.

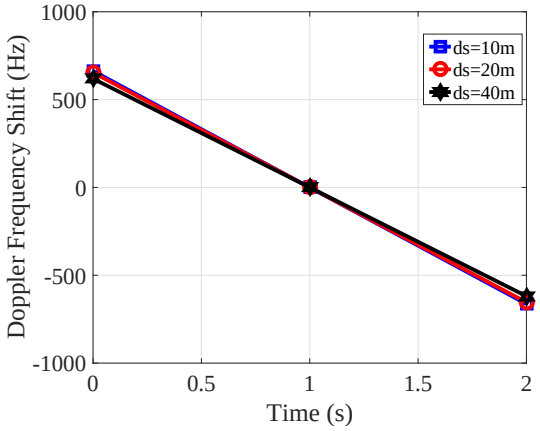

Figure 5.5: Doppler shift at 2GHz of a small cell BS which has a coverage area of 200m for a speed = 100m/s under a variable vertical distances.

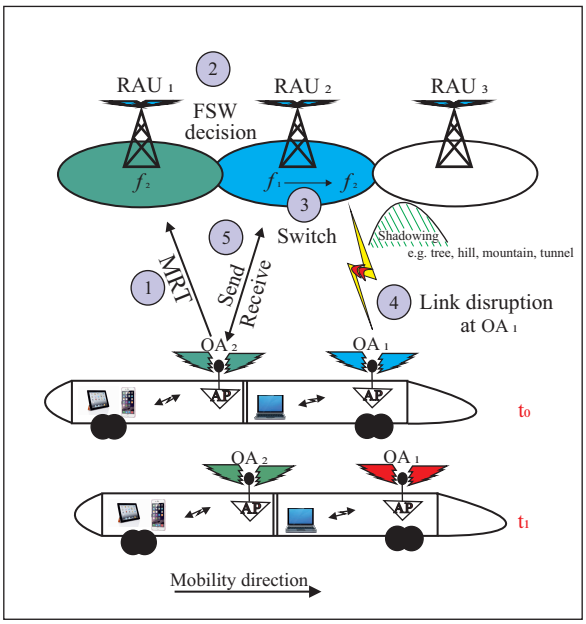

Figure 5.6: Partial interruption scenario, and it also represents the system architecture of the TFSW scheme.

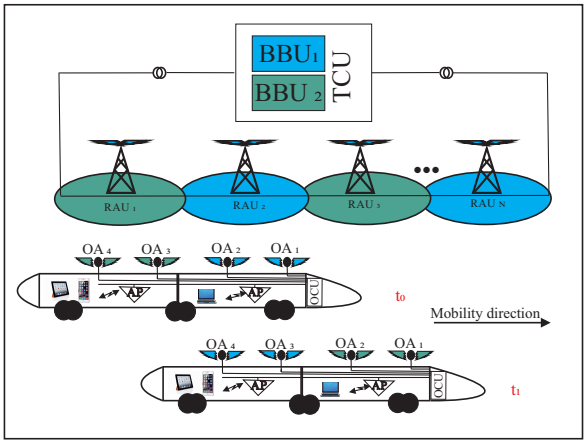

Figure 5.7: System architecture of the proposed scheme.

have a limited effect on the small cell deployment as the cell is of a small coverage range, and the vertical distance is limited by the cell radius. The Doppler shift effect on different cell sizes and small cell are shown respectively in Fig. 5.4 and Fig. 5.5 for varying vertical distances, which shows that the Doppler shift can be alleviated for macro cell only. In near future, Doppler shift can be made manifold as the speed will be tremendous and as a result of employing higher carrier frequencies in the millimetre wave band range. This leads to a further challenge that there is a high probability of the MRT exchanged at the cell edge failing.

5.1.1.2 Partial Interruption

The TFSW scheme might lose the link(s) established with one (or more) of the communicating RAUs (frequencies) due to the OA inherent asynchronous switching process. Since the scheme adopts the channel measurement to trigger the trackside scheme, a partial switch might happen, which leads to link connection failure and even cause the OA to enter the idle mode. To understand this scenario, consider this simple example depicted in Fig. 5.6 where two communication frequencies f_1 and f_2 are associated with RAU_2 and RAU_1, respectively, and two independent data streams are associated with OA_1 and

OA_2, respectively. Suppose that the train approaches the cell edge at time t_0 and OA_2 requests to switch to the next RAU i.e. RAU_2 by sending a MRT back to TCU once the predefined triggering condition is satisfied for example, the RSQ of the target is higher than or equal to a predefined condition. If TCU decides to switch OA_2 to RAU_2, OA_2's data stream will be switched from the current RAU_1 to RAU_2. Meanwhile, at time t_0, OA_1 has not issued any MRT to TCU yet as its current channel environment is still good enough for it to communicate through RAU_2 due to the presence of the shadowing effect e.g., trees, hill, mountain, which consequently prevents the RSQ of the target Ω_i^T from satisfying the predefined condition resulting in asynchronous triggering as illustrated in Fig. 5.6. After switching OA_2 to RAU_2 (which is currently OA_1's serving cell), at time t_1, OA_2 transmits and receives normally from RAU_2 using f_2, while OA_1 loses the link with RAU_2, which leads to a failure event. This leads consequently to the aforementioned partial interruption. Furthermore, it should be noted that one possible solution is that the TCU delays the switching process of all the OAs until it receives a MRT from all the associated OAs, so that a synchronous switching process could be achieved. However, this might also risk one or more of the associated OAs going through a poor channel condition, which leading to a failure event.

5.2 Onboard Switching Scheme

In this Section, by exploiting the two-hop architecture, striving to achieve ultra-reliable low-latency communications, the OAs are envisaged to execute an OFSW scheme when moving among RAUs belonging to different baseband units (BBUs) within the control of the same TCU, thereby expunging the necessity to perform HO. Prior to discussing the proposed scheme, the system architecture details are presented as follows.

5.2.1 System Architecture

Fig. 5.7 shows the proposed architecture which includes two main entities namely, the trackside (TCU and RAU) and the onboard entities. In the former, the TCU can include multiple BBUs in order to provide the users with their required capacity needs. Each BBU

within TCU controls a group of separated RAUs. The separation distance between RAUs or the frequency pattern allocation depends on how many BBUs the TCU includes which directly related to the train's dimensions. Particularly its length, and more specifically to the OA's and the associated RAU's footprint. TCU linked to RAUs via optical fibre links to transmit/receive to/from OA/TCU.

While in the latter, the network comprises a number of allocated access points (APs) along the trains' carriages. In contrast to the traditional architecture where each AP is linked to its correspondent OA, we propose to link the AP to an OCU. Thus, the OCU can reroute streams according to the upcoming RAU's RF as can be seen in Fig. 5.7. The OCU can realize the rerouting process of data streams by using an optical switch, where each OA includes an optical add drop multiplexer (OADM) to terminate a specific wavelength on its corresponding OA. After modulating the right wavelength on the intended RF, the signals are multiplexed and sent through the optical fibres which interconnect the OAs with the OCU. To conclude, rather than having a permanent RF associated with a specific OA, a temporary RF is dynamically assigned to each OA based on the OA's channel measurements. This results in a dynamic RF paradigm in which RFs used for communication can be frequently changed per each OA according to its current associated RAU's frequency.

5.2.2 The Proposed Onboard Switch Scheme

In this subsection, we propose an OFSW scheme which is composed of three phases: preparation phase, execution phase, and completion phase. In the following, without loss of generality, the OFSW process of the first OA is described. The proposed scheme is depicted in Fig. 5.8 and the details are as follows.

Phase I: Onboard Frequency Switch Preparation

1. Once the OA recovers the MC sent through the OA's current associated RAU, the OA will be aware of the candidate target RAU ID, the metrics used to perform measurement, and the conditions needed to trigger the process. Those conditions include the predefined RSQ threshold.

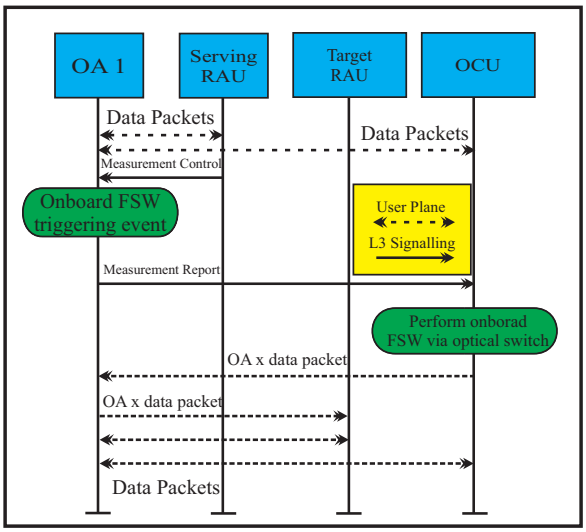

Figure 5.8: Onboard FSW scheme.

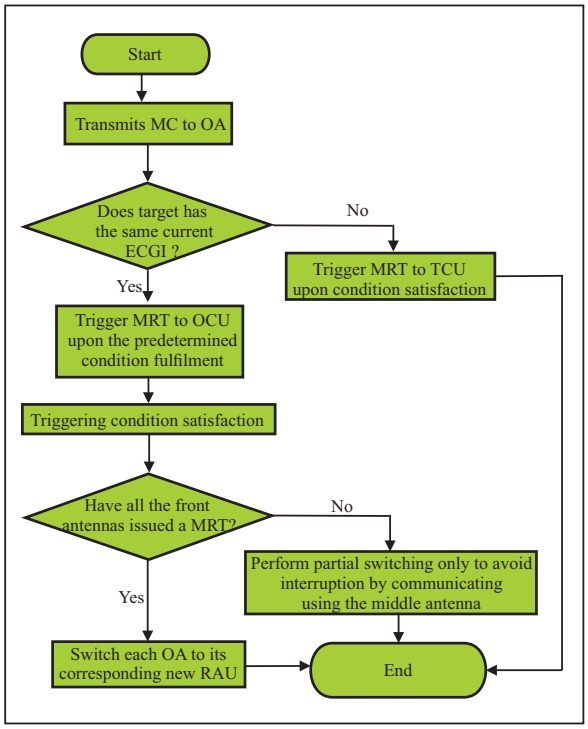

Figure 5.9: OFSW scheme execution process.

2. On triggering condition satisfaction, the OA issues a MRT to OCU. The transmitted MRT is not susceptible to retransmission attempts or failure event as the MRT is transmitted to the OCU through optical fibre. The MRT will include the RAU ID, which satisfies the triggering condition. Note that this RAU will always be the neighbouring RAU in HSR scenario due to the linear one-dimensional cell layout deployment.

3. In this phase, there is no need to execute the TFSW decision algorithm as the OA is moving under the control of the same TCU. However, the MC sent by TCU should include the E-UTRAN cell global identifier (ECGI) of the target RAU, so that the OCU could identify whether the target RAU is still controlled by the same TCU. If not, the OCU can either forward the MRT again to OA to be transmitted back to TCU, or the OCU can configure the OA to trigger the MRT back to TCU directly if the detected ECGI is different from the previous one. This would trigger a HO process by issuing the MRT back to the TCU in case the previous and the current ECGI is different (see Fig. 5.9).

   Phase II: Onboard Frequency Switch Execution

4. Based on the OA's MRT, OCU will reroute the requested OA's stream to another OA so that the switched OA can be associated with a proper RAU which propagates the same time-frequency set. For example, as Fig. 5.10 shows at time t_0, by assuming that OA_2 and OA_4 does not exist, OA_1 issues a MRT to OCU, reporting that RAU_3 is propagating a specific frequency (f_2) needed to be switched to, then OCU switches the stream associated with the target RAU i.e. RAN_3 to be propagated via OA_1, which is the same as OA_3's stream. In this situation, we only consider two communication frequencies i.e., f_1 and f_2. If OA_3 issues a MRT at the same time OA_1 does, OCU will switch each other streams to the other OA. If OA_1 and OA_3 did not trigger the MRT simultaneously, this will let the untriggered OA to lose the link with the serving RAU. In this case, an outage happens for f_1. f_1's OA then have to scan all the surrounded frequencies, as it does not know which RAU is the best to camp on since the switching process does not encounter a FSW/HO command which inform the OA with the chosen target. After choosing the best RAU to connect to, the OA starts the reestablishment procedure. This recovery process is very time-consuming and affects the user's QoS. Hence, we propose to place an extra antenna elaborately located at the middle of each carriage where an antenna is already deployed on the front of the carriage. As illustrated in Fig. 5.10, at time instant t_1, by adding the antennas OA_2 and OA_4, the antennas OA_1, OA_3 and OA_4 are communicating with RAU_3 using f_2 (the green colour in Fig. 5.10), while OA_2 is communicating with RAU_2 using f_1 (the blue colour in Fig. 5.10). It can be seen that no link interruption occurs among the trackside propagating RAUs, as it will be linked to the middle antennas i.e OA_2.

   Phase III: Onboard Frequency Switch Completion

5. At time instant t_1, deploying OA_2 and OA_4, any potential interruption can be totally avoided. As a result, OCU switches OA_1 from f_1 to f_2 using optical switch. The switching process for the first antenna OA_1 finishes successfully.

To conclude, the OFSW scheme can be triggered and performed totally internally within the train's network, consequently delivering a consistently successful scheme with no message command negotiation at the cell edge, reducing the trackside signalling. In

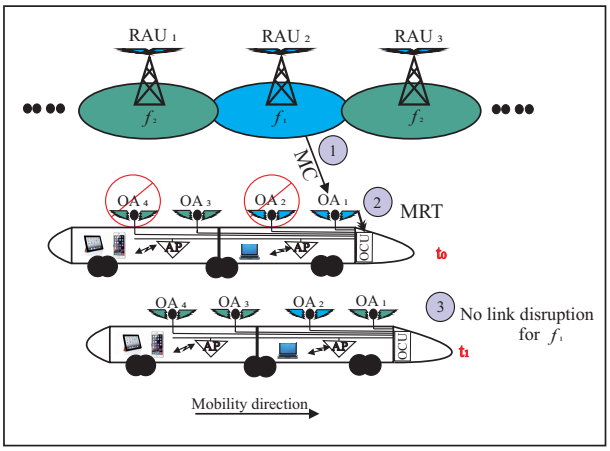

Figure 5.10: Partial interruption scenario.

order for the switched OA to be perfectly synchronized on time-frequency basis, the OCU should store the time-frequency information for each available BS within TCU and then track and update those information each time an onboard switching takes place for all the affected antennas.

5.3 System Model

Because railway tracks are generally constructed in a wide rural and/or viaduct area, where the multipath effect could be ignored most of the time and the FSW/HO scheme is less sensitive to the small scale fading, only the large scale fading is considered [5, 30, 88]. With equal power allocation among RAUs, the received signal power of OA $j \in \{f,\ m\}$, i.e. {front, middle} from RAU $k \in \{S,\ T\}$, i.e. {serving, target}, at the ith time interval denoted by P_{ij}^{k}, can be calculated as

$$P_{i_j}^{k}[dBm] = P_t[dBm] - P_{L_{i_j}}^{k}[dB]. \tag{5.1}$$

P_t is the transmitted power per RAU, given by

$$P_t[dBm] = 10\log_{10}\left(\frac{P_T/M}{N}\right), \tag{5.2}$$

where M denotes the number of subcarriers, P_T is the total transmitted power of CU_m, and N is the total number of RAUs under CU_m control. $P_{L_{i_j}}^{k}$ in (5.1) refers to the large scale fading between RAU k and OA j. According to WINNER II model, specifically,

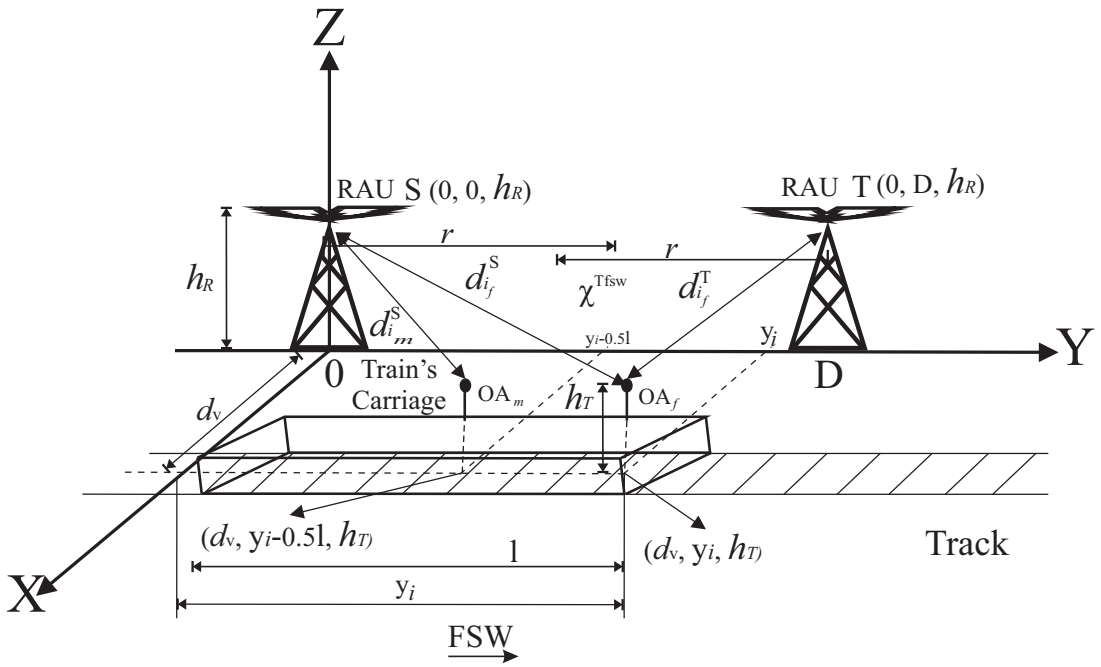

Figure 5.11: System model.

D2a rural moving networks scenario [89], $P_{L_{i_j}^k}$ can be given by

$$P_{L_{i_j}^k}[dB] = \begin{cases} 44.2 + 20\log_{10}(d_{i_j}^k) + 20\log_{10}(f[GHz]/5) + 10\log_{10} g_{i_j}^k, & 10m < d_{i_j}^k < d_{BR}, \\ 10.5 + 40\log_{10}(d_{i_j}^k) + 1.5\log_{10}(f[GHz]/5) - 18.5\log_{10}(h_R) & \\ -18.5\log_{10}(h_T) + 10\log_{10} g_{i_j}^k, & d_{BR} < d_{i_j}^k < 10km, \end{cases} \tag{5.3}$$

where $d_{i_j}^k$ is the distance between OA $j \in \{f,\ m\}$ and RAU $k \in \{S,\ T\}$. As shown in Fig. 5.11, $d_{i_f}^T$, $d_{i_f}^S$, $d_{i_m}^T$, and $d_{i_m}^T$, can be obtained as

$$d_{i_f}^T = \sqrt{(d_v)^2 + (D - y_i)^2 + (h_R - h_T)^2}, \tag{5.4}$$

$$d_{i_f}^S = \sqrt{(d_v)^2 + (y_i)^2 + (h_R - h_T)^2}, \tag{5.5}$$

$$d_{i_m}^T = \sqrt{(d_v)^2 + (D - (y_i - 0.5 \cdot l))^2 + (h_R - h_T)^2}, \tag{5.6}$$

and

$$d_{i_m}^S = \sqrt{(d_v)^2 + (y_i - 0.5 \cdot l)^2 + (h_R - h_T)^2}, \tag{5.7}$$

respectively, where l is the train's carriage length as shown in Fig. 5.11. D is the inter-RAU distance between two successive RAUs, y_i is OA_f's current location, and d_v is the distance between the RAU and the track. h_R and h_T are the heights of RAU and train, respectively. $d_{BR} = 4h_R h_T f_c/c$ is the breaking point distance. Shadowing at the ith time interval is represented by $g_{i_j}^k$ where $10\log_{10} g_{i_j}^k \sim \mathcal{N}\ (0, (\sigma_{i_j}^k)^2)$ follows a Gaussian distribution with a zero mean and a standard deviation $\sigma_{i_j}^k$. Since we always have $10m < (d_{i_j}^k) < d_{BR}$, our scenario fits the first sub-domain of (5.3).

Now, let $A[dBm] = 10\log_{10}\left(\frac{P_T/M}{N}\right) - 44.2 - 20\log_{10}(f[GHz]/5)$. (5.1) can be rewritten as

$$P_{i_j}^k[dBm] = A - 20\log_{10}(d_{i_j}^k) - 10\log_{10} g_{i_j}^k. \tag{5.8}$$

The RSQ at OA j[3] from RAU k can be obtained accordingly as

$$\omega_{i_j}^k = \frac{10^{P_{i_j}^k/10}}{(\Delta \cdot 10^{P_{i_j}^k/10}) + \sigma_o^2}, \tag{5.9}$$

where $\Delta = 1 - \int_{-1}^{1}(1-|x|)J_0(2\pi f_D T_s x)dx$ is the tight upper bound of the ICI power of orthogonal frequency division multiplexing (OFDM) system [90], as LTE-A is employed here which uses OFDM as a radio interface in the downlink. $J_0(.)$ is the zeroth-order Bessel function of the first kind. $f_D = (v \cdot f)/c$ is the maximum Doppler frequency shift, f is the carrier frequency, v is the OA's/train's speed, $c = 3 \times 10^8$ m/s is the speed of light in vacuum, and T_s is the symbol duration. σ_o^2 denotes the noise power. The RSQ can be then calculated as

$$\omega_{i_j}^k = \frac{10^{P_{i_j}^k/10}/\sigma_o^2}{(\Delta \cdot 10^{P_{i_j}^k/10})/\sigma_o^2 + 1}, \tag{5.10}$$

which can be obtained in dB as

$$\Omega_{i_j}^k[dB] = A - 20\log_{10}(d_{i_j}^k) - 10\log_{10} g_{i_j}^k - 10\log_{10}\sigma_o^2 - I_{i_j}^k[dBm], \tag{5.11}$$

where $I_{i_j}^k$ denotes the normalized noise and ICI power, given by

$$I_{i_j}^k[dBm] = 10\log_{10}\left[\frac{(10^{\frac{(P_t[dBm] - P_{L_{i_j}^k}[dB])}{10}}) \cdot \Delta}{\sigma_o^2} + 1\right], \tag{5.12}$$

[3]Without loss of generality a single OA is considered in the analysis, as the others have the same analysis.

Note that for the TFSW scheme we have assumed two carriages and each has one antenna located at the train's front denoted as OA_f, the same applies for the proposed OFSW scheme except each carriage has two antenna located at the train's front and middle dented as OA_f and OA_m, respectively.

5.4 Performance Comparison between TFSW and OFSW

In this Section, the proposed scheme will be analytically studied and compared with the TFSW scheme. More specifically, the triggering probability, the failure probability, the average latency, and finally the overlapping area required for each scheme are studied and compared with the TFSW scheme.

5.4.1 Triggering Probability

Both the proposed OFSW scheme and the TFSW have the same triggering probability as both have the same triggering condition, and this can be found as

$$\begin{aligned}\mathbf{P}_{trigg}^{fsw} &= \mathbf{P}\left\{\Omega_{i_f}^T \geqslant \beta_2\right\} = \mathbf{P}\left\{A - 20\log_{10}(d_{i_f}^T) - 10\log_{10} g_{i_f}^T - 10\log_{10}\sigma_o^2 - I_{i_f}^T \geqslant \beta_2\right\}, \\ &= 1 - Q\left(10\,\frac{A - \beta_2 - 20\log_{10}(d_{i_f}^T) - 10\log_{10}\sigma_o^2 - I_{i_f}^T}{10\cdot\sigma_{i_f}^T}\right), \end{aligned} \tag{5.13}$$

where β_2 is the predefined triggering condition and $Q(x) = \frac{1}{\sqrt{2\pi}}\int_x^\infty e^{\frac{-t^2}{2}}dt$ is the Q-function.

5.4.2 Failure Probability

Herein, the failure probability of both the OFSW and the TFSW schemes are investigated. In this chapter, the effect of the MC is taken into account for both schemes. More specifically, the effect of the MC failure probability is considered in calculating the schemes' total failure probability, since the FSW scheme in general faces a periodic frequency changing, whether the changing of frequencies happen on the OA side or on the RAU side where both IDs associate with different frequencies continuously. Thus, after each successful

FSW scheme, the OA should receive the MC in order to update the OA with the most recent frequency and the associated RAU ID (TFSW case) or updating the OAs with the upcoming RAU ID and the associated frequencies (OFSW case). Otherwise, in case the MC failed to be recovered the monitoring and measuring process which is necessary to detect the need for the FSW scheme cannot be performed and consequently this results in an outage scenario ultimately. Hence, it is worth considering the MC failure probability in the overall failure probability. As a result, the TFSW scheme's failure probability can be calculated as

$$\mathbf{P}_{f_f}^{Tfsw} = \mathbf{P}_{f_{mc}}^{Tfsw} + (1 - \mathbf{P}_{f_{mc}}^{Tfsw}) \cdot \underbrace{\prod_{z=1}^{\alpha_{mrt}} \left[Q \left(10 \frac{A - 20\log_{10}(d_{i_f,z}^S) - 10\log_{10}\sigma_o^2 - I_{i_f,z}^S - U}{10 \cdot \sigma_{i_f}^S} \right) \right]}_{(\mathbf{P}_{f_{mrt}}^{Tfsw}) \text{ MRT failure probability}}, \tag{5.14}$$

where $d_{i_f,z}^S$ and $I_{i_f,z}^S$ denote the distance and the normalized noise and ICI power between the front antenna and the serving RAU of the retransmission trial z. U is the minimum RSQ needed to recover the command successfully. α_{mrt} is the maximum retransmission trials permitted to recover the MRT and it can be obtained as

$$\alpha_{mrt} = \left\lfloor \frac{\chi^{Tfsw} - v \times T_{dec}}{v \cdot T_o} \right\rfloor, \tag{5.15}$$

where χ^{Tfsw} is the TFSW scheme's overlapping area. T_o is a one time delay cost of transmitting the MRT. $\mathbf{P}_{f_{mc}}^{Tfsw}$ is the MC failure probability and since the serving CU/RAU could send the MC anytime/anywhere within the serving RAU coverage area after finishing the FSW scheme (TFSW or OFSW), then the average failure probability for the MC can be obtained as

$$\begin{aligned} \mathbf{P}_{f_{mc}}^{Tfsw} &= \frac{1}{y_i} \int_{y_1}^{y_2} \left[\prod_{z=1}^{\alpha} \mathbf{P} \left\{ \Omega_{i_f,z}^S \leqslant U \right\} \right] \mathrm{d}y_i, \\ &= \frac{1}{y_i} \int_{y_1}^{y_2} \prod_{z=1}^{\alpha} \left[Q \left(10 \frac{A - 20\log_{10}(d_{i_f,z}^S) - 10\log_{10}\sigma_o^2 - I_{i_f,z}^S - U}{10 \cdot \sigma_{i_f}^S} \right) \right] \mathrm{d}y_i, \end{aligned} \tag{5.16}$$

where α is the maximum allowable retransmission trials needed for recovering the MC. y_1 and y_2 are the potential points where the serving RAU might send the MC in between.

(5.14) states that a TFSW failure event happens due to either a MC or MRT loss. While for the proposed OFSW scheme, the scheme only encounters the recovery of the MC to have a successful procedure, as the switching is performed onboard and the OA is moving within the same logical cell so there is no need to transmit the MRT over the air interface instead the MRT is sent to OCU via the fibre link. Hence, the overall failure probability of the proposed scheme can be expressed as

$$\mathbf{P}_{f_f}^{Ofsw} = \mathbf{P}_{f_{mc}}^{Ofsw} = \frac{1}{y_i} \int_{y_1}^{y_2} \prod_{z=1}^{\alpha} \left[Q \left(10 \frac{A - 20\log_{10}(d_{i_f,z}^S) - 10\log_{10}\sigma_o^2 - I_{i_f,z}^S - U}{10 \cdot \sigma_{i_f}^S} \right) \right] \mathrm{d}y_i. \tag{5.17}$$

5.4.3 Communication Interruption Probability

In order to investigate the proposed scheme ability to avoid the interruption scenario which happens when part of the OAs request a frequency switch while the others do not, we define a metric called the communication interruption probability. The interruption probability is therefore 1 when no OA is linked to a frequency during the FSW scheme. The lower the level of interruption, the more seamless scheme can be achieved.

Based on the aforementioned definition, we will study the interruption probability of the TFSW and the OFSW schemes in terms of two cases. The first case is the synchronous triggering across all the front OAs. The second case is the asynchronous triggering which happens when only some of the front OAs request to FSW. Both scenarios are discussed in the following

1. Synchronous FSW triggering

   Synchronous triggering can be encountered in both the TFSW and the proposed OFSW schemes, the details are as follows.

   (a) Trackside FSW Scheme

   TFSW scheme synchronous triggering takes place when both OAs request to switch frequency simultaneously. In this case, the TCU switches both frequencies to their intended RAUs. Therefore, the interruption probability of this

scenario is equivalent to the failure probability of the TFSW scheme, which can be expressed as

$$\mathbf{P}_{int}^{Tfsw} = \mathbf{P}_{f_f}^{Tfsw}. \tag{5.18}$$

(b) The Proposed OFSW Scheme

Synchronous triggering situation of the proposed OFSW scheme can occur when both front OAs trigger a MRT at the same time. Similar to the trackside case, the OCU switches both frequencies to the intended front OAs. Unlike the trackside scenario where there is only one OA linked to the same frequency/RAU, the proposed OFSW scheme has two antennas per carriage, so that the interruption probability of a specific frequency depends on both the failure probability of the proposed scheme (the front antenna of the first carriage) and the outage of the middle antenna (of the second carriage), and this can be derived as

$$\mathbf{P}_{int}^{Ofsw} = \mathbf{P}_{f_f}^{Ofsw} \cdot \mathbf{P}_{out_m}^{Ofsw}, \tag{5.19}$$

where $\mathbf{P}_{out_m}^{Ofsw}$ denotes the outage probability of the middle OA, given by

$$\begin{aligned}
\mathbf{P}_{out_m}^{Ofsw} &= \prod_{z=1}^{\alpha} \left[\mathbf{P}\left\{ \Omega_{i_m,z}^{S} < U \right\} \right], \\
&= \prod_{z=1}^{\alpha} \left[\mathbf{P}\left\{ A - 20\log_{10} d_{i_m,z}^{S} - 10\log_{10} g_{i_m,z}^{S} - 10\log_{10} \sigma_o^2 - I_{i_m,z}^{S} < U \right\} \right], \\
&= \prod_{z=1}^{\alpha} \left[Q\left(10 \frac{A - 20\log_{10}(d_{i_m,z}^{S}) - 10\log_{10} \sigma_o^2 - I_{i_m,z}^{S} - U}{10 \cdot \sigma_{i_m}^{S}} \right) \right],
\end{aligned} \tag{5.20}$$

where $d_{i_m,z}^{S}$ and $I_{i_m,z}^{S}$ denote the distance and the normalized noise and ICI power between the middle antenna and the serving RAU at the retransmission trial z.

2. Asynchronous FSW Triggering

Similarly, this scenario can be faced in both the TFSW scheme and the OFSW scheme and the details are presented as follows.

(a) TFSW Scheme

As the provided discussion of section 5.2.2, the TFSW scheme can encounter asynchronous triggering due to the existence of shadowing. Different from the synchronous case where we have an identical interruption probability, the asynchronous case has two interruption probabilities. The first is associated with the interrupted frequency while the other is associated with the uninterrupted frequency. The uninterrupted frequency is the frequency associated with the triggered OA while the interrupted frequency is the opposite. Since the TFSW scheme has only one antenna, the interruption probability of the interrupted frequency can be then found as

$$\mathbf{P}_{int}^{Tfsw} = 1. \tag{5.21}$$

Whereas, the interruption probability of the uninterrupted frequency depends on the failure probability of the TFSW scheme and can be obtained as in (5.14).

(b) The proposed OFSW scheme

Since at least one antenna can be linked to any available frequency in the case of the proposed OFSW scheme which is the middle antenna in this case, then the interruption probability can be expressed as

$$\mathbf{P}_{int}^{Ofsw} = \mathbf{P}_{out_m}^{Ofsw}. \tag{5.22}$$

Whilst, the interruption probability associated with the uninterrupted frequency depends on the failure/outage probabilities of all the linked antennas except the middle OA associated with the interrupted frequency which is three in this case. Hence, the interruption probability associated with this case can be found as

$$\mathbf{P}_{unint}^{Ofsw} = \mathbf{P}_{f_f}^{Ofsw} \cdot \mathbf{P}_{out_m}^{Ofsw} \cdot \mathbf{P}_{out_m}^{Ofsw}. \tag{5.23}$$

5.4.4 Overlapping Area Length

Overlapping area length highly depends on the encountered procedures contained in the applied schemes. As a result, the longer the scheme's procedures, the more overlapping

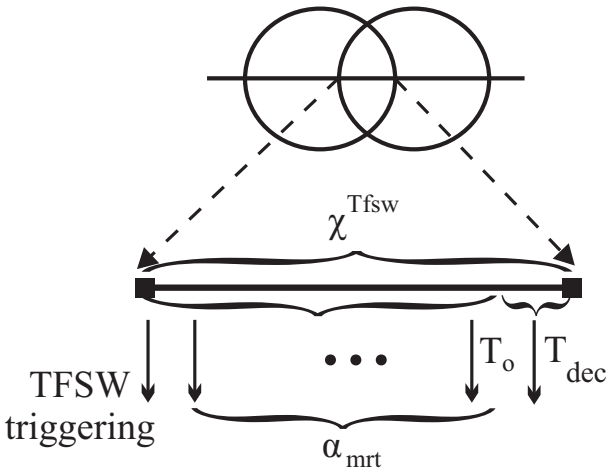

Figure 5.12: Operations taken place in the overlapping area for the TFSW scheme.

area required to keep the same performance compared with shorter procedure schemes. Shorter overlapping area has many benefits in terms of reducing the FSW rate, CAPEX and OPEX, by reducing the required number of RAUs to cover the same itinerary. To study the required amount of overlapping area length, we have neglect the effect of the optical switching time as we have considered the semiconductor optical amplifier (SOA) which has an opical switching time of 1ns [108]. The required overlapping area calculation is illustrated in Fig. 5.12. Consequently, the overlapping area length of the TFSW scheme can be derived as

$$\chi^{Tfsw} = v(\alpha_{mrt} \cdot T_o + T_{dec}), \tag{5.24}$$

where T_o and T_{dec} are the MRT's one time transmission delay and the TFSW decision algorithm, respectively. Since the proposed OFSW scheme does not encounter any MRT exchanging or decision algorithm and the optical switching time is 1ns. Hence, the need for overlapping area to perform the scheme's procedure can be neglected.

5.4.5 Average Latency

Herein, we introduce the latency cost for both the TFSW scheme and the proposed OFSW scheme of both success and failure event and the details are presented as follows.

1. Success Latency

(a) TFSW Scheme

The success latency of the TFSW scheme can be found as

$$T_{succ}^{Tfsw} = \overline{\alpha_s} \cdot T_o + \overline{\alpha_{mrt_s}} \cdot T_o + T_{dec}, \tag{5.25}$$

where $\overline{\alpha_s}$ is the expected value of the random variable of the retransmissions α_s required to recover MC successfully. Following the same assumption in page 88 of chapter 4. Then, the failure probability of the train's location can be represented as

$$\mathbf{P}_{f_{mc}}^{Tfsw} = \frac{1}{y_i} \int_{y_1}^{y_2} \left[Q \left(10 \frac{A - 20\log_{10}(d_{i_f}^S) - 10\log_{10}\sigma_o^2 - I_{i_f}^S - U}{10 \cdot \sigma_{i_f}^S} \right) \right]^{\alpha} \mathrm{d}y_i, \tag{5.26}$$

Therefore, $\overline{\alpha_s}$ can be derived as

$$\overline{\alpha_s} = \frac{1}{(1 - \mathbf{P}_{f_{mc}}^{Tfsw})} \sum_{n=1}^{\alpha} n \cdot \mathbf{P}\left\{\alpha_s = n\right\}, \tag{5.27}$$

where $\mathbf{P}(\alpha_s = n)$ denotes the probability of success transmission trial, given by

$$\mathbf{P}(\alpha_s = n) = \left[\mathbf{P}\left\{\Omega_{i_f}^S < U\right\}\right]^{n-1} \cdot \left[(1 - \mathbf{P}\left\{\Omega_{i_f}^S < U\right\})\right]. \tag{5.28}$$

The term $\sum_{n=1}^{\alpha} n \cdot \left[\mathbf{P}\left\{\Omega_{i_f}^S < U\right\}\right]^{n-1}$ can be simplified to

$$\frac{(\alpha \cdot \left[\mathbf{P}\left\{\Omega_{i_f}^S < U\right\}\right]^{(\alpha+1)} - (\alpha+1) \cdot \mathbf{P}_{f_{mc}}^{Tfsw} + 1)}{\left[\mathbf{P}\left\{\Omega_{i_f}^S < U\right\} - 1\right]^2}. \tag{5.29}$$

Similarly, $\overline{\alpha_{mrt_s}}$ is the expected value of the random variable α_{mrt_s} and this can be derived as

$$\overline{\alpha_{mrt_s}} = \frac{1}{(1 - \mathbf{P}_{f_{mrt}}^{Tfsw})} \sum_{n=1}^{\alpha_{mrt}} n \cdot \mathbf{P}\left\{\alpha_{mrt_s} = n\right\}, \tag{5.30}$$

where

$$\mathbf{P}(\alpha_{mrt_s} = n) = \left[\mathbf{P}\left\{\Omega_{i_f}^S < U\right\}\right]^{n-1} \cdot \left[(1 - \mathbf{P}\left\{\Omega_{i_f}^S < U\right\})\right]. \tag{5.31}$$

The term $\sum_{n=1}^{\alpha_{mrt}} n \cdot \left[\mathbf{P}\left\{\Omega_{i_f}^{S} < U\right\}\right]^{n-1}$ can be simplified further to

$$\frac{(\alpha_{mrt} \cdot \left[\mathbf{P}\left\{\Omega_{i_f}^{S} < U\right\}\right]^{(\alpha_{mrt}+1)} - (\alpha_{mrt}+1) \cdot \mathbf{P}_{f_{mrt}}^{fsw} + 1)}{\left[\mathbf{P}\left\{\Omega_{i_f}^{S} < U\right\} - 1\right]^{2}}. \tag{5.32}$$

The interruption time for this scheme is simply equaled to the optical switch time which can be neglected as mentioned before.

(b) Proposed Onboard FSW Scheme

Since the proposed OFSW scheme succeeds only if the MC is recovered successfully, then the latency of this case can be calculated as

$$T_{succ}^{Ofsw} = \overline{\alpha_s} \cdot T_o, \tag{5.33}$$

where $\overline{\alpha_s}$ is the expected value of the random variable of the retransmissions α_s required to recover MC successfully, this can be derived as

$$\overline{\alpha_s} = \frac{1}{(1 - \mathbf{P}_{f_{mc}}^{Ofsw})} \sum_{n=1}^{\alpha} n \cdot \mathbf{P}\left\{\alpha_s = n\right\}, \tag{5.34}$$

The interruption time for this scheme is simply equaled to the optical switch time which can be neglected as mentioned before.

2. Failure Latency

In case of failure event both schemes have the same latency and the details are as follows. The OA detects a RLF upon an indication that the maximum number of retransmission has been reached. Once the OA detects a RLF, it initiates T_{311} and starts the timer T_{311} for a cell reselection. In this case without receiving any command similar to the HO command, the OA is not aware of the target serving cell. As a result, the OA has to scan all the possible frequencies and then selects the best one. Once the OA selects a suitable cell, it starts reading all the required system information blocks (SIBs) to access the selected cell that is the neighbouring cell in the HSR case. If the needed SIBs are successfully acquired, the OA stops the timer T_{311} and starts the timer T_{301} in order to begin the connection re-establishment with the selected cell by sending RRC connection re-establishment request. The

re-establishment procedure succeeds only if the OA selects a prepared cell with the UE context. Therefore, re-establishment latency of the TFSW scheme in this case can be found as in (4.37). The total average latency is given by

$$T_{avg}^{Tfsw} = T_{succ}^{Tfsw} \cdot (1 - \mathbf{P}_{f_f}^{Tfsw}) + T_{rec}^{w/o[RCR]} \cdot \mathbf{P}_{ff}^{Tfsw}. \tag{5.35}$$

In the same way the total average latency of the proposed scheme can be obtained as

$$T_{avg}^{Ofsw} = T_{succ}^{Ofsw} \cdot (1 - \mathbf{P}_{f_f}^{Ofsw}) + T_{rec}^{w/o[RCR]} \cdot \mathbf{P}_{ff}^{Ofsw}. \tag{5.36}$$

Table 5.1: Default Simulation Parameters.

Parameter	Value
Number of Subcarrier M	1000
Bandwidth of Subcarrier	15 kHz
Carrier Frequency f	2 GHz
Power Density of Background Noise	-111 dBm/Hz
Speed of light in vacuum c	3 x 10^8 m/s
Symbol Duration T_s	1/14 ms
Total Transmit Power with normally noise power P_T	43 dBm
Shadow Fading Deviation σ_{i_j}	4 dB
Triggering Threshold β_2	1.3 dB
Signal Recovery Threshold U	1.1 dB
Total RAUs in each cell N	4
Inter-RAU distance D	200m
Cell radius r	105m
Overlap	10m
Length of Train	400m
Length of carriage l	200m
Distance between RAU and Track d_v	10m
Train height h_T	4m
RAU height h_R	32m
T304, T301, T311 in ms, respectively	50, 100, 1000
(y_1, y_2)	(-95, 95)

5.5 Results and Discussion

By mean of analytical model and validated via using simulations, the proposed OFSW scheme is investigated and compared with the TFSW scheme in terms of failure probability, communication interruption probability, overlapping area length, and average latency. These metrics are investigated under varying transmission trials to achieve the required performance. Single TCU is assumed, which controls 4 RAUs transmitting the same amount of power. OFSW/TFSW is performed when moving between two RAUs belong to the same TCU. The train length is assumed to be 400m with two carriages of 200m length each. Two antennas are mounted on the top of a carriage with one located on the front and the other in the middle of the carriage. The system parameters can be found in Table 5.1.

Fig. 5.13 shows the MRT failure probability of the TFSW scheme as a function of the front OA location for different speeds. As can be seen, as the speed increases, the failure probability increases assuming a fixed overlapping area of 2m. Since increases the speeds without extending the overlapping area means higher speed would not be able to finish the switching procedure successfully, as high speeds traversed the overlapping area in a shorter time compared with lower speed and/or it will have a lower chance to transmit more retransmissions. For example, for speed of 160 m/s, the failure probability is 1 due to the lack of overlapping area length, while the failure probability of speeds of 100 m/s, 80 m/s and 60 m/s are decreasing, respectively, as the speed decreases. Fig. 5.14, on the other hand, shows the same objective as Fig. 5.13 except a longer overlapping area of 4m is utilized. Comparing both figures, it can be seen that Fig. 5.14 has a lower failure probability under the same speeds shown in Fig. 5.13. For instant, under a speed of 160 m/s at OA's location of 100m, the failure probability is 0.03 at χ^{Tfsw} =4m, comparing with a failure probability of 1 at χ^{Tfsw} =2m, as increasing χ^{Tfsw} from 2m to 4m increases the retransmission trials from 0 to 2 trials to result in a decreasing gain of 1 in the failure probability.

The scheme's failure probability versus the front OA's location of the TFSW and the proposed OFSW schemes for a single transmission is shown in Fig. 5.15. As can be seen, the proposed scheme has a lower failure probability compared with the TFSW scheme,

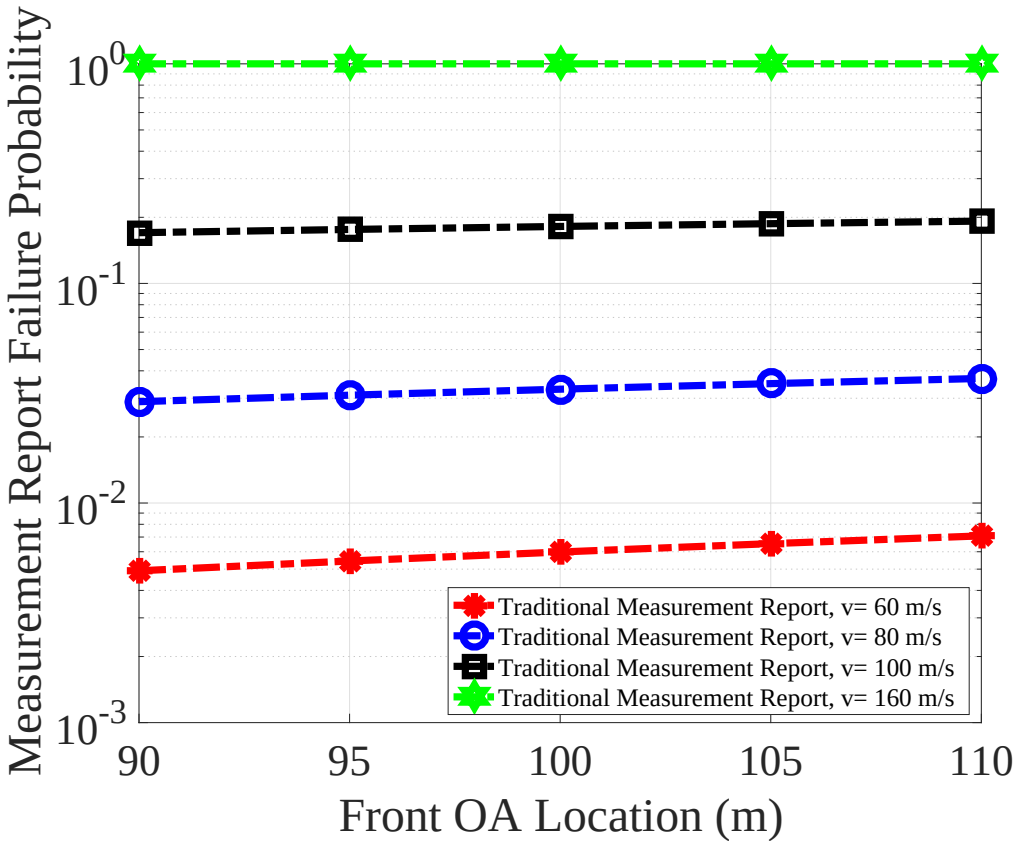

Figure 5.13: Failure probabilities of the MRT of the TFSW using single transmission as a function of the front OA location under χ^{Tfsw} =2 m

as the proposed scheme encounters the negotiation of only one command compared with two commands for the TFSW scheme. At OA's location of 100m, the proposed scheme reduces the failure probability from 0.2729 to 0.111, which means a reduction gain of 59.3% is possible by employing the proposed scheme which does not depend on the length of the overlapping region, as MC might be exchanged outside the overlapping region with a high probability. Also, it can be seen that th failure probability of the TFSW scheme is increasing as the OA moves away from the serving RAU, since the exchanged commands are correlated with the serving RAU, while the proposed scheme failure probability is a flat line, as it represents the average failure probability across the cell coverage area.

Furthermore, the scheme's failure probabilities as a function of the OA's location is shown in Fig. 5.16 under a varying number of retransmissions. As can be seen, as the number of retransmissions increase, the failure probability for both schemes decreases. However, increasing the number of retransmissions for the TFSW scheme means expanding

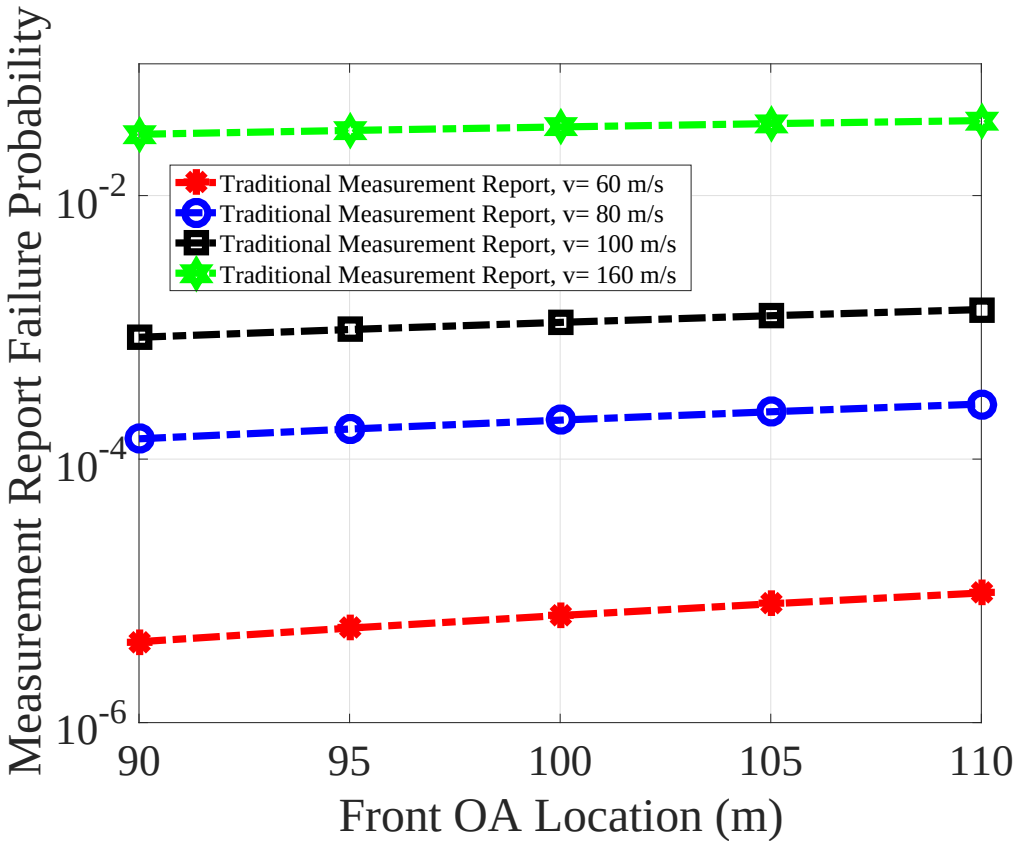

Figure 5.14: Failure probabilities of the MRT of the TFSW using single transmission as a function of the front OA location under χ^{Tfsw} =4 m

the overlapping area, while the proposed scheme does not. Moreover, the communication interruption probability as a function of the front OA location for the case of asynchronous switching is shown in Fig. 5.17. As can be seen, the interruption probability of the TFSW scheme is 1, since there is only one antenna linked to a specific RAU/communication frequency, which means switching that particular antenna leads to a total interruption to the original frequency. It should be noted that the TFSW interruption probability here is independent of the number of retransmission trials. In contrast, the proposed OFSW scheme shows a considerable performance improvement in terms of the interruption probability with different transmission trials single, quadruple and octuple. This performance improvement in the interruption probability compared with TFSW is due to the existence of the extra antenna used to be linked to a specific RAU/communication frequency. Also, it can be noticed that the interruption probability is decreasing as the transmission trials is increasing. For example, the interruption probabilities are 0.0622, 1.5×10^{-5} and

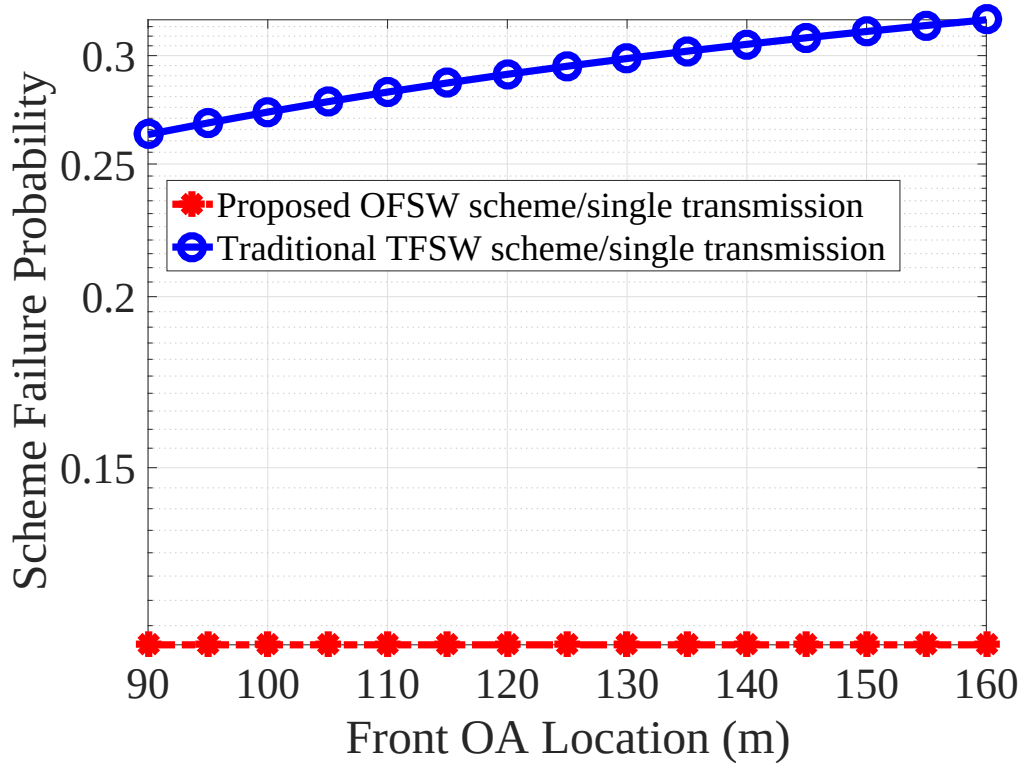

Figure 5.15: Failure probabilities of the TFSW and the proposed OFSW schemes using single transmission as a function of the front OA location, under a speed of 100 m/s.

2.25×10^{-10} at OA's location of 100m for single, quadruple and octuple transmission trials, respectively. In addition, the proposed OFSW scheme's interruption probability shows the lowest value at the OA's position of 100m. This is due to the fact that the proposed scheme elaborately deploys an extra antenna located at 100m away from the front antenna. And this is the exact location around which the switching process normally takes place. This elaborate deployment guarantees that the interruption will be at the lowest possible level, since the middle antenna will be near the RAU location, i.e. receiving with the best signal quality. After the 100m location, the interruption probability keeps increasing as the middle antenna will be moving away from the serving RAU.

Moreover, Fig. 5.18 shows the communication interruption probability versus the OA's location for the TFSW and the proposed OFSW schemes associated with the case of asynchronous switching for uninterrupted frequencies using single and quadruple transmissions. As can be seen, the proposed OFSW scheme shows a considerable reduction in

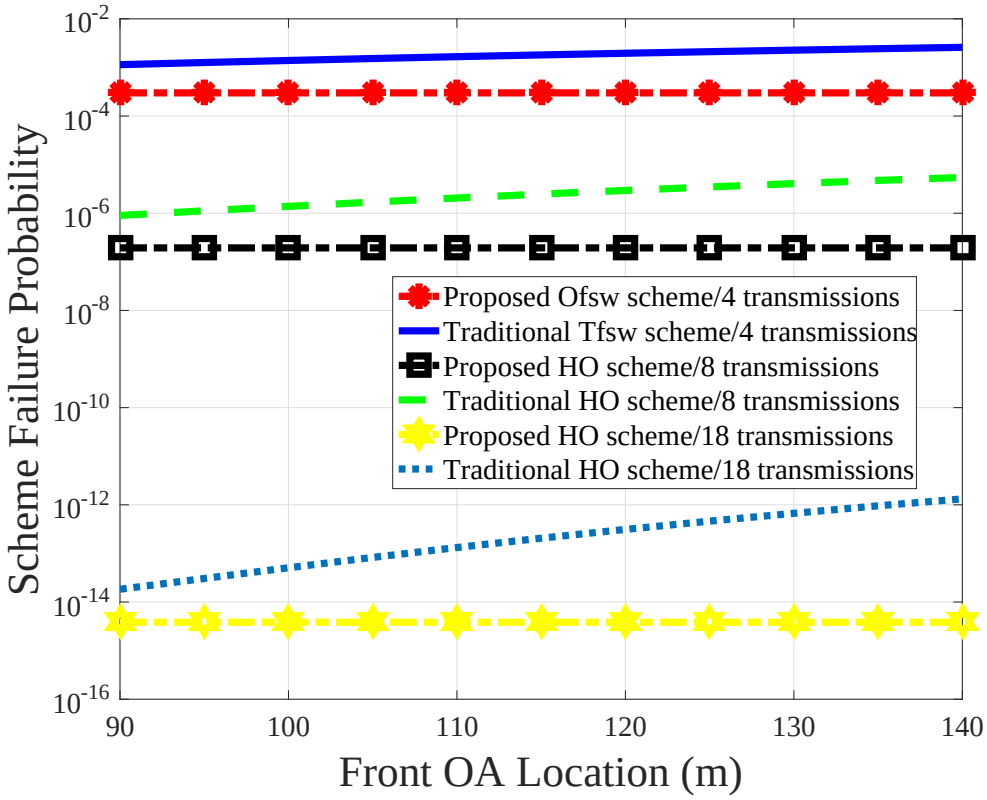

Figure 5.16: Failure probabilities of the TFSW and the proposed OFSW schemes using multiple transmissions as a function of the front OA location, under a speed of 100 m/s.

the interruption probability compared with the TFSW scheme for the same transmission trials. This stems from the fact that the TFSW scheme uses only single antenna to communicate with the serving RAU, while the proposed OFSW scheme uses three antennas to do so. Now, comparing Fig. 5.17 with Fig. 5.18 for the proposed OFSW scheme for a specific transmission trials, it can be noticed that the uninterrupted case has a lower interruption probability compared with the case of interruption. For instant, the interruption probabilities of the uninterrupted and the interrupted cases, respectively, are 0.001 and 2.47 $\times 10^{-8}$ compared with 0.0622 and 1.5×10^{-5} evaluated at OA's location of 100 for single and quadruple transmission trials, respectively. This reduction in the interruption probability of the uninterpreted case compared with the interrupted case is due to the fact that the uninterrupted case uses more antennas to be linked to a specific RAU. Thereby, the uninterrupted case can have a better QoS for the onboard users, since increasing the linked antennas not only reduces the interruption/failure probability but also reduces the

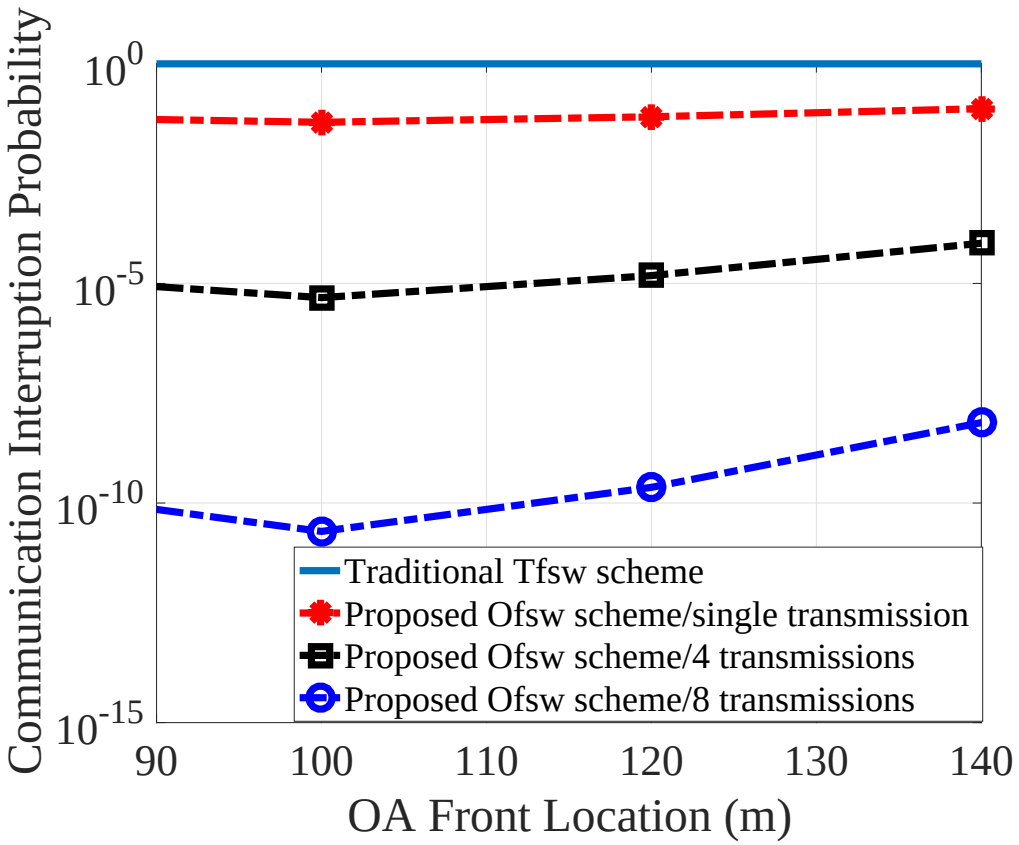

Figure 5.17: Communication interruption probabilities of the TFSW and the proposed OFSW schemes associated with the case of asynchronous interrupted frequencies using single and multiple transmissions as a function of the front OA location, under a speed of 100 m/s.

required number of retransmission to achieve a particular failure probability. On the other hand, the interruption probability of the synchronous case is depicted in Fig. 5.19 as a function of the front OA's location for the proposed OFSW scheme (single and quadruple transmission trials) and the TFSW scheme (quadruple and octuple transmission trials). Similarly, the proposed OFSW scheme exhibits a better performance compared with the TFSW scheme. Finally, the average latency as a function of the MR/train speeds is shown in Fig. 5.20, where α and α_{mrt} fixed to be four transmission trials. As can be seen, the proposed OFSW scheme experienced less latency compared with the TFSW scheme. A latency reduction of 61.16% can be achieved with the proposed OFSW scheme. Both schemes' latencies are the contribution of the success latency only, since both schemes have a low failure probability assuming a four transmission trials.

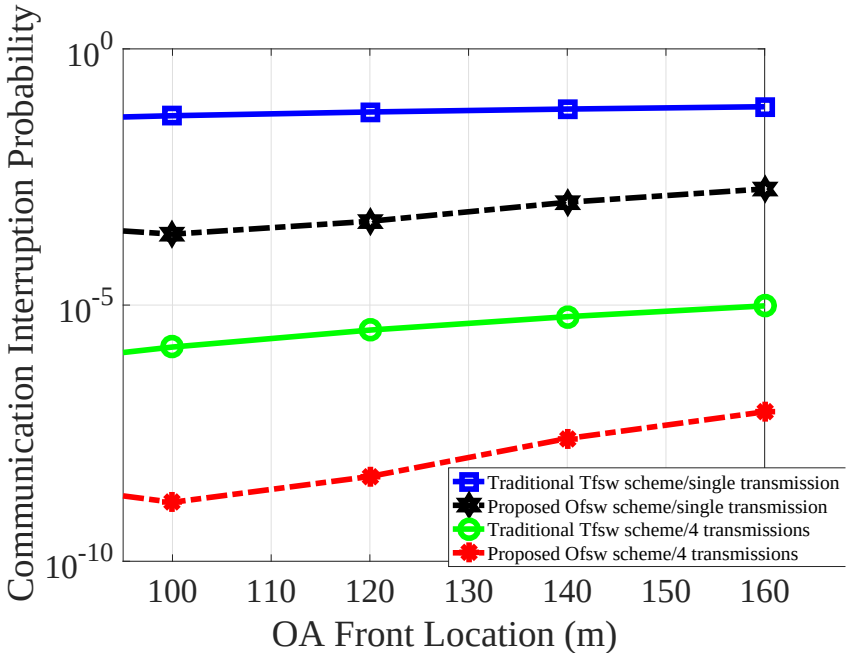

Figure 5.18: Communication interruption probabilities of the TFSW and the proposed OFSW schemes associated with the case of asynchronous switching for uninterrupted frequencies using single and multiple transmissions as a function of the front OA location, under a speed of 100 m/s.

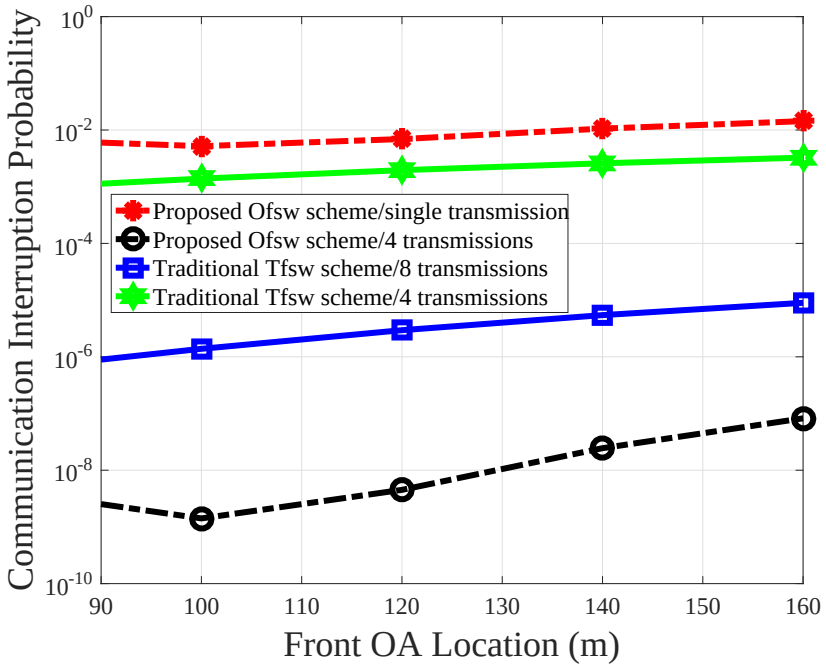

Figure 5.19: Communication interruption probabilities of the TFSW and the proposed OFSW schemes associated with the case of synchronous switching using single and multiple transmissions as a function of the front OA location, under a speed of 100 m/s.

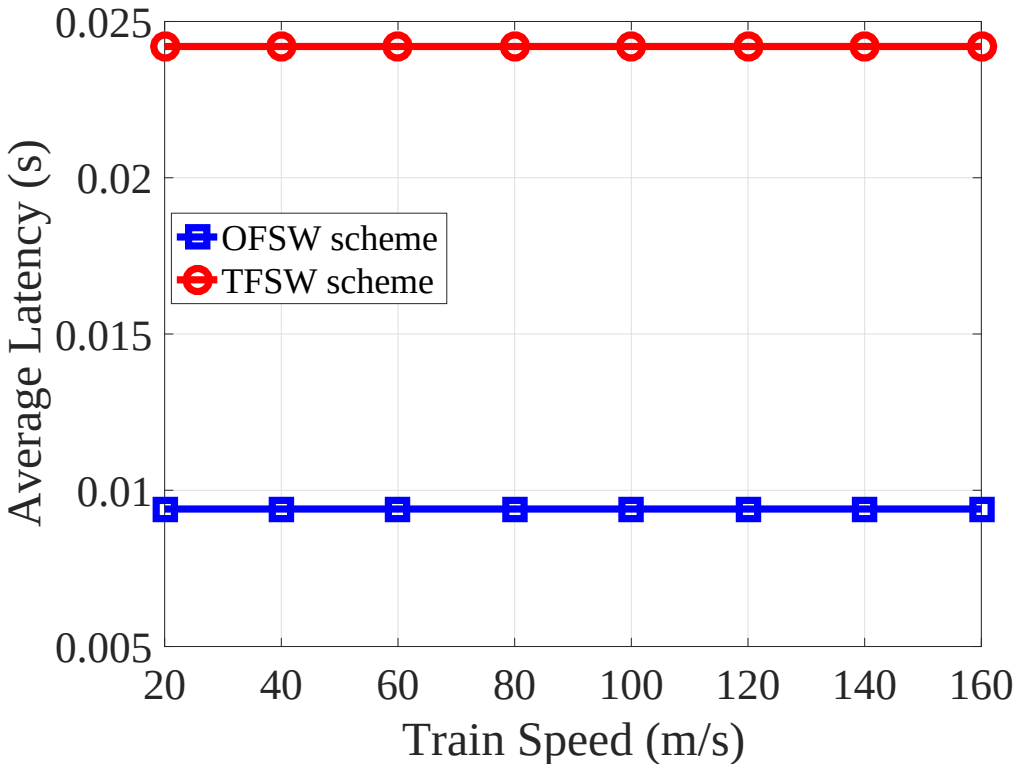

Figure 5.20: Average latency as a function of the MR/train speeds, where α and α_{mrt} fixed to be four transmission trials.

5.6 Conclusion

This chapter proposes a new scheme called as the OFSW scheme to replace the TFSW scheme when moving between two RAUs belong to the same TCU. The proposed OFSW scheme aims at enhancing the reliability and reduces the latency when moving among RAUs belong to the same TCU. Moreover, this chapter eliminate the possibility of the inherent interruption scenario when part of the OAs request to switch by employing multiple antennas on the carriage's roof. The analytical results verify the theoretical analysis and proves the proposed scheme superiority over the TFSW scheme by supporting lower failure, interruption probabilities and average latency. More specifically, the OFSW scheme shows a reduction gain of 59.3% and 61.16% in the failure probability and the average latency, respectively, compared with the TFSW scheme. Finally, the interruption scenario was totally avoided by adding an extra antenna on the middle of the carriage, so that the interruption probability is reduced from 1 in the TFSW scheme to 1.5×10^{-5} for only quadruple transmissions.

CHAPTER 6

CONCLUSION AND FUTURE WORKS

6.1 Conclusion

On one hand, using a small cell to serve the HSR might satisfy the users' needs in terms of capacity but it might also either increase the HO rate when moving between cells or increase the CAPEX and OPEX. However, these two issues can be eliminated or at least alleviated by using the DAS architecture, in which no HO is needed among RAUs under the control of the same CU. Instead a more fast and reliable FSW scheme is performed. CAPEX and OPEX on the other hand are reduced considerably when adopting the DAS architecture, in which the expensive BBUs can be centralized in one location compared with the traditional architecture, where BSs/BBUs are deployed along the train's route with large numbers. Also, the current trend of utilizing the milimetre wave frequencies, in which the path loss of these frequencies are high so the cells will tend to be of a small cell anyway in order to counteract this effect.

A HO process is needed when the MR crosses to RAU controlled by a different CU; thus, we have proposed a simplified HO scheme in chapter 3, in which the scheme triggers part of the preparation phase in advance so it can transmit the HO command immediately upon receiving the measurement report. This scheme was realized using the linear dedicated DAS.

Based on a dedicated DAS and the two-hop architecture, chapter 4 has proposed a

FSW scheme and a simplified HO schemes when moving among RAUs controlled by the same CU and different CUs, respectively. More specifically, a FSW scheme was proposed to avoid HOs when moving among RAUs controlled by the same CU. Therefore, the frequent HO issue is considerably alleviated as CU can control a large number of RAUs. However, the proposed FSW scheme has few issues such as the inherent interruption scenario as well as the long interruption time associated with failure/interruption event. While the proposed HO scheme performs the whole preparation phase in advance so that the HO command can be recovered with a high probability, yielding a more reliable scheme

Furthermore, To solve the issues associated with the FSW scheme, chapter 5 has proposed an onboard FSW scheme, which can eliminate the partial interruption issue by employing an extra antenna on the middle of each carriage to avoid it.

To this end, all the investigated schemes realized by exploiting the property of a dedicated DAS, where only one possible candidate is available to camp on. The proposed schemes have been analysed and compared with the traditional HO/FSW scheme. It has been proved analytically and by means of simulations that the proposed schemes outperform the traditional HO/FSW scheme and can deliver ultra-reliable low-latency communications. Finally, it has been proven that the proposed schemes require less overlapping area to support the same failure probability of the traditional HO/FSW scheme.

6.2 Future Works

HSR communications are now considering as the next 5G trending scenario. As a result, much more attention has been drawn to address this particular scenario's issues, especially the frequent HO issue.

In this context, and as a part of our future work, we will be investigating the system performance in terms of the failure probability, average latency, FSW/HO rate, and the required overlapping area length when considering massive MIMO/MIMO system instead of a SISO system. Employing massive MIMO technology by exploiting the train's long roof length should enhance the overall system reliability including the HO procedure, by sending and receiving multiple uncorrelated replica of the same message command. Moreover,

having multiple antennas to send and receive the message commands not only increase the reliability but also decrease the required time to finish the HO scheme successfully by reducing the required retransmission trials to achieve a certain reliability compared with a SISO system. Reducing the required time to conclude the HO scheme successfully results eventually in reducing the required overlapping area length, which reduces the FSW/HO rate. This results in decreasing the CAPEX and OPEX.

In addition, we will propose an expedited preparation phase scheme similar to what we have proposed earlier in chapter four of this thesis, however in conjunction with the most recent 5G network feature of synchronization, which eliminates the need to perform synchronization process between the MR and the target cell. As the new 5G BS is timely synchronized. Utilizing both approaches together would improve the HO scheme performance as the measurement report and the RCR command can be recovered successfully with low latency and the RA and RAR can be obsoleted due to the BSs synchronization feature, only the RCR complete command needs to be recovered successfully to conclude the scheme. This means only three commands need to be recovered successfully to finish the scheme two of them can be recovered with high probability. This scheme not only reduce the negotiated signalling commands and the failure probability but also reduce the interruption time associated with the obsoleted signallings. Thus, the proposed scheme enhances the users' QoS.

Furthermore, the drone BS will be also considered and investigated as the ultimate/vital solution to eliminate the frequent HO issue associated with HSR scenario. Employing the drone BS can reduces the HO rate since the HSR route can be divided to be covered by a number of drone. Also using the drone BS results in less Doppler shift since the drone can be moved at a speed relatively close to the train's speed, and less Doppler spread can be experienced due to the LOS availability. Moving at relatively close speed to the train's speed means less experienced ICI. Further, better channel gain can be obtained compared with a fixed BS which results in less radiated power towards a green environment. Building on the aforementioned, the proposed approach can achieve ultra reliability and low latency communication compared with the traditional fixed BS approach.

APPENDIX A

APPENDIX

Proof. let $Z = \mathbf{P}\left\{\Omega_i^S < U\right\}$, then

$$\sum_{n=1}^{n} n \cdot Z^{(n-1)} = 1 + 2Z + 3Z^2 + \cdots + nZ^{(n-1)}. \tag{1}$$

Now let $s = 1 + 2Z + 3Z^2 + \cdots + nZ^{(n-1)}$. Next, multiply both sides by Z.

$$sZ = Z + 2Z^2 + 3Z^3 + \cdots + nZ^n. \tag{2}$$

Subtract 2 from 1 as follows

$$\begin{array}{c} 1 + 2Z + 3Z^2 + 4Z^3 + \cdots + nZ^{(n-1)} \\ -\ Z - 2Z^2 - 3Z^3 - \cdots - nZ^n \\ \hline 1 + Z + Z^2 + Z^3 + \cdots + nZ^{(n-1)} - nZ^n = s - sZ \end{array} \tag{3}$$

Equality (3) can be then written as follows

$$1 + Z + Z^2 + Z^3 + \cdots + nZ^{(n-1)} - nZ^n = s(1 - Z) \tag{4}$$

We know that $1 + Z + Z^2 + Z^3 + \cdots + nZ^{(n-1)}$ is a geometric progression with first term 1 and a common ratio Z. So it can be expressed as

$$\sum_{k=1}^{n} aZ = \frac{1 - Z^n}{1 - Z}. \tag{5}$$

Consequently, equality (4) can be rewritten as follows

$$\frac{1-Z^n}{1-Z} - nZ^n = s(1-Z). \tag{6}$$

Now, divide both sides of (6) by $(1-Z)$. Accordingly, (6) can be expressed as follows

$$\frac{1-Z^n}{(1-Z)^2} - \frac{nZ^n}{1-Z} = s. \tag{7}$$

$$\frac{1-Z^n-(1-Z)nZ^n}{(1-Z)^2} = s. \tag{8}$$

Finally, equality (8) can be get as follows

$$\frac{nZ^{(n+1)} - Z^n(n+1)+1}{(1-Z)^2} = s. \tag{9}$$

Therefore, equality (9) is identical to equality (4.20). ■

BIBLIOGRAPHY

[1] A. Checko, H. L. Christiansen, Y. Yan, L. Scolari, G. Kardaras, M. S. Berger, and L. Dittmann, "Cloud ran for mobile networks a technology overview," *IEEE Communications Surveys Tutorials*, vol. 17, no. 1, pp. 405–426, Firstquarter 2015.

[2] Q. Li, R. Q. Hu, Y. Qian, and G. Wu, "Cooperative communications for wireless networks: techniques and applications in lte-advanced systems," *IEEE Wireless Communications*, vol. 19, no. 2, Apr. 2012.

[3] L. Tian, J. Li, Y. Huang, J. Shi, and J. Zhou, "Seamless dual-link handover scheme in broadband wireless communication systems for high-speed rail," *IEEE Journal on Selected Areas in Communications*, vol. 30, no. 4, pp. 708–718, May 2012.

[4] Y. Lin, S. Yang, and C. Wu, "Improving handover and drop-off performance on high-speed trains with multi-rat," *IEEE Transactions on Intelligent Transportation Systems*, vol. 15, no. 6, pp. 2720–2725, Dec 2014.

[5] H. Song, X. Fang, and L. Yan, "Handover scheme for 5g c/u plane split heterogeneous network in high-speed railway," *IEEE Transactions on Vehicular Technology*, vol. 63, no. 9, pp. 4633–4646, Nov. 2014.

[6] L. Yan, X. Fang, and Y. Fang, "A novel network architecture for c/u-plane staggered handover in 5g decoupled heterogeneous railway wireless systems," *IEEE Transac-*

tions on Intelligent Transportation Systems, vol. 18, no. 12, pp. 3350–3362, Dec 2017.

[7] M. S. Pan, T. M. Lin, and W. T. Chen, "An enhanced handover scheme for mobile relays in lte-a high-speed rail networks," *IEEE Transactions on Vehicular Technology*, vol. 64, no. 2, pp. 743–756, Feb. 2015.

[8] C. W. Lee, M. C. Chuang, M. C. Chen, and Y. S. Sun, "Seamless handover for high-speed trains using femtocell-based multiple egress network interfaces," *IEEE Transactions on Wireless Communications*, vol. 13, no. 12, pp. 6619–6628, Dec. 2014.

[9] M. Cheng, X. Fang, and W. Luo, "Beamforming and positioning-assisted handover scheme for long-term evolution system in high-speed railway," *IET Communications*, vol. 6, no. 15, pp. 2335–2340, October 2012.

[10] J. Wang, H. Zhu, and N. J. Gomes, "Distributed antenna systems for mobile communications in high speed trains," *IEEE Journal on Selected Areas in Communications*, vol. 30, no. 4, pp. 675–683, May 2012.

[11] S. Sesia, I.Toufik, and M. Baker, *LTE – The UMTS Long Term Evolution From Theory to Practice*, Second Edition, John Wiley and Sons, 2011.

[12] J. T. J. Penttinen, *The LTE-Advance Deployment Handbook the Planning Guidelines for the Fourth Generation Networks*, John Wiley and Sons, 2016.

[13] X. Zhang and X. Zhou, *LTE-Advanced Air Interface Technology*, Taylor and Francis Group, 2013.

[14] L. G. J. Acharya and S. Gaur, *Heterogeneous Networks in LTE-Advanced*, John Wiley and Sons, 2014.

[15] S. P. E. Dahlman and J. Skold, *4G, LTE-Advanced Pro and The Road to 5G*, Third Edition, Elsevier, 2016.

[16] M. Aguayo-Torres, P. Ameigeiras, J. Cullen, D. Fernández, A. Gil, G. Gómez, J. Guerrero, P. Hakalin, S. Hierrezuelo, and F. Kelly, *End-to-End Quality of Service over Cellular Networks Data Services Performance and Optimization in 2G/3G*, John Wiley and Sons, 2005.

[17] W. Zhan and L. Dai, "Massive random access of machine-to-machine communications in lte networks: Modeling and throughput optimization," *IEEE Transactions on Wireless Communications*, vol. 17, no. 4, pp. 2771–2785, April 2018.

[18] K. Abboud, H. A. Omar, and W. Zhuang, "Interworking of dsrc and cellular network technologies for v2x communications: A survey," *IEEE Transactions on Vehicular Technology*, vol. 65, no. 12, pp. 9457–9470, Dec 2016.

[19] G. Liu and D. Jiang, "5G: Vision and Requirements for Mobile Communication System towards Year 2020," *Chinese Journal of Engineering*, 2016.

[20] H. Park, Y. Lee, T. Kim, B. Kim, and J. Lee, "Handover mechanism in nr for ultra-reliable low-latency communications," *IEEE Network*, vol. 32, no. 2, pp. 41–47, March 2018.

[21] B. Lannoo, D. Colle, M. Pickavet, and P. Demeester, "Radio-over-fiber-based solution to provide broadband internet access to train passengers," *IEEE Communications Magazine*, vol. 45, no. 2, pp. 56–62, Feb. 2007.

[22] R. He, Z. Zhong, B. Ai, G. Wang, J. Ding, and A. F. Molisch, "Measurements and analysis of propagation channels in high-speed railway viaducts," *IEEE Transactions on Wireless Communications*, vol. 12, no. 2, pp. 794–805, Feb. 2013.

[23] R. He, Z. Zhong, B. Ai, and J. Ding, "An empirical path loss model and fading analysis for high-speed railway viaduct scenarios," *IEEE Antennas and Wireless Propagation Letters*, vol. 10, pp. 808–812, 2011.

[24] B. Chen, Z. Zhong, B. Ai, K. Guan, R. He, and D. G. Michelson, "Channel characteristics in high-speed railway: A survey of channel propagation properties," *IEEE Vehicular Technology Magazine*, vol. 10, no. 2, pp. 67–78, June 2015.

[25] C. X. Wang, A. Ghazal, B. Ai, Y. Liu, and P. Fan, "Channel measurements and models for high-speed train communication systems: A survey," *IEEE Communications Surveys Tutorials*, vol. 18, no. 2, pp. 974–987, Secondquarter 2016.

[26] L. Liu, C. Tao, J. Qiu, H. Chen, L. Yu, W. Dong, and Y. Yuan, "Position-based modeling for wireless channel on high-speed railway under a viaduct at 2.35 ghz," *IEEE Journal on Selected Areas in Communications*, vol. 30, no. 4, pp. 834–845, May 2012.

[27] K. Guan, Z. Zhong, B. Ai, and T. Kürner, "Propagation measurements and analysis for train stations of high-speed railway at 930 mhz," *IEEE Transactions on Vehicular Technology*, vol. 63, no. 8, pp. 3499–3516, Oct 2014.

[28] T. Zhou, C. Tao, S. Salous, Z. Tan, L. Liu, and L. Tian, "Graph-based stochastic model for high-speed railway cutting scenarios," *IET Microwaves, Antennas Propagation*, vol. 9, no. 15, pp. 1691–1697, 2015.

[29] W. Luo, X. Fang, M. Cheng, and Y. Zhao, "Efficient multiple-group multiple-antenna (mgma) scheme for high-speed railway viaducts," *IEEE Transactions on Vehicular Technology*, vol. 62, no. 6, pp. 2558–2569, July 2013.

[30] Z. Liu and P. Fan, "An effective handover scheme based on antenna selection in ground–train distributed antenna systems," *IEEE Transactions on Vehicular Technology*, vol. 63, no. 7, pp. 3342–3350, Sept 2014.

[31] C. V. N. I. Cisco, "Global mobile data traffic forecast update, 2015–2020," *white paper*, 2016.

[32] "Handbook of wireless networks and mobile computing," *John Willey and Sons.*, 2002.

[33] B. V. Quang, R. V. Prasad, and I. Niemegeers, "A survey on handoffs — lessons for 60 ghz based wireless systems," *IEEE Communications Surveys Tutorials*, vol. 14, no. 1, pp. 64–86, First 2012.

[34] N. D. Tripathi, J. H. Reed, and H. F. VanLandinoham, "Handoff in cellular systems," *IEEE Personal Communications*, vol. 5, no. 6, pp. 26–37, Dec 1998.

[35] S. . Wang and I. Wang, "Effects of soft handoff, frequency reuse and non-ideal antenna sectorization on cdma system capacity," in *IEEE 43rd Vehicular Technology Conference*, May 1993, pp. 850–854.

[36] J. Diederich and M. Zitterbart, "Handoff prioritization schemes using early blocking," *IEEE Communications Surveys Tutorials*, vol. 7, no. 2, pp. 26–45, Second 2005.

[37] C. N. Chuah, R. D. Yates, and D. J. Goodman, "Integrated dynamic radio resource management," in *1995 IEEE 45th Vehicular Technology Conference. Countdown to the Wireless Twenty-First Century*, vol. 2, July 1995, pp. 584–588 vol.2.

[38] W. Ali, J. Wang, H. Zhu, and J. Wang, "Seamless switching using distributed antenna systems for high-speed railway," in *2017 IEEE 85th Vehicular Technology Conference (VTC Spring)*, June 2017, pp. 1–5.

[39] X. Yu, Y. Luo, and X. Chen, "An optimized seamless dual-link handover scheme for high-speed rail," *IEEE Transactions on Vehicular Technology*, vol. 65, no. 10, pp. 8658–8668, Oct 2016.

[40] W. Ali, J. Wang, H. Zhu, and J. Wang, "An optimized fast handover scheme based on distributed antenna system for high-speed railway," in *2017 IEEE 86th Vehicular Technology Conference (VTC-Fall)*, Sep. 2017, pp. 1–5.

[41] "Visual networking index: Global mobile data traffic forecast update, 2012-2017," *San Jose, CA, USA, Tech. Rep.*, Feb. 2013.

[42] D. Gesbert, M. Kountouris, R. W. Heath, C. Chae, and T. Salzer, "Shifting the mimo paradigm," *IEEE Signal Processing Magazine*, vol. 24, no. 5, pp. 36–46, Sept 2007.

[43] J. Hoydis, S. ten Brink, and M. Debbah, "Massive mimo in the ul/dl of cellular networks: How many antennas do we need?" *IEEE Journal on Selected Areas in Communications*, vol. 31, no. 2, pp. 160–171, February 2013.

[44] S. Deb, P. Monogioudis, J. Miernik, and J. P. Seymour, "Algorithms for enhanced inter-cell interference coordination (eicic) in lte hetnets," *IEEE/ACM Transactions on Networking*, vol. 22, no. 1, pp. 137–150, Feb 2014.

[45] H. Zhou, Y. Ji, X. Wang, and S. Yamada, "eicic configuration algorithm with service scalability in heterogeneous cellular networks," *IEEE/ACM Transactions on Networking*, vol. 25, no. 1, pp. 520–535, Feb 2017.

[46] S. Bassoy, H. Farooq, M. A. Imran, and A. Imran, "Coordinated multi-point clustering schemes: A survey," *IEEE Communications Surveys Tutorials*, vol. 19, no. 2, pp. 743–764, Secondquarter 2017.

[47] C. Liu and L. Wang, "Optimal cell load and throughput in green small cell networks with generalized cell association," *IEEE Journal on Selected Areas in Communications*, vol. 34, no. 5, pp. 1058–1072, May 2016.

[48] G. Kardaras and C. Lanzani, "Advanced multimode radio for wireless and mobile broadband communication," *in Proc. EuWIT Conf.*, pp. 132–135.

[49] J. S. E. Dahlman, S. Parkvall and P. Beming, "3g evolution: Hspa and lte for mobile broadband," *Amsterdam, The Netherlands: Elsevier 2010, ser. 3G Evolution*, pp. 132–135.

[50] F. Anger, "Smart mobile broadband," *in Proc. RAN Evolution to the Cloud Workshop*, Jun. 2013.

[51] D. Xenakis, N. Passas, L. Merakos, and C. Verikoukis, "Mobility management for femtocells in lte-advanced: Key aspects and survey of handover decision algorithms," *IEEE Communications Surveys Tutorials*, vol. 16, no. 1, pp. 64–91, First 2014.

[52] R. Aggarwal, M. Assaad, C. E. Koksal, and P. Schniter, "Joint scheduling and resource allocation in the ofdma downlink: Utility maximization under imperfect

channel-state information," *IEEE Transactions on Signal Processing*, vol. 59, no. 11, pp. 5589–5604, Nov 2011.

[53] K. Yang, "Interference management in LTE wireless networks [Industry Perspectives]," *IEEE Wireless Communications*, vol. 19, no. 3, pp. 8–9, June 2012.

[54] C. Kosta, B. Hunt, A. U. Quddus, and R. Tafazolli, "On interference avoidance through inter-cell interference coordination (icic) based on ofdma mobile systems," *IEEE Communications Surveys Tutorials*, vol. 15, no. 3, pp. 973–995, Third 2013.

[55] P. Marsch and G. Fettweis, "Coordinated multi-point in mobile communications: From theory to practice," *Cambridge U.K.: Cambridge*, Univ. Press, 2011.

[56] J. Lee, Y. Kim, H. Lee, B. L. Ng, D. Mazzarese, J. Liu, W. Xiao, and Y. Zhou, "Coordinated multipoint transmission and reception in lte-advanced systems," *IEEE Communications Magazine*, vol. 50, no. 11, pp. 44–50, November 2012.

[57] M. Sawahashi, Y. Kishiyama, A. Morimoto, D. Nishikawa, and M. Tanno, "Coordinated multipoint transmission/reception techniques for lte-advanced [coordinated and distributed mimo]," *IEEE Wireless Communications*, vol. 17, no. 3, pp. 26–34, June 2010.

[58] Y. Liu, Y. Dai, and Z. Luo, "Coordinated beamforming for MISO interference channel: Complexity analysis and efficient algorithms," *IEEE Transactions on Signal Processing*, vol. 59, no. 3, pp. 1142–1157, March 2011.

[59] A. Alorainy and M. J. Hossain, "Cross-layer performance of downlink dynamic cell selection with random packet scheduling and partial cqi feedback in wireless networks with cell sleeping," *IEEE Transactions on Wireless Communications*, vol. 16, no. 8, pp. 5353–5369, Aug 2017.

[60] "Wireless LAN Medium Access Control (MAC) and physical layer (PHY) specifications," *IEEE 802.11 Standard*, 2007.

[61] L. C.-S. et al., "A neighbor caching mechanism for handoff in IEEE 802.11 wireless networks," *in Proc. Int. Conf. on Multimedia and Ubiquitous Eng.*, pp.48-53, 2007.

[62] D. Gesbert, S. Hanly, H. Huang, S. Shamai Shitz, O. Simeone, and W. Yu, "Multi-cell mimo cooperative networks: A new look at interference," *IEEE Journal on Selected Areas in Communications*, vol. 28, no. 9, pp. 1380–1408, December 2010.

[63] G. Liu, F. R. Yu, H. Ji, V. C. M. Leung, and X. Li, "In-band full-duplex relaying: A survey, research issues and challenges," *IEEE Communications Surveys Tutorials*, vol. 17, no. 2, pp. 500–524, Secondquarter 2015.

[64] A. Naeem, M. H. Rehmani, Y. Saleem, I. Rashid, and N. Crespi, "Network coding in cognitive radio networks: A comprehensive survey," *IEEE Communications Surveys Tutorials*, vol. 19, no. 3, pp. 1945–1973, thirdquarter 2017.

[65] M. Salem, A. Adinoyi, M. Rahman, H. Yanikomeroglu, D. Falconer, Y. Kim, E. Kim, and Y. Cheong, "An overview of radio resource management in relay-enhanced ofdma-based networks," *IEEE Communications Surveys Tutorials*, vol. 12, no. 3, pp. 422–438, Third 2010.

[66] H. Phan, T. Q. Duong, M. Elkashlan, and H. Zepernick, "Beamforming amplify-and-forward relay networks with feedback delay and interference," *IEEE Signal Processing Letters*, vol. 19, no. 1, pp. 16–19, Jan 2012.

[67] A. Vashistha, S. Sharma, and V. A. Bohara, "Outage analysis of a multiple-antenna cognitive radio system with cooperative decode-and-forward relaying," *IEEE Wireless Communications Letters*, vol. 4, no. 2, pp. 125–128, April 2015.

[68] Y. Tan and X. Yuan, "Compute-compress-and-forward: Exploiting asymmetry of wireless relay networks," *IEEE Transactions on Signal Processing*, vol. 64, no. 2, pp. 511–524, Jan 2016.

[69] L. Li, H. V. Poor, and L. Hanzo, "Non-coherent successive relaying and cooperation: Principles, designs, and applications," *IEEE Communications Surveys Tutorials*, vol. 17, no. 3, pp. 1708–1737, thirdquarter 2015.

[70] L. Yan, X. Fang, and Y. Fang, "Control and data signaling decoupled architecture for railway wireless networks," *IEEE Wireless Communications*, vol. 22, no. 1, pp. 103–111, February 2015.

[71] H. Song, X. Fang, L. Yan, and Y. Fang, "Control/user plane decoupled architecture utilizing unlicensed bands in lte systems," *IEEE Wireless Communications*, vol. 24, no. 5, pp. 132–142, October 2017.

[72] L. Zhu, F. R. Yu, B. Ning, and T. Tang, "Handoff performance improvements in mimo-enabled communication-based train control systems," *IEEE Transactions on Intelligent Transportation Systems*, vol. 13, no. 2, pp. 582–593, June 2012.

[73] H. Jiang, V. C. M. Leung, C. Gao, and T. Tang, "Mimo-assisted handoff scheme for communication-based train control systems," *IEEE Transactions on Vehicular Technology*, vol. 64, no. 4, pp. 1578–1590, April 2015.

[74] W. Luo, R. Zhang, and X. Fang, "A comp soft handover scheme for lte systems in high speed railway," *EURASIP Journal on Wireless Communications and Networking*, vol. 2012, 12 2012.

[75] H. J. Kim and J. . Linnartz, "Virtual cellular network: a new wireless communications architecture with multiple access ports," in *Proceedings of IEEE Vehicular Technology Conference (VTC)*, June 1994, pp. 1055–1059 vol.2.

[76] M. Flament and A. Svensson, "Virtual cellular networks for 60 ghz wireless infrastructure," in *IEEE International Conference on Communications, 2003. ICC '03.*, vol. 2, May 2003, pp. 1223–1227 vol.2.

[77] B. L. D. et al., "Radio-over-fiber based architecture for seamless wireless indoor communication in the 60 ghz band," in *Elsevier Comput. Commun.*, vol. 30, no. 18, 2007, pp. 3598–3613.

[78] C. D. Gavrilovich, "Broadband communication on the highways of tomorrow," *IEEE Communications Magazine*, vol. 39, no. 4, pp. 146–154, Apr. 2001.

[79] N. Pleros, K. Tsagkaris, and N. D. Tselikas, "A moving extended cell concept for seamless communication in 60 ghz radio-over-fiber networks," *IEEE Communications Letters*, vol. 12, no. 11, pp. 852–854, November 2008.

[80] R. Q. Hu and Y. Qian, "An energy efficient and spectrum efficient wireless heterogeneous network framework for 5g systems," *IEEE Communications Magazine*, vol. 52, no. 5, pp. 94–101, May 2014.

[81] O. B. Karimi, J. Liu, and C. Wang, "Seamless wireless connectivity for multimedia services in high speed trains," *IEEE Journal on Selected Areas in Communications*, vol. 30, no. 4, pp. 729–739, May 2012.

[82] Z. Liu and P. Fan, "An effective handover scheme based on antenna selection in ground train distributed antenna systems," *IEEE Transactions on Vehicular Technology*, vol. 63, no. 7, pp. 3342–3350, Sept. 2014.

[83] W. Ali, J. Wang, H. Zhu, and J. Wang, "Distributed antenna system based frequency switch scheme evaluation for high-speed railways," *Accepted by IEEE Int. Conf. Commun. (ICC) 2017, Paris, 21-25 May*, 2017.

[84] J. Wang and L. Dai, "Asymptotic rate analysis of downlink multi-user systems with co-located and distributed antennas," *IEEE Transactions on Wireless Communications*, vol. 14, no. 6, pp. 3046–3058, Jun. 2015.

[85] 3GPP RAN2 R2-140089, "Mobility Performance in Real Networks," *3rd Generation Partnership Project (3GPP), Qualcomm Incorporated*, Feb. 2014.

[86] T. Han and N. Ansari, "Radiate: radio over fiber as an antenna extender for high-speed train communications," *IEEE Wireless Communications*, vol. 22, no. 1, pp. 130–137, Feb. 2015.

[87] D. Lopez-Perez, I. Guvenc, and X. Chu, "Mobility management challenges in 3gpp heterogeneous networks," *IEEE Communications Magazine*, vol. 50, no. 12, pp. 70–78, Dec. 2012.

[88] S. Jeon and S. Lee, "A relay-assisted handover technique with network coding over multihop cellular networks," *IEEE Communications Letters*, vol. 11, no. 3, pp. 252–254, Mar. 2007.

[89] P. Kyösti, J. Meinilä, L. Hentilä, X. Zhao, T. Jämsä, C.Schneider, M. Narandzić, M. Milojević, A. Hong, J. Ylitalo, V. Holappa, M. Alatossava, R. Bultitude, Y. de Jong, and T. Rautiainen, "Winner ii channel model," *Techincal Report*, Sep. 2007, [Available Online:http://www.ist-winner.html].

[90] Y. Li and L. J. Cimini, "Bounds on the interchannel interference of ofdm in time-varying impairments," *IEEE Transactions on Communications*, vol. 49, no. 3, pp. 401–404, Mar. 2001.

[91] 3GPP R3-120233, "Performance Analysis for Candidate Architectures Supporting Mobile Relay," *3rd Generation Partnership Project (3GPP), Sophia-Antipolis,France*, Feb. 2012.

[92] 3GPP TS 36.331, "Evolved Universal Terrestrial Radio Access (E-UTRA); Radio Resource Control (RRC); Protocol Specification," *3rd Generation Partnership Project (3GPP), Sophia-Antipolis, France*, Jul. 2012.

[93] C. X. Wang, F. Haider, X. Gao, X. H. You, Y. Yang, D. Yuan, H. M. Aggoune, H. Haas, S. Fletcher, and E. Hepsaydir, "Cellular architecture and key technologies for 5g wireless communication networks," *IEEE Communications Magazine*, vol. 52, no. 2, pp. 122–130, Feb. 2014.

[94] H. Zhu, S. Karachontzitis, and D. Toumpakaris, "Low-complexity resource allocation and its application to distributed antenna systems [coordinated and distributed mimo]," *IEEE Wireless Communications*, vol. 17, no. 3, pp. 44–50, Jun. 2010.

[95] H. Zhu and J. Wang, "Radio resource allocation in multiuser distributed antenna systems," *IEEE Journal on Selected Areas in Communications*, vol. 31, no. 10, pp. 2058–2066, Oct. 2013.

[96] H. Zhu, "On frequency reuse in cooperative distributed antenna systems," *IEEE Communications Magazine*, vol. 50, no. 4, pp. 85–89, Apr. 2012.

[97] H. Osman, H. Zhu, D. Toumpakaris, and J. Wang, "Achievable rate evaluation of in-building distributed antenna systems," *IEEE Transactions on Wireless Communications*, vol. 12, no. 7, pp. 3510–3521, July 2013.

[98] T. Alade, H. Zhu, and J. Wang, "Uplink spectral efficiency analysis of in-building distributed antenna systems," *IEEE Transactions on Wireless Communications*, vol. 14, no. 7, pp. 4063–4074, July 2015.

[99] H. Zhu and J. Wang, "Performance analysis of chunk-based resource allocation in multi-cell ofdma systems," *IEEE Journal on Selected Areas in Communications*, vol. 32, no. 2, pp. 367–375, Feb. 2014.

[100] R. Raoof, C. Pan, H. Zhu, and J. Wang, "Dynamic pilot reuse in distributed massive mimo systems," in *2017 IEEE 85th Vehicular Technology Conference (VTC Spring)*, June 2017, pp. 1–5.

[101] R. Sabbagh, C. Pan, and J. Wang, "Pilot allocation and sum-rate analysis in cell-free massive mimo systems," in *2018 IEEE International Conference on Communications (ICC)*, May 2018, pp. 1–6.

[102] W. Ali, J. Wang, H. Zhu, and J. Wang, "Distributed antenna system based frequency switch scheme evaluation for high-speed railways," in *2017 IEEE International Conference on Communications (ICC)*, May 2017, pp. 1–6.

[103] P. T. Dat, A. Kanno, N. Yamamoto, and T. Kawanishi, "Wdm rof-mmw and linearly located distributed antenna system for future high-speed railway communications," *IEEE Communications Magazine*, vol. 53, no. 10, pp. 86–94, Oct. 2015.

[104] W. Ali, J. Wang, H. Zhu, and J. Wang, "An expedited predictive distributed antenna system based handover scheme for high-speed railway," in *GLOBECOM 2017 - 2017 IEEE Global Communications Conference*, Dec. 2017, pp. 1–6.

[105] 3GPP TS 36.300, "Overall description;Stage 2," *3rd Generation Partnership Project (3GPP), v11.2.0,Sophia-Antipolis, France*, Jun. 2012.

[106] T. Taleb, K. Samdanis, and A. Ksentini, "Supporting highly mobile users in cost-effective decentralized mobile operator networks," *IEEE Transactions on Vehicular Technology*, vol. 63, no. 7, pp. 3381–3396, Sept. 2014.

[107] 3GPP R3 060741, "Inter-RAT Mobility for Real-time flows," *3rd Generation Partnership Project (3GPP), Shanghai, China*, May 2006.

[108] G. H. S. R. Ramaswami, K. N. Sivarajan, "Optical networks a practical perspective," *Morgan Kaufmann, ELSEVIER*, vol. Third Edition, 2010.

[109] 3GPP TR 25.912, "Technical Specification Group Radio Access Network; Feasibility Study for Evolved Universal Terrestrial Radio Access (UTRA) and Universal Terrestrial Radio Access Network (UTRAN) Release 10," *3rd Generation Partnership Project (3GPP), Sophia-Antipolis, France*, Mar. 2011.

[110] Institute for Information Industry, "Performance Analysis for Candidate Architectures Supporting Mobile Relay," *3rd Generation Partnership Project (3GPP), 3GPP TSG RAN WG3 Meeting 75*, Feb. 2012.

[111] 3GPP TS 36.331, "Radio Resource Control (RRC);Protocol specification," *3rd Generation Partnership Project (3GPP), v11.1.0,Sophia-Antipolis, France*, Sep., 2012.

[112] 3GPP TS 36.413, "S1 Application Protocol (S1AP)," *3rd Generation Partnership Project (3GPP), v11.1.0,Sophia-Antipolis, France*, Sep. 2012.

[113] 3GPP TS 36.423, "X2 Application Protocol (X2AP)," *3rd Generation Partnership Project (3GPP), v11.2.0,Sophia-Antipolis, France*, Sep. 2012.

[114] H. Zhang, N. Liu, X. Chu, K. Long, A. H. Aghvami, and V. C. M. Leung, "Network slicing based 5g and future mobile networks: Mobility, resource management, and challenges," *IEEE Communications Magazine*, vol. 55, no. 8, pp. 138–145, 2017.

[115] Y. Y. Lan and T. D. Chiueh, "Turbo receiver with dual-loop dual-list update for inter-cell interference mitigation in heterogeneous networks," *IEEE Transactions on Wireless Communications*, vol. 16, no. 4, pp. 2288–2299, April 2017.